F 1503/2

BULETINUL INSTITUTULUI POLITEHNIC DIN IAȘI

Tomul XXIX(XXXIII)

Fasc. 1—4

L: 040721

Secția II

CHIMIE ȘI INGINERIE CHIMICĂ

1983

ORSZÁGOS MŰSZAKI INFORMÁCIÓS KÖZPONT ÉS KÖNYVTÁR 1883

BULETINUL INSTITUTULUI POLITEHNIC DIN IAŞI

Tomul XXIX (XXXIII)

Fasc. 1—4

Secţia II

CHIMIE
ŞI
INGINERIE CHIMICĂ

1982

COLEGIUL DE REDACŢIE

Prof. dr. doc. **VAL. BLIDARU**
Prof. dr. doc. **N. V. BOŢAN**
Prof. dr. ing. **GH. CAŞLER,**
Prof. dr. ing. **M. GAFIŢANU** (preşedinte)
Prof. dr. **P. MÂLCOMETE**
Prof. dr. doc. **D. MANGERON**
Prof. dr. ing. **T. SILION**
Acad. prof. dr. doc. **CR. SIMIONESCU**
Prof. dr. ing. **I. VLAD**

COMITETUL DE REDACŢIE AL SECŢIEI II. CHIMIE ŞI INGINERIE CHIMICĂ

Prof. dr. ing. **N. ASANDEI**
Prof. dr. doc. **MAGDA PETROVANU**
Prof. dr. doc. **RADU TUDOSE**

REDACŢIA

Prof. dr. doc. **D. MANGERON**
(redactor responsabil)
Prof. dr. ing. **HUGO ROSMAN**
(secretar)
ECATERINA IRIMIEA
(tehnoredactor)

BULETINUL INSTITUTULUI POLITEHNIC DIN IAŞI
BULLETIN OF THE POLYTECHNIC INSTITUTE OF JASSY
ИЗВЕСТИЯ ЯССКОГО ПОЛИТЕХНИЧЕСКОГО ИНСТИТУТА
Tom XXIX (XXXIII), fasc. 1–4 1983

Secţia II

CHIMIE ŞI INGINERIE CHIMICĂ

SUMAR

Pag

N. CALU, L. ODOCHIAN, A. HÎRTOPEANU şi E. MIHAI, Studiul termogravimetric al unor complecşi ai 2-hidroxi 3,5 dicloracetofenon oximei cu metale tranziţionale (engl., rez. rom.) 7

I. ROŞCA, M. PALAMARU şi C. ADAM, Interacţiunea poliuretanilor cu ionii metalelor tranziţionale (IV) (engl. rez. rom.) 13

AL. NACU, D. NACU şi D. BÎLBĂ, Coprecipitarea unor chelaţi metalici pe colectori organici indiferenţi (engl. rez. rom.) 19

N. AELENEI, A. TARHON, GH. IONESCU, O. ROMAN şi M. ŞCHIOPU, Ecuaţii pentru curba presiunii de vapori a lichidelor pure (franc., rez. rom.) 25

D. P. LAZĂR, Despre piroliza spumelor poliuretanice (rom. rez. engl.) . . . 33

E. POPOVICI şi M. CRUCEANU, Unele corelaţii compoziţie—proprietăţi la site moleculare de tip NaA (rom., rez. engl.) 39

GH. MIHĂILĂ, N. BÎLBĂ, P. ONU, C. LUCA şi N. NAUM, Comportarea unor derivaţi cloruraţi organici la adsorbţie pe tufuri vulcanice (engl., rez. rom.) 45

I. CURIEVICI, S. MATACHE, V. NICU, ŞT. UNGUREANU, C. PETRILĂ şi E. IONESCU, Modelarea matematică a unui reactor catalitic pentru hidrogenarea benzenului (engl. rez. rom.) 51

L. IFRIM, C. LEONTE, AL. SZÉP şi C. CALISTRU, Cercetări de inginerie chimică în cadrul procesului de obţinere a $Mg(OH)_2$ (I) (engl., rez. rom.) . . . 59

C. HAGIU şi C. CALISTRU, Controlul procesului de oxidare catalitică a amoniacului prin intermediul modelelor matematice de bilanţ (rom., rez. engl.) . 65

M. APOSTOLESCU, ŞT. IVĂŞCAN şi F. BRANDABUR, Cercetări privind posibilitatea de recuperare a cuprului şi zincului din soluţii acide (engl., rez. rom.) 73

C. LUCHIAN, V. BĂRBOIU, GH. SURPĂŢEANU şi M. PETROVANU, 1, 2, 4-triazoliu-ilide (VII) (franc., rez. rom.) 77

T. LIXANDRU, M. DUMITRU, M. PĂSTRĂVANU şi I. COCÎRLĂ, Poliacenaftenchinoniminimide (engl., rez. rom.) 83

AL. CAŞCAVAL, Compuşi organici ai sulfului (XVI), (XI) (engl., rez. rom.) . 89

V. GORDUZA, GH. LUPUŞOR şi V. PESCARU, Noi pigmenţi azoici de condensare (rom., rez. engl.) 93

S. OPREA, E. DUMITRU şi I. C. DIEAC, Reactivitatea monomerilor acrilici (X) (engl., rez. rom.) 99

BULETINUL INSTITUTULUI POLITEHNIC DIN IAŞI
BULLETIN OF THE POLYTECHNIC INSTITUTE OF JASSY
ИЗВЕСТИЯ ЯССКОГО ПОЛИТЕХНИЧЕСКОГО ИНСТИТУТА
Tom XXIX (XXXIII), fasc. 1—4 1983

Section II

CHEMISTRY and CHEMICAL INGINEERING

CONTENTS

Pp.

N. CALU, L. ODOCHIAN, A. HÎRTOPEANU and E. MIHAI, Thermogravimetrical Study of some Complexes of 2-Hydroxy 3,5-dichloroacetophenone Oxime with Transitional Metals (English, Romanian summary) 7

I. ROŞCA, M. PALAMARU and C. ADAM, Interaction of Polyuretanes with the Element Ions from *d* Block (IV) (English, Romanian summary) . . 13

AL. NACU, D. NACU and D. BÎLBĂ, Coprecipitation of Some Metalic Chelates on Indifferent Organic Collectors (English, Romanian summary) 19

N. AELENEI, A. TARHON, GH. IONESCU, O. ROMAN et M. ŞCHIOPU, Équation pour la courbe de la pression de vapeur pour les liquides purs (French, Romanian summary) 25

D. P. LAZĂR, About the Pyrolysis of the Polyurethane Foames (Romanian, English summary) 33

E. POPOVICI and M. CRUCEANU, Some Correlations Composition—Properties on the Molecular Sieves of the NaA Type (Romanian, English summary) 39

GH. MIHĂILĂ, N. BÎLBĂ, P. ONU, C. LUCA and N. NAUM, Adsorption Behaviour of Some Organic Chloroderivatives on Volcanic Tuffs (English, Romanian summary) 45

I. CURIEVICI, S. MATACHE, V. NICU, ŞT. UNGUREANU, C. PETRILĂ and E. IONESCU, Mathematical Modelling of a Catalytic Reactor for Benzene Hydrogenation (I) (English, Romanian summary) 51

L. IFRIM, C. LEONTE, AL. SZÉP and C. CALISTRU, Chemical Engineering Researches on the Process of $Mg(OH)_2$ Preparation (I) (English, Romanian summary) 59

C. HAGIU and C. CALISTRU, Controle of Catalytic Oxydation Process of Ammonia by means of Balance Mathematical Model (Romanian, English summary) 65

M. APOSTOLESCU, ŞT. IVĂŞCAN and F. BANDRABUR, On the Possibility of Recovering Copper and Zinc from Acid Solutions (English, Romanian summary) 73

C. LUCHIAN, V. BĂRBOIU, GH. SURPĂŢEANU et M. PETROVANU, 1,2,4-Triazolium-Ylures (VII) (French, Romanian summary) 77

T. LIXANDRU, M. DUMITRIU, M. PĂSTRĂVANU and I. COCÎRLĂ, Polyacenaphthenequinoniminimides (English, Romanian summary) 83

AL. CAŞCAVAL, Organic Sulphur Compounds (XVI), (XI) (English, Romanian summary) 89

V. GORDUZA, GH. LUPUŞOR and V. PESCARU, New Condensing Azopigments (Romanian, English summary) 93

S. OPREA, E. DUMITRIU and I. C. DIEAC, Reactivity of Acrylic Monomers (X) (English, Romanian summary) 99

BULETINUL INSTITUTULUI POLITEHNIC DIN IAŞI
BULLETIN OF THE POLYTECHNIC INSTITUTE OF JASSY
ИЗВЕСТИЯ ЯССКОГО ПОЛИТЕХНИЧЕСКОГО ИНСТИТУТА
Том XXIX (XXXIII), Вып. 1—4 1983 г.

Секция II

ХИМИЯ и ХИМИЧЕСКАЯ ПРОМЫШЛЕННОСТЬ

СОДЕРЖАНИЕ

Стр.

Н. КАЛУ, Л. ОДОКЯН, А. ХЫРТОПЯНУ и Е. МИХАЙ, Термогравиметрические изучение некоторых комплексов 2-хидрокси 3,5 дихлорацетофенон оксима с переходными металлами (англ., рез. рум.) 7

И. РОШКА, М. ПАЛАМАРУ и К. АДАМ, Взаимодействие полиэстеруретанов с ионами переходных металлов (IV) (англ., рез. рум.) . . 13

АЛ. НАКУ, Д. НАКУ и Д. БЫЛБЭ, Соосождение некоторых хелатов элементов с индиферентными органическими сосадителями (англ., рез. рум.) 19

Н. АЕЛЕНЕЙ, А. ТАРХОН, Г. ИОНЕСКУ, О. РОМАН и М. ШКИОПУ, Уравнение для кривой давления пары чистых жидкостей (франц., рез. рум.) 25

Д. П. ЛАЗЭР, Об пиролизе полиуретанских лен (рум., рез. англ.) 33

Е. ПОПОВИЧ и М. КРУЧЯНУ, Некоторые корреляции состав — свойства на молекулярных сит (рум., рез. англ.) 39

Г. МИХЭИЛЭ, Н. БЫЛБЭ, П. ОНУ, К. ЛУКА и Н. НАУМ, Поведение некоторых хлорорганических производных в адсорбции на вулканические туффы (англ., рез. рум.) 45

И. КУРИЕВИЧ, С. МАТАКЕ, В. НИКУ, ШТ. УНГУРЯНУ, К. ПЕТРИЛЭ и Е. ИОНЕСКУ, Математическое моделирование каталитического реактора для гидрогенизации бензола (англ., рез. рум.) 51

Л. ИФРИМ, К. ЛЕОНТЕ, АЛ. СЕП и К. КАЛИСТРУ, Исследование процесса осаждения гидрата окиси магния ($Mg(OH)_2$) (I) (англ., рез. рум.) 59

К. ХАДЖИУ и К. КАЛИСТРУ, Контроль процесс окисление аммиака с помощю математические модели баланса (рум., рез. англ.) . . . 65

М. АПОСТОЛЕСКУ, ШТ. ИВЭШКАН и Ф. БАНДРАБУР, Исследования относительно к возможности рекуперации меди и цинка из кислых растворов (англ., рез. рум.) 73

К. ЛУКЯН, В. БЭРБОЮ, Г. СУРПЭЦЯНУ и М. ПЕТРОВАНУ, 1, 2, 4-триазолю-илиды (VII) (франц., рез. рум.) 77

Т. ЛИКСАНДРУ, М. ДУМИТРИУ, М. ПЭСТРЭВАНУ и И. КОКЫРЛЭ, Полиаценафтенхинониминимиды (англ., рез. рум.) 83

АЛ. КАШКАВАЛ, Серосодержание органические соединения. (XVI), (XI) (англ., рез. рум.) 89

В. ГОРДУЗА, Г. ЛУПУШОР и В. ПЕСКАРУ, Новые конденсационные азопигменты (рум., рез. англ.) 93

С. ОПРЯ, Е. ДУМИТРИУ и И. К. ДИЕАК, Реакционоспособность акриловых мономеров (X) (англ., рез. рум.) 99

BULETINUL INSTITUTULUI POLITEHNIC DIN IAŞI
Tomul XXIX (XXXIII), Fasc. 1—4, 1983
Secţia II
CHIMIE şi INGINERIE CHIMICĂ

D.C.547.574.2; 545.1

THERMOGRAVIMETRICAL STUDY OF SOME COMPLEXES OF 2-HYDROXY 3,5-DICHLOROACETOPHENONE OXIME WITH TRANSITIONAL METALS

BY

N. CALU, LUCIA ODOCHIAN, A. HÎRTOPEANU and ELENA MIHAI

1. Introduction

The compounds of the *o*-hydroxy-acetophenonoxime type act as ligands with a series of metallic ions. The resulted complexes are of interest both for the structural point of view and for analytical purposes, being used in dosing some elements.

For the thermogravimetrical study a series of complexes of 2-hydroxy-3,5-dichloro-acetophenonoxime (L) with transitional metals (M) with general formula $M(n)L_n$, namely: $Mn(II)L_2$, $Cu(II)L_2$, $Ni(II)L_2$, $Co(II)L_2$ and $Fe(III)L_3$ have been synthesised and characterized [1]. Data obtained by chemical analysis determinations of molecular weights, spectral measurements (IR, visible and UV) indicate a structure of chelate type, with a normal bond, obtained by the elimination of phenolic proton and another covalent—coordinative one by the nitrogen of the oxime group.

In the present paper the thermogravimetrical study of the above mentioned complexes was carried out to obtain informations on their behaviour on heating, certain appreciations on the chemical composition, kinetics, thermal decomposition and thermal stability being made.

2. Experimental

The $M(n)L_n$ complexes were synthesised under established conditions of pH and temperature. Thus, the $Mn(II)L_2$ and $Fe(III)L_3$ complexes were obtained starting from 2-hydroxy-3,5-dichloroacetophenonoxime and the corresponding metallic ion, in aqueous ethylic alcool medium and a buffer system of pH=9...10 and 3...4.5, respectively. The obtained complexes crystallized in time at the room temperature.

The other complexes ($Cu(II)L_2$, $Ni(II)L_2$ and $Co(II)L_2$) were synthesised in a similar manner but at different pH (=3.5; 5...6 and 5...6, respectively) and by warming.

The investigations were performed by means of dynamic thermogravimetry with constant heating rate, using a MOM—Budapest derivatograph of Paulik-Paulik-Erdey type. The experimental conditions were the following; heating rate — 12,4°C/min, maximum temperature — 900°C, ambient atmosphere, sample wight — 18 mg.

3. Results and Discussion

The experimental results indicated the thermal decomposition to take place stepwise. The calculation of the weight losses and analysis of the residue allowed the determination of composition of the investigated combinations [2], [3].

The data listed in Table 1 indicate the chemical composition to correspond to the oxydation state of the metallic ion. Thus the M^{2+} ions lead to $M(II)L_2$ complexes with the combination ratio 1 M : 2 L as in complexes with Ni, Cu, Co and Mn while those M^{3+} give complexes $M(III)L_3$ with the combination ratio 1 M : 3 L, such as the Fe complex. This fact was confirmed by the elemental analysis and pleads for the formation of some internal nonelectrolite complexes.

Table 1

Elemental and Thermogravimetrical Analysis Data

Nr.	Sample	Elemental analysis								Thermogravimetrical analysis				
		C, [%]		H, [%]		N, [%]		Me, [%]		W_∞, [mg]		Residue, [mg]		
		calc.	found	calc.	found	calc.	found	calc.	found	calc.	found	nature	calc.	found
1	Ligand	43.64	43.72	3.18	3.68	6.36	6.10	—	—	18.00	18.00	—	—	—
2	$Ni(II)L_2$	38.66	39.83	2.42	2.96	5.64	5.49	11.82	11.34	15.30	16.00	NiO	2.700	2.50
3	$Cu(II)L_2$	38.28	37.76	2.39	2.47	5.58	5.54	12.67	12.70	15.15	15.50	CuO	2.850	1.75
4	$Co(II)L_2$	38.63	39.24	2.42	2.80	5.64	5.35	11.86	11.03	15.28	15.20	CoO	2.716	2.80
5	$Fe(III)L_3$	40.40	39.70	2.53	2.46	5.89	5.35	7.83	8.06	16.18	16.70	FeO	1.814	1.30
6	$Mn(II)L_2$	38.95	37.96	2.43	3.05	5.68	5.53	11.14	11.28	13.88	13.78	MnO_2	2.900	2.80

As can be seen in Fig. 1, where the thermograms of ligand and Ni and Fe complex are given (Fig. 1 *a* and 1 *b*, respectively) the mechanism of thermal decomposition complicates from the ligand to complexes being characteristic for every complex combination.

By applying the Freeman-Carroll method [4] for the recorded thermograms the data listed in Table 2 were obtained.

Table 2

Kinetic Parameters for the Decomposition Steps

Nr.	Sample	Step I		Step II		Step III		Step IV	
		n	E_a Kcal/mol	n	E_a Kcal/mol	n	E_a Kcal/mol	n	E_a Kcal/mol
1	$C_8H_7O_2Cl_2N$	0	22.52	4	117.58	—	—	—	—
2	$(C_8H_6O_2Cl_2N)_2Ni$	0.5	28.79	—	—	—	116.38	3.5	53.35
3	$(C_8H_6O_2Cl_2N)_2Cu$	0.4	125.67	—	109.68	3	111.05	—	—
4	$(C_8H_6O_2Cl_2N)_2Co$	—	88.13	2	66.69	6	79.97	—	—
5	$(C_8H_6O_2Cl_2N)_3Fe$	0.4	18.20	1.5	21.76	—	—	—	—
		2.2	32.36	3.2	33.39	—	—	—	—
6	$(C_8H_6O_2Cl_2N)_2Mn$	1	25.38	—	—	—	167.49	—	—
		—	49.50						

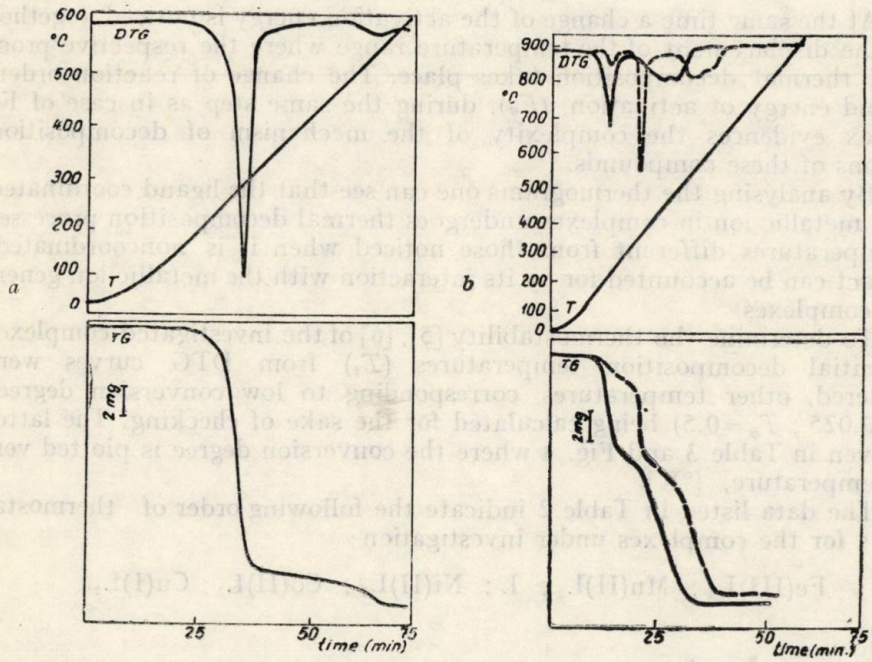

Fig. 1. — Thermograms of ligand : *a* — Ni complex (—) ; *b* — Fe complex (— —).

It must be pointed out that the evaluation of the kinetic parameters by this method is not possible for all decomposition steps due to the fact that the step separation is not very clear. In addition, the narrow temperature range did not allow the application of the calculating method with a satisfactory accuracy.

From the data obtained with help of Freeman-Carroll analysis (Table 2, Figs. 2 and 3) it result the increasing of the reaction order from 0...0.4, when diffusion is the rate determining step to $n > 1$, when the chemical reaction is the determining step.

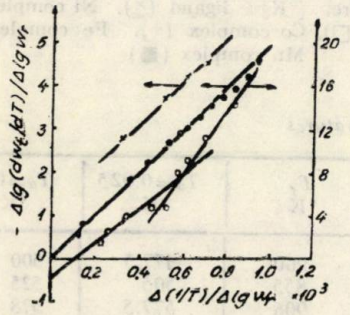

Fig. 2. — Freeman-Carroll plots for the first decomposition step for : ligand (•), Co complex (×) and Fe com plex (○).

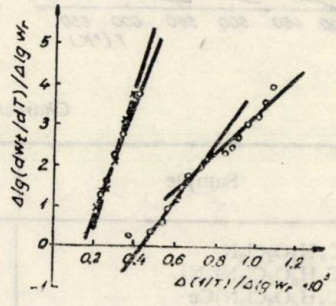

Fig. 3. — Freeman-Carroll plots for the second decomposition step : for ligand (×), Co complex (•) and Fe complex (○).

At the same time a change of the activation energy is noticed together with the displacement of the temperature range where the respective process of thermal decomposition takes place. The change of reaction order, (n), and energy of activation, (E_a), during the same step as in case of Fe complex evidences the complexity of the mechanism of decomposition reactions of these compounds.

By analysing the thermograms one can see that the ligand coordinated to the metallic ion in complexes undergoes thermal decomposition processes at temperatures different from those noticed when it is noncoordinated. This fact can be accounted for by its interaction with the metallic ion generating complexes.

To determine the thermostability [5], [6] of the investigated complexes the initial decomposition temperatures (T_i) from DTG curves were considered, other temperatures corresponding to low conversion degrees ($T_\alpha=0.025$; $T_\alpha=0.5$) being calculated for the sake of checking. The latter are given in Table 3 and Fig. 4 where the conversion degree is plotted versus temperature, [°K].

The data listed in Table 2 indicate the following order of thermostabilities for the complexes under investigation:

$$Fe(III)L_3\ ;\ Mn(II)L_2\ ;\ L\ ;\ Ni(II)L_2\ ;\ Co(II)L_2\ ;\ Cu(I)L_2.$$

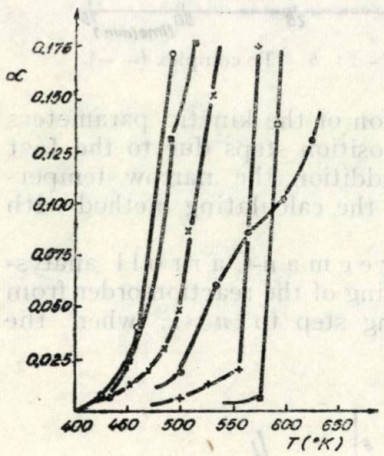

Fig. 4. — Dependence of the conversion degree α on temperature, [°K]: ligand (×), Ni complex (•), Cu complex (□), Co complex (+), Fe complex (○), Mn complex (■).

Table 3

Characteristic Temperatures

Nr.	Sample	T_i °K	T_f °K	$T_\alpha=0.025$ °K	$T_\alpha=0.05$ °K
1	$C_8H_7O_2Cl_2N$	421	960	477.5	500
2	$(C_8H_6O_2Cl_2N)_2Ni$	466	855	505	525
3	$(C_8H_6O_2Cl_2N)Cu$	573	906	577.5	578
4	$(C_8H_6O_2Cl_2N)_2Co$	513	913	555	557
5	$(C_8H_6O_2Cl_2N)_3Fe$	393	863	447	465
6	$(C_8H_6O_2Cl_2N)_2Mn$	423	921	450	465

In this sequence the thermal stability increase (with some small deviations) towards the $Cu(II)L_2$ complex corresponding to a cation with d^{10} electronic configuration whose π donating ability and polarizing activity are streangthened.

By applying the kinetic criterion of thermostability [7], that is the values of activation energies for the first decomposition stage, the same sequence as above can be settled.

4. Conclusions

Based on the thermogravimetrical study under dynamic temperature conditions on the above mentioned complexes the following conclusions can be drawn :

1. The composition of complex combinations resulted from thermogravimetrical data is in good agreement with that obtained by elemental chemical analysis.

2. The mechanism of thermal decomposition reactions as well as the thermostability is specific to every complex combination and dependent on the metal nature.

Received, February 2, 1982

Polytechnic Institute, Jassy,
Department of Inorganic and Analytical Chemistry
and
University, Galaţi

REFERENCES

1. Hîrtopeanu A., *Combinaţii complexe ale metalelor tranziţionale cu liganzi din clasa hidrazonelor şi oximilor*. Ph. D. Diss., Polyt. Inst., Jassy, 1982.
2. Hurduc N., Odochian L., Schneider I. A., Segal E., Rev. Roumaine Chim., **11**, 1453 (1966).
3. Vicol O., Hurduc N., Schneider I. A., J. Inorg. Nucl. Chem., **41**, 309 (1979).
4. Freeman E. S., Carroll B., J. Phys. Chem., **62**, 394 (1958).
5. Popa-Luchian M., Rozmarin Gh., Schneider I. A., J. Thermal Analysis, **1**, 211 (1969).
6. Odochian L., Mihai E., Fişel S., Mitoşeriu O., Rev. Roumaine Chim., **26**, 383 (1981).
7. Simionescu Cr., Schneider I. A., Hurduc N., Dumitriu S., Cellulose Chem. Technol., **11**, 577 (1977).

STUDIUL TERMOGRAVIMETRIC AL UNOR COMPLECŞI AI 2-HIDROXI 3,5 DICLORACETOFENON OXIMEI CU METALE TRANZIŢIONALE

(Rezumat)

S-a întreprins un studiu termogravimetric al descompunerii termice a unor combinaţii complexe a 2-hidroxi 3,5 dicloracetofenon oximei cu metale tranziţionale, folosind ca metodă de investigaţie termogravimetria în condiţii dinamice de temperatură.

Rezultatele obţinute au condus la concluzii privind compoziţia chimică, termostabilitatea şi cinetica descompunerii termice.

BULETINUL INSTITUTULUI POLITEHNIC DIN IAŞI
Tomul XXIX (XXXIII), Fasc. 1—4, 1983
Secţia II
CHIMIE şi INGINERIE CHIMICĂ

D.C. 678.664 ; 546.4/5

INTERACTION OF POLYURETANES WITH THE ELEMENT IONS FROM *d* BLOCK

IV. STABILITY IN AQUEOUS MEDIUM AND CALORIFIC EFFECT ACTION ON MODIFIED POLYESTERURETANES WITH THE GROUP II TRANSITION METAL IONS

BY

I. ROŞCA, MIRCEA PALAMARU and CORNELIU ADAM

1. Introduction

The interaction capacity of the transition metal ions with polyesteruretanes is of interest from both theoretical and practical point of view [1]...[8].

The experimental data show that due to their electronic structure, ionic potential and all consequences that follow from these, the group II transition metal ions interact with polyesteruretanes giving products with special properties. These interaction products exhibit a high thermal stability and are stable enough in aqueous medium, which confer them a different behaviour.

Due to their stability in aqueous medium, it can predict that these compounds can be used as retention agents for respectively ions in waste waters or other wastes. The methods employed in this study reveal a strongly complexation capacity of the polyesteruretanes.

The group II transition metal ions in polyesteruretanes transmit not only colour modification of these products, but also other properties such as viscosity, density, which constitute certain evidences for new structures.

2. Experimental

2.1. Reagents

a) Two polyesteruretanes, as intermediate in the polyaddition reaction, have been employed [5], [6]. Their general formula is :

$$-\underset{\underset{O}{\|}}{C}-NH-M-NH-\underset{\underset{O}{\|}}{C}-O-P-O-\underset{\underset{O}{\|}}{C}-NH-M-NH-\underset{\underset{O}{\|}}{C}-O-G-,$$

where :

$$M = -\langle\bigcirc\rangle-\left(-CH_2-\right)_n-\langle\bigcirc\rangle-, \quad (n=1,2)\,; \quad G = -\left(-CH_2-\right)_n-\,;$$

$$P=-O-(-CH_2-)_n-O-\overset{\overset{O}{\|}}{C}-(-CH_2-)_n-\overset{\overset{O}{\|}}{C}-O-$$

For the polyesteruretane (I), in M, $n=1$ and for polyesteruretane (II), in M, $n=2$.

b) Purified dimethylformamide with 500 p.p.m. water and traces of formic acid and dimethylamine

c) Inorganic salts of respective metals reagent grade.

2.2 Stability of the Polyesteruretanes Modified with the Zn^{2+}, Cd^{2+} and Hg^{2+} Ions in Aqueous Medium

a) *Preparation of Samples*

To a solution of polyesteruretane in dimethylformamide (DMF) the solution of transition metal salt is added drop by drop, under stirring at 25°C. Both solutions have equimolecular concentration in active component (uretane groups and inorganic salt, respectively). The solutions of salt is added until the separation of polymer-transition cation compounds takes place. Exceeding solvent is removed by settling. The samples were placed in a drying stove at 105°C for a 24 h in order to remove main part of DMF. After that, the samples were placed in a vacuum oven for 48 h at 40°C in order to remove the solvent traces.

b) *Determination of Metal Amount in Complexes*

The amount of metal in samples has been determined conductometrical and by atomic absorption spectroscopy [9], [10]. Therefore the complexes were suspended in distilled water and nonstop refluxed for 48 h. After cooling, the aqueous layer was analysed. Distilled water employed to carry out these experiments has a specific conductivity of 0.012 mS. Conductometric analyses have bean carried out on OK-102 Budapest conductometer. In order to eliminate the temperature influence, the conductometric cell has been thermostated at 25°C. Experimental was previously described [8].

Determinations by atomic absorbtion spectroscopy have been carried out only for the samples containing zinc, using a SP-90 A Pye-Unicam apparatus. Zinc was determined in air—acetylene flame, wave length equal to 2 138 Å. The best concentration was comprised between 0.5 and 5.0 g/ml, the sensitivity was about 0.03 g/ml. The method with the calibration curve has been used. The obtained results are set on in Table 1.

As it comes ont from Table 1, after extraction, no traces of metal has been found in the filtered samples probably because the amount of metal is placed under the detection limit of the employed apparatus.

c) *Behaviour at Immersion in Water*

The behaviour at immersion in water of the complexes obtained as above, after separation, was studied. The samples were placed in glass flasks with ground-glass stopper in which there are already 25 ml distilled water with known specific conductivity. All flasks were heated simultaneously at 100°C and refluxed for 4, 8, 12, 14 and 16 h, respectively. After each period of time, the samples were taken out cooled and thermostated precisely. Specifical conductivity obtained for each complex at each instant are sumarised in Table 2.

Table 1

Maximum Amount of Metal in the Complexes Synthesized by Interaction of Polyesteruretanes I and II with Group II Transitions Metal Ions

No.	Cation	Ligand	Specific conductivity $ohm^{-1}cm^{-1}$	Concentration, [g/ml]	
				Conductometricaly	Atomic absorbtion
1	Zn^{2+}	I	0.85	0.2851	0.30
2	Zn^{2+}	II	6.38	2.1400	2.000
3	Cd^{2+}	I	0.62	1.0420	—
4	Cd^{2+}	II	2.35	0.2749	—
5	Hg^{2+}	I	0.31	0.1940	—
6	Hg^{2+}	II	0.58	0.3631	—

T ble 2

Specific Conductivity of Aqueous Solutions of Polyesteruretanes Complexes with Group I Transition Metal Ions for Different Immersion Time

No.	Cation	Ligand	Immersion time, [h]				
			4	8	12	14	16
1	Zn^{2+}	I	0.73	0.73	0.76	0.78	0.82
2	Zn^{2+}	II	3.72	3.90	4.05	4.43	6.30
3	Cd^{2+}	I	0.57	0.57	0.57	0.58	0.58
4	Cd^{2+}	II	2.20	2.20	2.23	2.30	2.30
5	Hg^{2+}	I	0.178	0.130	0.210	0.250	0.286
6	Hg^{2+}	II	0.330	0.340	0.570	0.410	1.580

Transfer of the ions in solution versus immersion time is represented in Fig. 1.

At it comes ont from Fig. 1 and Tables 1 and 2, the polyesteruretanes (I) that contain only a methylenic group between the aromatic rings of the starting isocyanates, retain a smaller quantity of metal, which is heavily liberate. This fact allows to consider that the strength of the metal—macromolecular ligand bound is higher in the case of polyesteruretane (I) than that in (II) ; except for cadmium ions, that give with polyesteruretanes (I) and (II) the bounds of comparable strength.

d) *Action of the Calorific Effect*

In order to study the modifications occuring in heated polyesteruretanes versus temperature, a microscope type Boetius with heating plate has been used. Determinations were carried out under a heating rate of 4°C/min. We could see in detail the modifications that took place as well as modifications of the investigated samples in comparison with the reference polyesteruretanes.

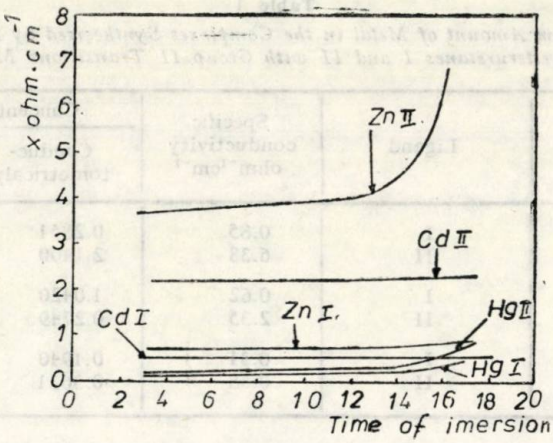

Fig. 1

Fig. 1. — Transfer of the ions in solution vs. immersion time.

α) *Polyesteruretane (I) modified with* Zn^{2+} *Ions.* In the range of temperature from 25° to 138°C there are not seen important modifications as regards the aspect of sample. At 138°C the image is indistinct accompanied also by volatile products release. At 185°C, the thin layer becomes yellow and the image is clearly. After this temperature, the sample becomes easily dark in colour. At 298°C, the image becomes brick-coloured and at 315°C it becomes to grow dim. No details can be seen after 328°C.

β) *Polyesteruretane (II) modified with* Zn^{2+} *Ions.* The behaviour at heating is similarly to that of previous sample. At the begining, the complex is light-brown. In the range of temperature from 25° to 145°C there are not seen modifications as regards the aspect of sample. At 152°C, the image becomes light in colour to orange, phenomenon that indicates a softennly process. After 185°C, the image becomes dark in colour and at 285°C it becomes again light in colour as if the sample has a second softennly internal. At 298°C the image becomes brick-coloured. After 336°C no detail can be seen.

γ) *Polyesteruretane (I) Modified with* Cd^{2+} *Ions.* The obtained complex is light yellow. There is not possible to see the crystalls of dispersed salt in mass of sample. In the range of temperature from 25° to 95°C there are not seen essential modifications, but at 95°C a release of volatile products takes place. At 142°C, the image becomes dark in colour ; in the range of 195°...215°C the sample is hightening again, a typical behaviour for a softennly internal. After this temperature, up to 322°C, the image becomes dark in colour again and details cannot be seen.

δ) *Polyesteruretane (II) modified with* Cd^{2+} *Ions.* The obtained complex is light yellow. In the temperature range of 132°...152° C the image becomes light transparent and is yellow ; that is a typical behaviour for a softennly internal. At 210°C, the image becomes troubled and dark in colour to brown again. In the range of 218°...248°C the image becomes light in colour, fact that points out the second internal of steeping. At 263°C, the image becomes to grow dim to dark brown, while at 304°C no details can be seen.

ε) *Polyesteruretane (I) modified with Hg^{2+} Ions.* The complex obtained is green-yellow. At 110°C the image becomes light in colour while at 138°C the image becomes to trouble simultaneously with the volatile products release. In the range of 144°...161°C the image becomes light again and the sample melts. In the range 181°...203°C the image becomes brown in colour and the second steeping internal cannot he seen. After this temperature, the image becomes dark in colour against temperature increase, while over 327°C the image becomes dark-grey.

ζ) *Polyesteruretane (II) modified with Hg^{2+} Ions.* The obtained complex is dark-yellow. At 115°C the found becomes easily dark in colour, the image becomes to grow dim accompanied by a release of volatile products. At 123°C the image becomes light yellow. In the range of 140°...148°C the sample melts. In the temperature range of 168°...216°C the image becomes dark in colour to orange again. The second steeping internal may be observed between 216° and 228°C, when the image becomes light again, the sample seems like a thin layer. Over 258°C, the image becomes to grow dim while at 330°C no details can be seen.

3. Conclusions

The obtained compounds by interaction of polyesteruretanes (I) and (II) with the Zn^{2+}, Cd^{2+} and Hg^{2+} ions provide a great stability in aqueous medium under usual conditions, but at refluxation temperature for long time, their hydrolises is almost complete.

The group II transition metal ions in polyesteruretanes transmit not only colour modification of these products but also other properties such as: melting point, thermal stability, chemical stability and viscosity.

Received, July 6, 1981

Polytechnic Institute, Jassy,
Department of Inorganic and Analytical Chemistry

REFERENCES

1. Străjescu N., Teodor F., *Elemente de chimie bioanorganică.* Ed. Dacia. Cluj-Napoca 1979, 384.
2. Roman L., Bârzu O., *Implicațiile biomedicale ale combinațiilor complexe.* Ed. Dacia, Cluj-Napoca, 1979, 52.
3. Lewis I., Wilkinson R. G., *Modern Coordination Chemistry.* Intersci. Publ., New-York, 1960.
4. Spacu P., Brezeanu M., *Chimia combinațiilor complexe.* EDP. Buc., 1970.
5. Roșca I., Palamaru M., Bul. Inst. polit., Iași, **XXV (XXIX)**, *1—4*, s. VII, 13 (1979).
6. Roșca I., Palamaru M., Bul. Inst. polit., Iași, **XXVI (XXX)**, *1—4*, s. VII, 19 (1980).
7. Roșca I., Palamaru M., Bul. Inst. polit., Iași, **XXVII (XXXI)**, *1—4*, s. VII, (1981).
8. Roșca I., Palamaru M., Temciuc M., Bul. Inst. polit. Iași, **XXVIII (XXXII)**, *1—4*, s. II (1981).
9. Doboș D., *Electrochemical Data.* Academiai Kiado, Budapest, 1979.
10. Price W. J., *Analytica Atomic Absorbtion Spectroscopy.* London, 1974.

INTERACŢIUNEA POLIURETANILOR CU IONII METALELOR TRANZIŢIONALE

IV. Stabilitatea în mediu apos şi acţiunea efectului caloric asupra poliesteruretanilor interacţionaţi cu ionii grupei a II-a secundare

(Rezumat)

Continuînd studiile anterioare se prezintă rezultatele obţinute privind stabilitatea în mediu apos şi acţiunea efectului caloric asupra poliesteruretanilor modificaţi cu ionii de zinc, cadmiu şi mercur. Acest studiu răspunde necesităţilor practice de a cunoaşte comportarea poliesteruretanilor modificaţi chimic, în mediu apos, mediu în care se găsesc ionii metalelor tranziţionale. Din rezultatele obţinute rezultă tăria legăturii metal—ligand şi capacitatea de complexare a poliesteruretanilor, diferită, în funcţie de natura cationului. Din datele experimentale rezultă participarea catalitică a ionilor metalelor din grupa II-a secundară la destrucţia termică a poliesteruretanilor.

BULETINUL INSTITUTULUI POLITEHNIC DIN IAŞI
Tomul XXIX (XXXIII), Fasc. 1—4, 1983
Secţia II
CHIMIE şi INGINERIE CHIMICĂ

C.D. 541.57

COPRECIPITATION OF SOME METALLIC CHELATES ON INDIFFERENT ORGANIC COLLECTORS

BY

AL. NACU, DIDINA NACU and DOINA BÎLBĂ

1. Introduction

Of real interest for concentration and separation of some trace elements is the type of metallic chelates coprecipitation, using as coprecipitation agents indifferent organic collectors [1]...[5]. Mechanism of the metallic chelates coprecipitation on indifferent collectors is not well enough elucidated. According to some authors [3] the coprecipitation processes should be similar with the extraction processes of chelate complexes, except that in the case of coprecipitation one can be talking about an „extraction in solid phase". For this reason we expect that the factors which influence the metallic chelates extraction to be the same in their coprecipitation.

Starting with this assumption, we investigated the coprecipitation of some metallic chelates formed by interaction of Pd(II), Co(II) and Mo(VI) ions with *p*-phenetidide of thioglycolic acid, $H_5C_2O-C_6H_4-NH-CO-CH_2-SH$ (R_1), *p*-phenetidide of 1-mercaptopropionic acid, $H_5C_2O-C_6H_4-NH-CO-CH(CH_3)-SH$ (R_2) and *p*-phenetidide of 2-mercaptopropionic acid, $H_5C_2O-C_6H_4-NH-CO-CH_2-CH_2-SH$ (R_3). These metallic chelates have been studied in detail by the authors and employed for photometrical determination by extraction of the above mentioned elements [6]...[9].

2. Experimental

The coprecipitation technique on indifferent organic collectors of metallic chelates is relatively simple : to solution of the investigated element is added the chelating agent and the pH is adjusted corresponding to chelate formation. In this step, usually, chelate formation is not observed because concentration of the components in solution is below the limit of needed value. After this, the solution of indifferent collector with different concentration is added under stirring. The collector precipitate together with solution is maintained in contact for one to 12 hours, then is filtered, washed, dried and calcinated to complete mineralization, followed by trace element analysis.

In our experiment, there were employed solutions of chlorides and sulphates and in the case of Mo(VI), ammoniumparamolibdate. Metal concentration in the initial solution ranged between 1...10 μg/100 ml. Chelating reagents have been synthesized by previous described method [6]. Their solutions in ethylic alcohol or methylic alcohol had the initial concentration equal to 10^{-3} M. Solutions of phenolphtalein and 2-naphtol 5%

in alcohols have been employed as collectors. The formed precipitate was filtered on white band filter paper and after combustion was dissolved with 1 : 2 hydrochloric acid solution, determining the trace element by spectrophotometrical method or by atomic absorption spectroscopy.

In order to find the optimal conditions of coprecipitation, a series of factors have been studied, namely : type and concentration of collector, nature and concentration of chelating agent, coprecipitation time, pH and coprecipitation in the presence of the other elements.

2.1. Influence of Collector and Chelating Agent

The data summarized in the Table 1 show that the coprecipitation yield does not depend on nature of employed collector, but it depends on the nature of chelating agent.

Table 1

Data as Regards the Coprecipitation against the Nature of Chelating Agent and Collector

No.	Added chelating agent, 2 mg/100 ml	Coprecipitation yield, [%]					
		Pd(II)		Co(II)		Mo(VI)	
		F	N	F	N	F	N
1	*p*-Phenetidide of thioglycolic acid	93.2	94.5	76.7	74.4	93.5	91.6
2	*p*-Phenetidide of 1-mercapto-propionic acid	98.2	91.8	47.0	46.2	88.8	83.6
3	*p*-Phenetidide of 2-mercapto-propionic acid	53.2	49.8	98.5	95.8	48.7	47.5

F — Phenolphtalein 1.5 g ; N — 2-Naphtol 1.5 g

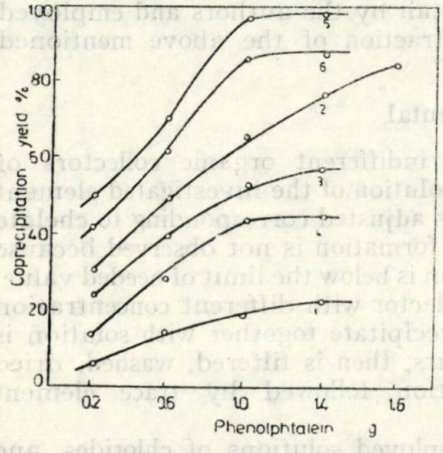

Fig. 1. — Coprecipitation of Pd(II), Co(II) and Mo(VI) chelates against the concentration of chelating agent (R_2) and indifferent collector (F) : *1* — Co : R_2= 1 : 10 ; *2* — Pd : R_2= 1 : 10 ; *3*— Mo : R_2 = 1 : 10 ; *4* — Co : R_2= 1 : 100 ; *5* — Pd : R_2= 1 : 100 ; *6* — Mo : R_2 = 1 : 100.

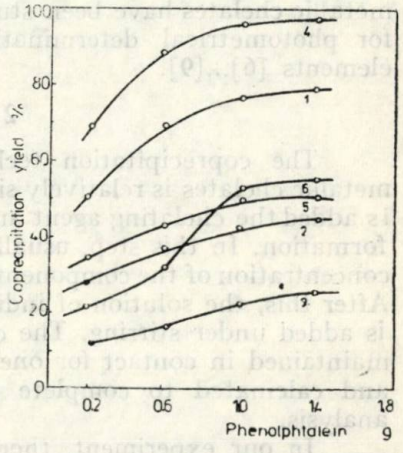

Fig. 2. — Coprecipitation of Pd(II), Co(II) and Mo (VI) chelates against the concentration of chelating agent (R_3) and collector (F) : *1* — Co : R_3 = 1 : 10 ; *2*—Pd : R_3= 1 : 10 ; *3*—Mo : R_3 = 1 : 10 ; *4*—Co : R_3= 1 : 100 ; *5*—Pd : R_3= 1 : 100; *6* — Mo : R_3= 1 : 100.

p-Phenetidide of 1-mercaptopropionic acid favours maximal coprecipitation of the Pd(II) and Mo(VI) ions, while *p*-phenetidide of 2-mercaptopropionic acid favours coprecipitation of the Co(II) ions. Increase of the complexante concentration favours coprecipitation (Figs. 1 and 2). Also, it can be seen a maximal coprecipitation for amounts of collectors ranging between 1...1.5 g.

2.2. Influence of Coprecipitation Time

The data listed in Table 2 show that the optimal coprecipitation time is about 4...5 hours, depending on the employed chelate.

Table 2

Data as Regards the Coprecipitation Yield versus Time

No.	Time h	Coprecipitation yield, [%]		
		$Pd-R_2$	$Co-R_3$	$Mo-R_2$
1	1.0	66.2	75.5	65.8
2	2.0	80.2	86.6	79.8
3	3.0	93.7	92.4	91.0
4	4.0	98.7	97.4	92.2
5	5.0	98.2	98.6	94.3
6	6.0	98.4	98.3	94.4
7	7.0	98.3	98.7	94.7
8	12.0	98.6	98.4	95.1

2.3. Influence of pH

As it comes out from the data summarized in Table 3, optimal coprecipitation values of pH depends on the nature of chelating agent and metal. Thus, chelate of Pd(II) coprecipitates well in the strong acid medium, that of Mo(VI) in weak acid medium and that of Co(II) in weak alkaline medium.

If percentage of metallic chelates coprecipitation is compared with the percentage extraction of the same chelates against pH, a close corel-

Table 3

Coprecipitation Yield at Different pH using Phenolphtalein as Collector

No.	Metallic chelate	pH						
		0.0	1.0	3.5	5.5	7.0	9.0	10.0
1	$Pd-R_2$	97.3	98.1	97.6	83.6	12.0	8.3	2.8
2	$Co-R_2$	—	—	1.3	21.4	35.2	46.6	47.4
3	$Mo-R_2$	61.7	94.2	92.3	62.4	5.3	—	—
4	$Co-R_3$	—	—	3.2	52.7	85.5	91.0	98.5

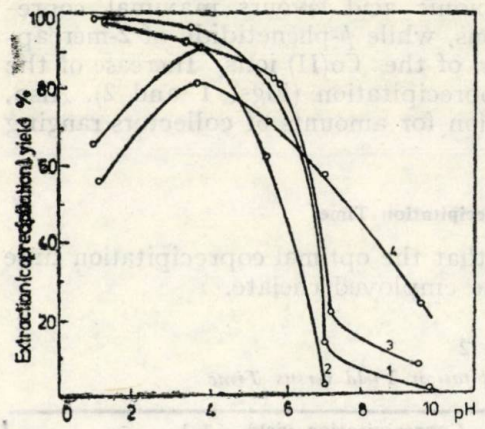

Fig. 3. — Influence of the pH on the coprecipitation and extraction of the Pd(II) and Mo(VI) chelates. Coprecipitation: *1* — Pd— $-R_2$; *2* — Mo— R_2; collector — F; extraction: *3* — Pd— R_2 in chloroform; *4* — Mo— R_2 in mixture of isoamylic alcohol — benzene

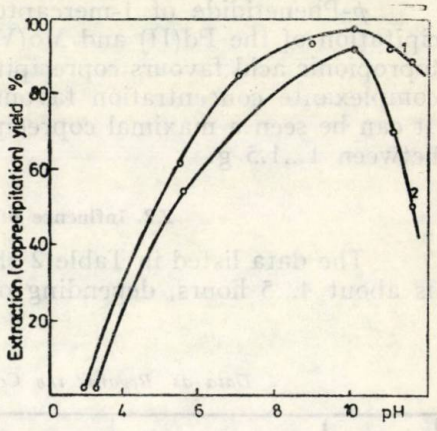

Fig. 4. — Coprecipitation and extraction of Co(II) chelate versus pH: *1* — coprecipitation Co— R_3, collector — F; *2* — extraction Co— R_3 in chloroform.

ation will be seen, optimal domain of extraction is the same with optimal domain of coprecipitation (Figs. 3 and 4).

There is a close correlation between the values of molar absorption coefficients of metallic chelates and coprecipitation yield, as the data from Table 4 show.

Table 4

Values of the Extraction Yield, Coprecipitation Yield and Molar Absorption Coefficients for Some Metallic Chelates

No.	Metallic chelate	ε_{max}	Yield, [%]	
			Extraction	Coprecipitation
1	Pd— R_2	15 120	92.5	98.3
2	Co— R_2	7 920	42.3	47.8
3	Pd— R_3	6 290	53.7	52.6
4	Co— R_3	19 700	96.2	98.8

Coprecipitation yield increases as the molar absorption coefficient increases for certain complex, but this fact cannot be generalized without investigation of the other group of metallic chelates.

2.4. Coprecipitation of Pd(II), Co(II) and Mo(VI) in the Presence of Other Elements

Coprecipitation of metallic chelates on indifferent organic collectors has been investigated also in the presence of other elements, which usually accompany them and whose separation is difficult. For this reason the copre-

cipitation of Pd(II) in the presence of platinum metals, the coprecipitation of Mo(VI) in the presence of wolfram and coprecipitation of Co(II) in the presence of nickel have been studied. The experiments have been carried out under the conditions found for complet coprecipitation of Pd(II), Co(II) and Mo(VI). The obtained results are summarized in Table 5.

Table 5

Data as Regard the Separation of Pd(II), Mo(VI) and Co(II) from some Interferent Elements using Coprecipitation Procedure: Collector — F; Chelating Agent R_1 and R_2 for Pd and Mo and R_3 for Co

No.	Ground element	Interfering element	Elements ratio	
			Initial	After coprecipitation
1	Pd(II)	Pt(II), Rh(III), Ir(III)	$1 : 10^7$	$1 : 10^2$
2	Mo(VI)	W(VI)	$1 : 10^7$	$1 : 10$
3	Co(II)	Ni(II)	$1 : 10^6$	$1 : 10^3$

The data in Table 5 show a good separation of Pd(II) and Pt(II) Ir(III), Rh(III), of Mo(VI) and W(VI) and less satisfactory separation of Co(II) and Ni(II).

3. Conclusions

1. Coprecipitation of some metallic chelates formed by interaction of Pd(II), Co(II) and Mo(VI) ions with *p*-phenetidide of thioglycolic acid and of 1- and 2-mercaptopropionic acid depends on the nature and excess of reagent employed, amount of collector, pH and coprecipitation time.

2. The parameters that influence the metallic chelates extraction, do in the same measure over their coprecipitation. There is also a correlation between values of absorption molar coefficients and coprecipitation yield.

3. Using the procedure of chelate complexes coprecipitation on indifferent organic collectors, the concentration and separation of trace elements in the presence of interfering elements can be made. Thus separation of Pd(II) can be performed quantitatively in the presence of Pt(II), Rh(III) and Ir(III) and Mo(VI) in the presence of W(VI)

Received, December 3, 1981

Polytechnic Institute, Jassy,
Department of Inorganic and Analytical Chemistry

REFERENCES

1. Mitchell R. L., Scott R. O., J. Soc. Chem. Ind., **66**, 330 (1974).
2. Кузнецов В. И., ЖАХ, **9**, 199 (1954).
3. Pickett E. E., Hankins B. E., Analyt. Chem., **30**, 47 (1958).
4. Herbest V. W., Schipman W. H., Analyt. Chem., **34**, *8*, 1010 (1962).
5. Кузнецов В. И., Маругин В. А., Зав. лаб., **1**, 1297 (1970).
6. Бусев А. И., Наку А., Рудзит Г. П., ЖАХ, **19**, *4*, 475 (1964).

7. Nacu Al., Nacu D., An. şt. Univ. „Al. I. Cuza", Iaşi, s. I, 18, 25 (1968).
8. Бусев А. И., Наку А., ЖАХ, 18, *12*, 1479 (1963).
9. Nacu Al., Nacu D., An. şt., Univ. „Al. I. Cuza", Iaşi, s. I, 13, 29 (1967).

COPRECIPITAREA UNOR CHELAŢI METALICI PE COLECTORI ORGANICI INDIFERENŢI

(Rezumat)

Se cercetează coprecipitarea unor chelaţi metalici formaţi prin interacţiunea ionilor de Pd(II), Co(II), Mo(VI) cu *p*-fenetidida acizilor tioglicolic, 1-mercaptopropionic şi 2-mercaptopropionic, în vederea concentrării şi separării urmelor de elemente, pe colectori organici indiferenţi (fenolftaleina şi β-naftolul).

Sînt studiaţi o serie de factori care pot influenţa randamentul coprecipitării: pH-ul mediului, natura şi concentraţia reactivilor timpul de coprecipitare etc. Se constată că există analogie între factorii ce influenţează extracţia chelaţilor şi coprecipitarea lor.

Pe baza rezultatelor obţinute s-au găsit condiţiile optime de separare prin coprecipitare a paladiului de alte elemente platinice şi a molibdenului de wolfram şi alte elemente.

BULETINUL INSTITUTULUI POLITEHNIC DIN IAŞI
Tomul XXIX (XXXIII), Fasc. 1—4, 1983
Secţia II
CHIMIE şi INGINERIE CHIMICĂ

C.D. 536.423.15

ÉQUATION POUR LA COURBE DE LA PRESSION DE VAPEUR POUR LES LIQUIDES PURS

PAR

N. AELENEI, ANA TARHON, GH. IONESCU, OVIDIU ROMAN et M. ŞCHIOPU

1. Introduction

Les données expérimentales concernant l'équilibre liquide—vapeur constituent les données de base pour la résolution d'innombrables problèmes scientifiques et techniques liés à l'utilisation des liquides purs ou des solutions liquides. De telles données sont nécessaires, en particulier, pour le calcul des procédés technologiques et le calcul des installations de séparation par rectification des composants d'une solution. Comme élément essentiel nécessaire à la résolution des problèmes ci-dessus, on peut citer la recherche de l'équilibre liquide—vapeur dans les substances pures. De tels équilibres de phase sont rigoureusement exprimés par l'équation différentielle de Clapeyron, mais les solutions intégrales de celle-ci ont un caractère approximatif.

En littérature sont publiées plusieurs équations empiriques ou semi-empiriques pour décrire l'indépendance entre la pression de vapeur et la température [1]...[14]. Plusieurs d'entre elles sont discutées comparativement dans différents manuels [16]...[21].

Dans ce qui suit on démontre l'utilité de l'évaluation d'une fonction „résiduelle" de type exponentiel, pour améliorer la concordance de la relation $p = p(T)$ avec les données expérimenteles et en même temps pour que cette relation contienne un nombre minimum de constantes individuelles. Ce choix permet à exprimer la pression de vapeur par une relation unique valable pour tout le domaine d'existence de la phase liquide.

2. Considérations théoriques

La relation thermodynamique rigoureuse pour l'équilibre liquide—vapeur dans un système à une seule composante est donnée par l'équation différentielle de Clapeyron :

$$\frac{dp}{dT} = \frac{\Delta H_v}{T[V_m^{(g)} - V_m^{(l)}]}, \tag{1}$$

dans laquelle : $\Delta H_v = H_m^{(g)} - H_m^{(l)}$ représente la chaleur latente de vaporisation, tandis que $V_m^{(g)}$ et $V_m^{(l)}$ sont les volumes molaires de vapeur et de liquide, à la température T. Les volumes molaires peuvent être remplacés par les facteurs de compressibilité correspondants :

$$Z^{(g)} = \frac{pV_m^{(g)}}{RT}, \tag{2}$$

$$Z^{(l)} = \frac{pV_m^{(l)}}{RT}. \tag{3}$$

On peut calculer les facteurs de compressibilité en fonction de la température si on connaît les densités des phases coexistentes le long de la courbe d'équilibre en tenant compte des équations (2) et (3). L'équation (1) peut être écrite sous la forme :

$$-\frac{\mathrm{d}\ln p}{\mathrm{d}(1/T)}=\frac{\Delta H_v}{R\Delta Z}, \tag{4}$$

où $\Delta Z=Z^{(g)}-Z^{(l)}$.

Des données expérimentales concernant la pression des vapeurs en fonction de la température on peut approximer la dérivée $\mathrm{d}(\ln p)/\mathrm{d}(1/T)$ par le rapport des croissances finies :

$$Y=-\frac{\Delta \ln p}{\Delta(1/T)}, \tag{5}$$

valable pour la température moyenne $T_m=-\Delta(\ln T)/\Delta(1/T)$. Dans le domaine de l'existence de la phase liquide, Y varie avec T_m selon une courbe ayant un minimum, illustrée dans la Fig. 1 pour le benzène et l'eau sur la base des données fournies par [22]. Dans ce diagramme, en abscisse on a

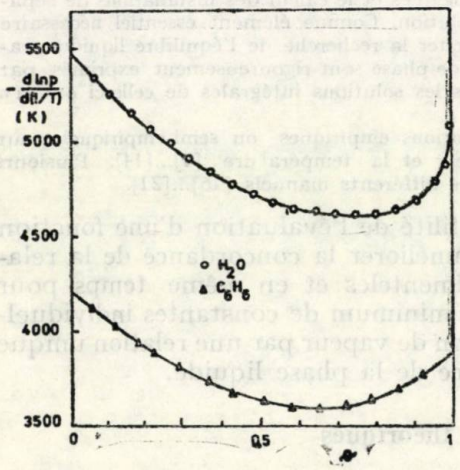

Fig. 1

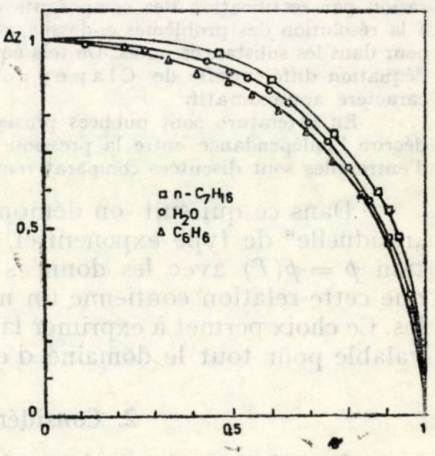

Fig. 2

introduit, à la place de la température, le paramètre adimensionnel θ, qui norme à l'unité l'intervalle de température dans lequel existe la phase liquide :

$$\theta=\frac{T-T_0}{T_c-T_0}, \tag{6}$$

où T_0 est la température du point triple, tandis que T_c est la température du point critique. Dans le même domaine de température, ΔZ décroît de la valeur 1, correspondante au point triple, à la valeur zéro, correspondante au point critique. Dans la Fig. 2 est représentée la variation de ΔZ avec θ

pour l'eau, le benzène et l'heptane, évaluée à partir des densités des phases coexistentes fournies par la littérature [22]. Dans ces coordonnées adimensionnelles les courbes de la Fig. 2 s'approchent d'un arc de cercle.

Au voisinage du point triple, la fonction Y croît avec la température, cependant, dans le même domaine, ΔZ décroît beaucoup plus rapidement avec la température de façon que ΔH_v doit décroître sur tout l'intervalle de température.

L'équation (4) ne peut pas être intégrée rigoureusement, vus que aussi bien ΔZ que ΔH_v sont des fonctions compliquées de température. Une intégration approximative peut être effectuée pour des températures au voisinage du point triple, quand $\Delta Z \to 1$, tandis que ΔH_v peut être considérée comme une fonction linéaire de température :

$$\Delta H_v = a + bT. \tag{7}$$

Par intégration on obtient :

$$\ln p = -\frac{A}{T} + C \ln T + B. \tag{8}$$

L'équation (8) devrait être strictement valable seulement à la température du point triple. Pour n'importe quelle autre température comprise entre la température du point triple et celle du point critique, l'équation de la pression de vapeur pourrait être écrite sous la forme :

$$\ln p = -\frac{A}{T} + C \ln T + B + \psi, \tag{9}$$

où ψ est une fonction de correction qui peut être déterminée en se basant sur des données expérimentales sur tout le domaine de température de l'existence de la phase liquide :

$$\psi = \ln p_{exp} - (-A/T + B + C \ln T). \tag{10}$$

De l'analyse des données expérimentales pour plusieurs systèmes, nous avons abouti à la conclusion que la fonction résiduelle est décrite de façon satisfaisante par une équation de la forme :

$$\psi = m(T - T_0)^n, \tag{11}$$

T_0 étant la température du point triple.

Des données expérimentales on peut calculer la fonction :

$$Y = -\frac{\Delta \ln p}{\Delta(1/T)} = A - C\frac{\Delta \ln T}{\Delta(1/T)} - \frac{\Delta\psi}{\Delta(1/T)}. \tag{12}$$

Aux températures approchées de T_0, quand $\Delta\psi \to 0$, et $\Delta\psi/\Delta(1/T) \to 0$, de ces données on peut obtenir les valeurs des constantes A, B et C et la fonction ψ de l'équation (10). Si l'équation (11) représente une bonne approximation pour ψ, alors la relation (9) offre une solution pour l'équation (1).

Pour des motifs d'ordre théorique, la pression de vapeur de l'eau a été bien étudiée, par voie expérimentale et technique, les données expérimentales qui se trouvent dans la littérature étant probablement les plus sûres.

3. L'interprétation des données expérimentales

Dans le but de vérifier les équations (9) et (10) on utilise les données expérimentales relatives à la pression de vapeur de l'eau [22]. Dans ce but, l'équation (12) s'écrit sous la forme :

$$Y=-\frac{\Delta \ln p}{\Delta(1/T)}=A+CT_0+C(T_m-T_0)-\frac{\Delta\psi}{\Delta(1/T)}, \tag{13}$$

où :

$$T_m=-\frac{\Delta \ln T}{\Delta(1/T)}=\frac{2T_1T_2}{T_1+T_2}. \tag{14}$$

Cette expression pour T_m est obtenue en tenant compte du fait que $\Delta \ln T=\ln(T_2/T_1)$, tandis que du développement en série du therme logarithmique on retient seulement le premier therme. L'équation (13) peut s'écrire pour le point triple, quand $\Delta\psi/\Delta(1/T)=0$, sous la forme :

$$Y=A+CT_0+C(T_m-T_0). \tag{15}$$

On peut supposer que pour T_m-T_0 relativement petit, Y devient :

$$Y=a_0+a_1(T_m-T_0)+a_2(T_m-T_0)^2+a_3(T_m-T_0)^3. \tag{16}$$

En utilisant pour la pression de vapeur les données expérimentales jusqu'à la température de 100°C, inscrites dans la troisième colonne du tableau 1, on calcule les coefficients a_i de l'équation (16) par la méthode des moindres carrés ; on obtient :

$$a_0=5\,422{,}112483, \qquad a_1=-5{,}179333619,$$
$$a_2=8{,}2320026\cdot10^{-3}, \qquad a_3=-1{,}66162\cdot10^{-5}.$$

En comparant l'équation (15) avec (16) il résulte que :

$$C=a_1=-5{,}179333619, \quad A=a_0-273{,}15\,C=6\,836{,}8645.$$

Tableau 1

t °C	T °K	p Torr	$Y=-\frac{\Delta \ln p}{\Delta(1/T)}$	$T_m=-\frac{\Delta \ln T}{\Delta(1/T)}$	T_m-T_0	Y'
0	273,15	4,581	—	—	—	55,6078132
10	283,15	9,204	5 396,342173	278,0900796	4,9400796	55,6077661
20	293,15	17,53	5 347,836256	288,0921574	14,9421574	55,6080131
30	303,15	31,81	5 295,376107	298,0940949	24,9440949	55,6086122
40	313,15	55,32	5 253,066334	308,0959064	34,945906	55,6096218
50	323,15	92,52	5 204,331323	318,096156	44,9476156	55,6111000
60	333,15	149,4	5 158,24925	328,0992017	54,9492020	55,6131051
70	343,15	233,7	5 115,586407	338,1007083	64,950708	55,6156952
80	353,15	355,2	5 073,256348	348,1021185	74,95119	
90	363,15	525,9	5 032,775297	358,1034631	84,953463	
100	373,15	760,0	4 989,556492	368,1047301	94,954730	

Pour déterminer la constante B on calcule d'abord la fonction :

$$Y' = \ln p + \frac{6\,836{,}8645}{T} + 5{,}179333619 \ln T, \tag{17}$$

de sorte que :

$$B = \lim_{T \to 273{,}15°K} Y'.$$

Aux températures approchées de $T_0 = 273{,}15°K$, Y' peut être approximé par un polynôme en $T_m - T_0$:

$$Y' = b_0 + b_1(T_m - T_0) + b_2(T_m - T_0)^2 + b_3(T_m - T_0)^3 \tag{18}$$

et donc $B = b_0$.

Les coefficients b_i sont déterminés par la méthode des moindres carrés avec les données du tableau 1, colonnes 6 et 7, jusqu'la à température de 70°C. On obtient :

$$b_0 = 55{,}60781321, \qquad b_1 = -1{,}746838 \cdot 10^{-5},$$
$$b_2 = 1{,}1790429 \cdot 10^{-6}, \qquad b_3 = 9{,}7011691 \cdot 10^{-9}.$$

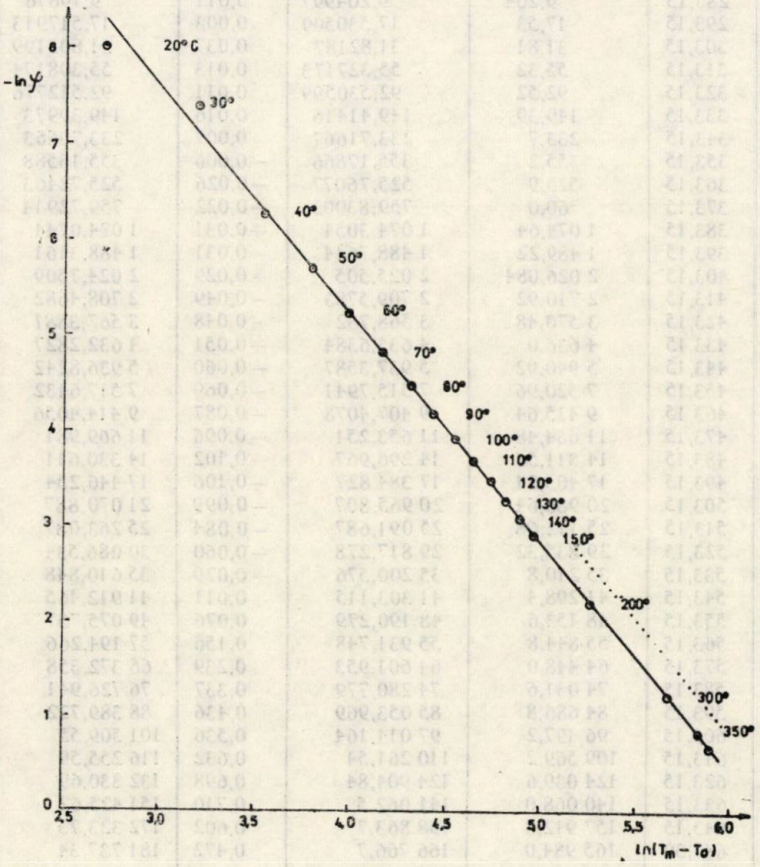

Fig. 3

On obtient donc :

$$B = 55{,}6078132.$$

Avec les valeurs des constantes A, B et C ci-dessus la fonction de correction va s'écrire :

$$(19) \qquad \psi = \ln p_{exp} + \frac{6\,836{,}8645}{T} + 5{,}179333619 \ln T - 55{,}6078132.$$

À l'aide de la rélation (19) on calcule les valeurs de ψ pour tout le domaine d'existence de l'eau liquide. Si la relation (11) est valable en coordonnées $\ln \psi$ et $\ln(T - T_0)$, on doit obtenir une droite, conformément à l'équation :

Tableau 2

t °C	T °K	p, [1] Torr	p, Eq. (21) Torr	$100\,\delta_p$	p, Eq. (22) Torr	$100\,\delta_p$
0	273,15	4,581	4,581082	0,002	4,576554	−0,097
10	283,15	9,204	9,204997	0,011	9,19676	−0,079
20	293,15	17,53	17,530509	0,003	17,517913	−0,069
30	303,15	31,81	31,82187	0,037	31,805199	−0,015
40	313,15	55,32	55,327173	0,013	55,308174	−0,021
50	323,15	92,52	92,530599	0,011	92,512776	−0,008
60	333,15	149,39	149,41416	0,016	149,39973	0,007
70	343,15	233,7	233,71667	0,007	233,70663	0,003
80	353,15	355,2	355,17866	−0,006	355,16588	−0,010
90	363,15	525,9	525,76077	−0,026	525,72463	−0,033
100	373,15	760,0	759,83002	−0,022	759,72914	−0,036
110	383,15	1 074,64	1 074,3054	−0,031	1 074,0744	−0,053
120	393,15	1 489,22	1 488,7644	−0,031	1 488,3161	−0,061
130	403,15	2 026,084	2 025,505	−0,029	2 024,7509	−0,066
140	413,15	2 710,92	2 709,5783	−0,049	2 708,4682	−0,090
150	423,15	3 570,48	3 568,782	−0,048	3 567,3881	−0,087
160	433,15	4 636,0	4 633,6384	−0,051	4 632,2827	−0,080
170	443,15	5 940,92	5 937,3587	−0,060	5 936,8242	−0,069
180	453,15	7 520,96	7 515,7941	−0,069	7 517,6432	−0,044
190	463,15	9 415,64	9 407,4078	−0,087	9 414,4056	0,013
200	473,15	11 664,48	11 653,251	−0,096	11 669,981	0,047
210	483,15	14 311,56	14 296,967	−0,102	14 330,611	0,133
220	493,15	17 403,24	17 384,827	−0,106	17 446,254	0,247
230	503,15	20 986,64	20 965,807	−0,099	21 070,887	0,401
240	513,15	25 112,68	25 091,687	−0,084	25 263,087	0,599
250	523,15	29 835,32	29 817,278	−0,060	30 086,534	0,842
260	533,15	35 210,8	35 200,576	−0,029	35 610,848	1,136
270	543,15	41 298,4	41 303,115	0,011	41 912,465	1,487
280	553,15	48 153,6	48 190,279	0,076	49 075,757	1,915
290	563,15	55 844,8	55 931,748	0,156	57 194,266	2,416
300	573,15	64 448,0	64 601,953	0,239	66 372,358	2,986
310	583,15	74 031,6	74 280,779	0,337	76 726,941	3,641
320	593,15	84 686,8	85 053,969	0,436	88 389,722	4,372
330	603,15	96 497,2	97 014,164	0,536	101 509,55	5,194
340	613,15	109 569,2	110 261,54	0,632	116 255,59	6,102
350	623,15	124 039,6	124 904,84	0,698	132 830,69	7,079
360	633,15	140 068,0	141 062,5	0,710	151 425,62	8,109
370	643,15	157 912,8	158 863,7	0,602	172 323,73	9,126
374,1	647,30	165 984,0	166 766,7	0,472	181 737,34	9,491

$$\ln \psi = \ln m + n \ln (T - 273{,}15). \tag{20}$$

De la Fig. 3 on observe que la linéarité de cette courbe est satisfaisante dans l'intervalle 50°...350°C. On peut calculer les coefficients m et n à l'aide de la méthode des moindres carrés, en excluant les valeurs approchées du point triple et celles approchées du point critique où les erreurs expérimentalles pour p sont plus grandes. En utilisant les valeurs de ψ dans l'intervalle de température 50°...350°C, on obtient :

$$m = 2{,}157896 \cdot 10^{-7}, \quad n = 2{,}474878.$$

Avec ces valeurs, l'équation des pressions de vapeur pour l'eau devient :

$$\ln p = -\frac{6\,836{,}8645}{T} + 55{,}6078132 - 5{,}179333619 \ln T + \\ + 2{,}157896 \cdot 10^{-7} (T - 273{,}15)^{2{,}474878}. \tag{21}$$

Les valeurs de la pression de vapeur calculées avec l'équation (21) sont inscrites dans la tableau 2, colonne 4. Les erreurs relatives (en pourcents par rapport aux valeurs de la littérature) sont inscrites dans la colonne 5.

Pour comparaison on considère l'équation de K e y e s [8], valable dans l'intervalle 273°...423°K :

$$\lg p = -\frac{2\,892{,}3693}{T} + 19{,}3011421 - 2{,}892736 \lg T - 4{,}9369728 \cdot 10^{-3} T + \\ + 5{,}606905 \cdot 10^{-6} T^2 - 4{,}645869 \cdot 10^{-9} T^3 + 3{,}7874 \cdot 10^{-12} T^4. \tag{22}$$

Les valeurs de la pression de vapeur calculées avec l'équation K e y e s sont inscrites dans la colonne 6 du tableau 2.

4. Conclusions

À partir des simplifications effectuées à l'intégration de l'équation de C l a p e y r o n, la solution de l'intégrale représentée par l'équation (8) est valable seulement aux températures basses mais d'une façon rigoureuse pour le point triple. De l'analyse des résultats obtenus avec l'équation (22) résulte que pour l'extention de l'équation (8) pour les températures élevées, on ne peut pas ajouter les termes de la forme $a_1 T + a_2 T^2 + a_3 T^3 + a_4 T^4$, par exemple, dans l'équation de K e y e s. En effet, la fonction résiduelle ψ, donnée par l'équation (10), reste pratiquement nulle jusqu'à une certaine valeur de la température où elle commence à croître. Une telle fonction ne peut pas être approximée avec un polynôme en T sans changer sensiblement les valeurs des constantes A, B et C, trouvées dans le domaine des basses températures. La fonction résiduelle proposée s'annule au point triple, où l'équation à trois constantes doit être rigoureuseument valable, elle a des valeurs négligeables dans le domaine des basses températures et devient appréciable à des températures élevées. Implicitement cette fonction met en évidence l'effet de la variation non-linéaire de ΔH_v avec la température, la déviation des vapeurs par rapport au comportement idéal et la variation du volume molaire du liquide avec la température, étant peu probable que sa forme puisse expliquer tous les détails concernant la

courbe des vapeurs des liquides purs. Pour cela, la forme de la fonction et la méthode d'évaluation peuvent être considérées comme un élément expérimental capable d'offrir une relation relativement simple et précise sur le domaine entier de température, utile dans l'interprétation des données expérimentales consistentes du point de vue thermodynamique.

Reçue le 14 avril 1980

Institut Polytechnique, Jassy,
Chaire de Chimie Physique

BIBLIOGRAPHIE

1. Frost A. A., Kalkwarf D. R., J. Chem. Phys., **21**, 264 (1963).
2. Van Laar J., *Die Zustandsgleichung*. Leipzig, 1924.
3. Harmin C. E., Thodos G., J. Chem. Phys., **35**, 899 (1961).
4. Planck R., Riedel L., Ing. Arch., **16**, 255 (1948).
5. Michels A., Physica, **17**, 874 (1951).
6. Prausnitz J. M., Chueh P. L., *Computer Calculation for High Pressure Vapor—Liquid Equilibria*. Prentice Hall Englewood Cliffs, New Jersey, 1968.
7. Renon H., Asselineau L., Cohen G., Raimbault C., *Calcul sur ordinateur des Équilibres Liquide—Vapeur et Liquide — Liquide*. Technik., Paris, 1971.
8. Keyes F. G., J. Chem. Phys., **15**, 607 (1947).
9. Reynes G. E., Thodos G., Amer. Inst. Chem. Eng. J., **8**, 357 (1962).
10. Thomson, Chem. Rev., 38, 1 (1946).
11. Calingaert G., Davis S., Ind. Eng. Chem., **17**, 1287 (1925).
12. Kollar G., Proszt J., Z. Phys. Chem., **219**, 47 (1962).
13. Reynes G. E., Thodos G., Ind. Eng. Chem. Fundam., **1**, 127 (1962).
14. Shou J. K., Harmin Ch. E., J. Chem. Eng. Data, **16**, *1*, 37 (1971).
15. Oehley E., Chem.-Ztg., **85**, 913 (1961).
16. Reid R. C., Sherwood T. K., *Properties of Gases and Liquids*. Mc. Graw Hill, New York, 1966.
17. Карапетянц М. Х., Чех Х. Ж., *Температуры кипения и давлении пара углеводородов*. Москва, 1961.
18. Partington J., *An Advanced Treatise on Physical Chemistry*. Longmans & Green, London, 1954.
19. Miller D., Ind. Eng. Chem., **56**, 46 (1964).
20. Gothard F. A., *Echilibre lichid—vapori*. Ed. Acad. R.S.R., Buc., 1975.
21. Sternberg S., Daneş F., *Termodinamică chimică aplicată*. Ed. Acad. R.S.R., Buc., 1978.
22. * * * *Landolt—Börnstein Zahlenwerte und Funktionen aus Physik, Chemie, Astronomie, Geophysik und Technik*. Bd. **II**, part. 2, Springer Verlag, 1960.

ECUAŢIE PENTR U CURBA PRESIUNII DE VAPORI A LICHIDELOR PURE

(Rezumat)

Pentru exprimarea presiunii de vapori a lichidelor pure se propune o ecuaţie de forma

$$\ln p = -A/T + C \ln T + B + m(T - T_0)^n,$$

unde T_0 este temperatura punctului triplu al lichidului. Ultimul termen din această ecuaţie se evaluează din presiunile de vapori experimentale. Ecuaţia poate fi utilizată pentru calcularea presiunii de vapori pe întreg domeniul de existenţă a fazei lichide cu o eroare relativă procentuală sub 1%. Se exemplifică utilizarea ecuaţiei pentru presiunea de vapori a apei.

BULETINUL INSTITUTULUI POLITEHNIC DIN IAŞI
Tomul XXIX (XXXIII), Fasc. 1—4, 1983
Secţia II
CHIMIE şi INGINERIE CHIMICĂ

C.Z. 66.069.85; 678.664

DESPRE PIROLIZA SPUMELOR POLIURETANICE

DE

D. P. LAZĂR

1. Introducere

S-a cercetat piroliza unui lot de opt spume poliuretanice (SPU), în condiţii statice, într-un spaţiu de reacţie insuficient aerat, cu ajutorul unei instalaţii de laborator prezentată în fig. 1.

Probele analizate au fost împărţite în două grupe: E·XX (E·57, E·59, E·62 şi E·63) şi E·XXX (E·956, E·964, E·983 şi E·992), potrivit codului de fabricaţie. Piroliza s-a efectuat în condiţii dinamice de temperatură, între temperatura camerei şi 800°C. Evoluţia în timp a procesului de piroliză a fost urmărită prin analiza gaz cromatografică a gazelor rezultate. S-au formulat unele concluzii privind periclitatea (toxicitatea) gazelor rezultate din piroliză, precum şi pericolele de incendiu şi explozie.

2. Rezultate experimentale

1.1. Descrierea instalaţiei de piroliză (fig. 1)

Piesa principală a instalaţiei este reactorul (*1*), a cărei parte inferioară este confecţionată din cuarţ şi are dimensiunile $L=120$ mm şi $\varnothing=30$ mm; partea superioară a reactorului este confecţionată din sticlă Pyrex, joncţiunea dintre cele două părţi fiind realizată printr-o trecere cuarţ/Pyrex (*2*). Partea superioară a reactorului se termină printr-o joncţiune N.S. 29/32 mm (*3*) care susţine solidar un tub de cuarţ/Pyrex (*4*) închis la partea inferioară şi care serveşte drept locaş pentru sudura caldă (*5*) a termocuplului de cromel—alumel.

Tot în partea superioară a reactorului, imediat sub joncţiunea (*3*), este prevăzută o tubulură laterală pe care este sudat un robinet cu o cale (*6*), ambele servind pentru dirijarea gazelor rezultate din piroliză către barbotorul (*9*). Legătura dintre reactor şi barbotor se realizează prin două legături elastice (*7*) între care se află intercalată o valvă metalică cu septum (*8*), care serveşte pentru luarea probelor de gaze în vederea analizei lor pe cale cromatografică. Barbotorul (*9*) este prevăzut cu un difuzor de gaze (*10*) şi cu o tubulură laterală care, de asemenea, prin intermediul unei joncţiuni elastice (*7*), face legătura cu o a doua valvă metalică cu septum (*8'*), prin care se iau probe de gaz după ce acestea au fost trecute prin soluţia de NaOH 2M conţinută în barbotorul (*9*). Încălzirea reactorului (*1*) se efectuează

cu ajutorul unui cuptoraş electric cu rezistenţă (*11*, *12*), care are un gol de încălzire cu dimensiunile $L=150$ mm şi $\varnothing=50$ mm. În partea superioară cuptoraşul este închis cu ajutorul unui capac de şamotă (*13*) format din

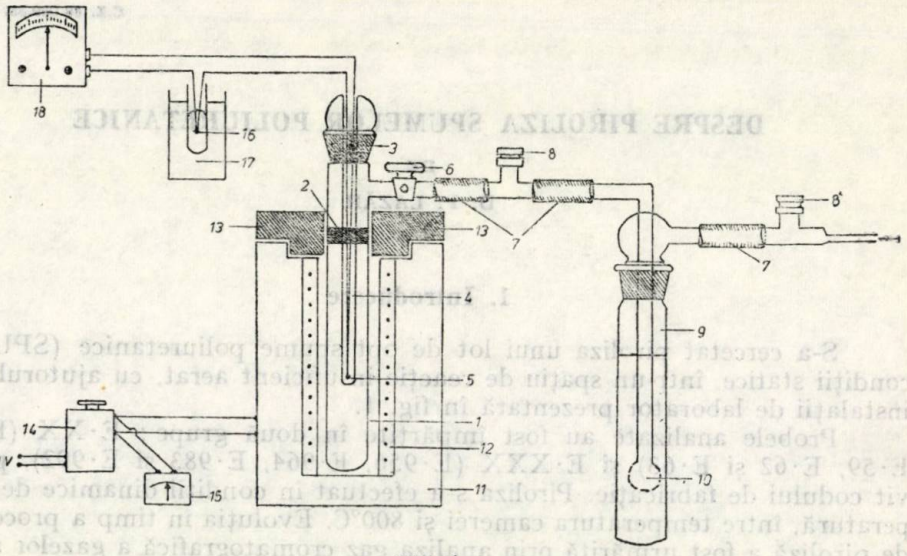

Fig. 1

două piese care cuprind între ele corpul reactorului (*1*). Alimentarea cu energie electrică a cuptoraşului (*11*) s-a realizat cu ajutorul unui autotransformator reglabil (*14*), începînd de la tensiunea de 50 V c.a., în trepte a cîte 5 V, măsuraţi cu ajutorul voltmetrului (*15*). Sudura rece a termocuplului de cromel—alumel a fost plasată într-un mic termostat de 0°C (apă+ +gheaţă) (*17*), iar tensiunea electromotoare furnizată de termocuplu a fost măsurată cu un microvoltmetru B.M. 483 (R. S. Cehoslovacia) (*18*).

1.2. Modul de lucru

Probele de SPU , în greutate de 0,1...0,3 g, s-au introdus pe rînd în reactorul (*1*), în spaţiul situat sub sudura caldă a termocuplului. În barbotorul (*9*) s-au introdus 50...60 ml soluţie NaOH 2M. Încălzirea treptată a probelor s-a efectuat de la temperatura camerei pînă la 900°C, aplicînd cuptoraşului electric tensiuni din ce în ce mai mari, în trepte a cîte 5 V, între 50 V şi 220 V. Începînd cu temperatura de aproximativ 100°C, s-a procedat la sondarea gaz cromatografică a gazelor rezultate din piroliză. Probele de gaz s-au recoltat prin valva (*8*) situată între reactor şi barbotor. Durata unei analize gaz cromatografice a fost de 5 min. şi în raport cu această durată s-a procedat şi la creşterea tensiunii de alimentare a cuptoraşului electric. Numărul sondajelor gaz cromatografice a variat de la o probă la alta între 30 şi 35, ceea ce revine la o analiză cromatografică pentru fiecare creştere cu 20°...30°C a temperaturii reactorului. Rezultatele cantitative ale analizelor gaz cromatografice sînt redate în tabelul 1 pentru proba E.62 şi în tabelul 2 pentru proba E.956.

Tabelul 1

Compoziția procentuală a gazelor de piroliză, în funcție de timp și temperatură (E.62).

Timpul min.	Temperatura °C	Compoziția procentuală a amestecului gazos, raportată la temperatura respectivă					
		CO_2	$NH_3 + H_2O$	NO	N_2O	NO_2	C_4H_{10}
0	98	7,69	92,30	—	—	—	—
5	107	5,81	94,18	—	—	—	—
10	121	5,08	94,91	—	—	—	—
15	137	10,95	89,04	—	—	—	—
20	164	14,28	85,71	—	—	—	—
25	191	53,64	46,35	—	—	—	—
35	265	89,92	10,07	—	—	—	—
40	275	89,39	10,60	—	—	—	—
45	285	77,95	22,04	—	—	—	—
50	300	80,05	19,87	—	—	—	*u*
55	320	86,52	11,96	—	—	—	1,50
60	345	90,70	8,65	—	0,26	—	0,37
65	377	88,08	10,83	—	0,48	—	0,60
70	397	67,13	9,98	—	1,28	*u*	1,54
75	417	87,56	9,79	—	1,82	0,06	0,76
80	440	81,10	10,57	—	2,11	0,11	6,08
85	463	78,62	10,52	0,70	3,41	0,35	6,32
90	483	79,54	9,74	0,92	3,40	0,36	4,01
95	514	56,79	13,72	17,35	4,89	1,57	5,65
100	545	60,84	7,60	20,28	4,18	2,83	4,24
105	567	63,73	6,58	19,37	4,78	2,46	3,05
110	600	37,34	11,32	22,05	4,52	3,56	2,81
115	626	45,15	6,58	32,73	5,78	8,04	1,69
120	650	53,15	7,24	26,49	4,95	7,30	0,84
125	674	39,24	8,50	36,04	6,15	9,61	0,49
130	695	38,86	6,73	36,52	3,96	7,90	0,29
140	757	43,95	6,79	36,25	4,49	8,15	0,33
145	794*)	47,50	7,39	34,09	2,09	8,73	0,17
155	875	23,18	1,35	87,73	1,38	3,88	1,45
160	890	15,67	3,21	64,62	1,04	3,05	1,04
165	905	19,08	10,02	66,14	0,94	2,98	0,81

u — urme; *) temperatura la care aria totală a peak-urilor G.C. a fost maximă.

Tabelul 2

Compoziția procentuală a gazelor de piroliză, în funcție de timp și temperatură (E. 956)

Timpul min.	Temperatura °C	Compoziția procentuală a amestecului gazos, raportată la temperatura respectivă					
		CO_2	NH_3+H_2O	NO	N_2O	NO_2	C_4H_{10}
0	63	4,92	95,00	—	—	—	—
5	85	5,53	94,47	—	—	—	—
10	101	7,45	92,55	—	—	—	—
15	122	10,20	89,79	—	—	—	—
20	144	9,50	90,50	—	—	—	—
25	166	9,52	90,47	—	—	—	—
30	190	9,43	90,56	—	—	—	—
35	214	38,29	61,70	—	—	—	—
40	227	40,69	59,31	—	—	—	*u*
45	236	57,10	42,90	—	—	—	*u*
50	271	72,52	27,45	—	—	—	*u*
55	333	75,41	18,05	—	—	—	6,50
60	354	52,93	40,40	—	0,16	0,10	6,40
65	416	60,34	26,45	—	1,60	1,11	10,50
70	422	55,35	18,51	1,38	2,50	1,49	20,77
75	439	50,37	26,04	3,90	3,46	3,02	13,21
80	462	48,01	29,09	5,61	7,42	5,86	13,55
85	845	37,70	16,84	22,52	4,27	6,75	11,85
90	564	38,45	12,28	29,20	4,71	8,62	6,72
95	595	21,85	14,47	36,44	5,36	8,57	5,31
100	633*)	9,58	5,58	74,15	3,42	5,89	1,36
105	652	19,63	5,89	60,05	4,96	8,95	0,51
110	666	14,67	8,11	63,36	4,00	8,47	1,37
115	697	12,39	4,43	77,82	3,02	5,92	—
125	757	13,13	11,62	68,48	3,11	3,65	—
130	783	11,12	6,81	77,55	1,72	2,79	—
135	798	10,01	7,69	78,59	1,39	2,71	—
140	822	6,71	10,28	79,84	0,91	2,25	—
145	848	6,11	8,72	82,86	0,73	1,77	—
150	858	9,26	8,50	79,77	0,70	1,75	—

u — urme ; *) temperatura la care aria totală a peak-urilor G.C. este maximă.

Aceste două probe au fost selectate pentru ilustrarea cantitativă a compoziției gazelor de piroliză deoarece sînt cele mai gazeificabile spume din grupele respective [1]. Pentru celelalte spume poliuretanice, analizele GC sînt foarte asemănătoare și nu prezintă aspecte deosebite. Analizele cromatografice s-au efectuat cu un cromatograf Chromatron HFGC 18.3 (R.D.G.) echipat cu un detector khatarometric ; coloana cromatografică a fost din oțel inoxidabil, cu lungimea de 1 000 mm și $\varnothing = 4$ mm, umplută cu Porapak Q, 80/100 mesh. Drept gaz purtător s-a folosit argonul uscat, cu un debit de 36 cm³/min.

Soluțiile alcaline culese din barbotorul (*9*) s-au adus la volum constant și s-au analizat potențiometric în privința ionilor CN^-, folosind un electrod selectiv Radelkis, O.P. — CN 7112 D, un electrod de referință Ag/AgCl (Beckmann) iar ca instrument de măsură un pH-metru M.V. 84 (R.D.G.). Rezultatele determinărilor cantitative privind ionii CN^- sînt redate în tabelul 3.

Tabelul 3

Rezultatele analizei potențiometrice pentru ionii CN^-

Codul SPU	Greutatea probei m_p g	T.E.M. a pilei E_p mV	Concentrația CN^- ioni—g/l*)	Concentrația CN^- g la 100 g SPU
E.57	0,2619	133	$2{,}23 \cdot 10^{-4}$	2,291
E.59	0,2416	130	$3{,}54 \cdot 10^{-4}$	3,932
E.62	0,2132	158	$4{,}36 \cdot 10^{-4}$	5,534
E.63	0,2465	100	$0{,}89 \cdot 10^{-4}$	5,030
E.951	0,3361	88	$6{,}76 \cdot 10^{-5}$	0,541
E.964	0,2940	75	$2{,}23 \cdot 10^{-5}$	0,204
E.983	0,1249	84	$5{,}01 \cdot 10^{-5}$	1,081
E.992	0,1934	93	$7{,}50 \cdot 10^{-5}$	1,044

*) din curba de etalonare

3. Discuții și concluzii

Spumele poliuretanice, încălzite în spații închise insuficient aerate, se gazeifică fără a se topi. Principalele date cantitative privind piroliza celor opt spume analizate sînt redate în tabelul 4.

Aplicarea calculului statistic [2] datelor cantitative cuprinse în tabelul 4, atît pentru produsele gazoase cît și pentru reziduurile solide (tabelul 5), arată că ambele grupe de spume au o comportare termocinetică sensibil apropiată (v. mărimile $\sum x$ și x), cu unele deosebiri nesemnificative în privința deviației standard (δn) și a deviației standard a mărimii ($\delta n - 1$), care sînt cu puțin mai mici în cazul spumelor E.XXX.

Analiza gaz cromatografică a pus în evidența faptul că amestecul gazos obținut în procesul de piroliză are o compoziție completă la temperaturi de piroliză T_p sensibil apropiate de temperaturile T_1 la care se termină primul proces termogravimetric raportat într-o lucrare anterioară [1]. Această comparație între valorile T_p și T_1 este redată în tabelul 6.

Tabelul 4

Rezultatele experimentale obținute în procesul de piroliză a SPU

Cod SPU	Greutatea m_p g	Produse gazoase		Reziduu	
		g	%	g	%
E.57	0,2619	0,1831	69,91	0,0788	30,08
E.59	0,2416	0,1628	67,38	0,0788	32,61
E.62	0,2132	0,1196	56,09	0,0936	43,94
E.63	0,2465	0,1747	70,87	0,0718	29,30
E.956	0,3361	0,2598	77,29	0,0763	22,70
E.964	0,2940	0,1856	63,12	0,1084	36,87
E.983	0,1249	0,0781	62,53	0,0468	37,46
E.992	0,1934	0,1215	62,82	0,0719	37,18

Tabelul 5

Analiza statistică a datelor experimentale din tabelul 4

Cod SPU	Mărimi statistice					
	n	x, [%]	Σx	$\bar{x}$	δn	$\delta n-1$
A. Produși gazoși de piroliză						
E.57		69,91				
E.59	4	67,38	264,25	66,06	5,897	6,809
E.62		56,09				
E.63		70,87				
E.951		77,29				
E.964	4	63,12	265,76	66,44	6,267	7,237
E.983		62,53				
E.992		62,82				
B. Reziduuri						
E.57		30,08				
E.59	4	31,61	135,93	33,98	5,877	6,797
E.62		43,94				
E.63		29,30				
E.956		22,70				
E.964	4	36,87	134,21	33,55	6,289	7,239
E.983		37,46				
E.992		37,18				

n — populația ; x — valoarea individuală a mărimii ; δn — deviația standard ; $\delta n-1$ — deviația standard a mărimii.

Compoziția procentuală a gazelor de piroliză, în funcție de timpul și temperatura de piroliză, este redată în tabelul 1 pentru spuma E.62 și în tabelul 2 pentru spuma E.956. Pentru celelalte spume analizele gaz cromatografice sînt asemănătoare.

După cum se poate constata din analiza datelor cuprinse în tabelele 1 și 2, piroliza s-a condus cu o viteză de încălzire de circa 5...6 grade pe minut.

Tabelul 6

Comparație între temperaturile T_p și T_1

Cod SPU	T_p °C	T_1 °C
E.57	372	350
E.59	368	360
E.62	377	360
E.63	367	360
E.956	354	390
E.964	359	330
E.983	375	370
E.992	358	420

Detectarea tuturor componentelor gazoase rezultate din piroliză s-a realizat la temperaturi destul de înalte (tabelul 6), după timpi de piroliză care au variat de la probă la probă, între 70 și 80 min. Pentru toate gazele de piroliză (cu excepția oxidului de azot, NO), compoziția acestora crește la început cu temperatura pînă la o valoare maximă, apoi scade fie pînă la dispariția compusului din sistem sau pînă la o valoare staționară, ca urmare a antrenării acestor gaze în diferitele reacții posibile în sistemul dat, la temperaturile ridicate la care s-a condus procesul de piroliză.

Oxidul de azot apare în amestecul gazelor de piroliză la temperaturi de peste 400°C ; concentrația lui crește cu temperatura fără să treacă printr-un maxim astfel că la terminarea procesului de piroliză NO constituie componentul principal al gazelor de piroliză, urmat de CO_2 și NH_3, restul gazelor avînd rol de componente minore.

După cum se poate constata din datele cantitative și calitative prezentate, piroliza spumelor poliuretanice în spații închise conduce la formarea unei mari cantități de gaze (peste 66% din greutatea spumei pirolizate) care, prin compoziția cantitativă și calitativă, se prezintă ca un amestec gazos extrem de coroziv, inflamabil și deosebit de toxic prin acidul cianhidric, amoniac și oxizii de azot.

Primită la 5 iulie 1980

Institutul politehnic, Iași,
Catedra de chimie fizică

BIBLIOGRAFIE

1. Lazăr D. P., Bul. Inst. polit. Iași, **XXVIII (XXXII)**, *1—4*, s. III, 47—50 (1982).
2. Ceaușescu D., *Tratarea statistică a datelor chimico-analitice*. Buc., Ed. Tehn, 1973, 20, 32, 43.

ABOUT THE PYROLYSIS OF THE POLYURETHANE FOAMES

(Summary)

The pyrolysis of the eight different polyurethane foames, divided into two groups (E.XX and E.XXX) had been studied in static conditions, in a confined, insufficienly aerated vessel, using a laboratory installation working between room temperature and 900°C. The evolution of the pyrolysis process has been gas chromatographicaly investigated. Some kinetic conclusions had been formulated.

Detectarea tuturor componentelor gazoase rezultate din piroliză s-a realizat la temperaturi destul de înalte (tabelul 6), după timpi de piroliză care au variat de la probă la probă, între 70 și 80 min. Pentru toate gazele de piroliză (cu excepția oxidului de azot, NO), compoziția acestora crește la început cu temperatura până la o valoare maximă, apoi scade fie până la dispariția compusului din sistem sau până la o valoare staționară, ca urmare a antrenării acestor gaze în diferitele reacții posibile în sistemul dat, la temperaturile ridicate la care s-a condus procesul de piroliză.

Oxidul de azot apare în amestecul gazelor de piroliză la temperaturi de peste 400°C, concentrația lui crește cu temperatura fără să treacă printr-un maxim astfel că la terminarea procesului de piroliză NO constituie componentul principal al gazelor de piroliză, urmat de CO_2 și NH_3, restul gazelor avînd rol de componente minore.

După cum se poate constata din datele cantitative și calitative prezentate, piroliza spumelor poliuretanice în spații închise conduce la formarea unei mari cantități de gaze (peste 65%, din greutatea spumei pirolizate) care, prin compoziția cantitativă și calitativă, se prezintă ca un amestec gazos extrem de coroziv, inflamabil și deosebit de toxic prin acidul cianhidric, amoniac și oxizii de azot.

Primită la 5 iulie 1980

Institutul politehnic, Iași.
Catedra de chimie fizică

BIBLIOGRAFIE

1. Lazăr D. P., Bul. Inst. polit. Iași, XXVIII (XXXII), 1–4, s. III, 47–50 (1982).
2. Ceausescu B., Tratarea statistică a datelor chimico-analitice. Buc., Ed. Tehn., 1975, 20, 32, 43.

ABOUT THE PYROLYSIS OF THE POLYURETHANE FOAMES

(Summary)

The pyrolysis of the eight different polyurethane foames, divided into two groups (F XX and E XXX) had been studied in static conditions, in a confined, insufficiently aerated vessel, using a laboratory installation working between room temperature and 900°C. The evolution of the pyrolysis process has been gas chromatographically investigated. Some kinetic conclusions had been formulated.

BULETINUL INSTITUTULUI POLITEHNIC DIN IAŞI
Tomul XXIX (XXXIII), Fasc. 1—4, 1983
Secţia II
CHIMIE şi INGINERIE CHIMICĂ

C.Z. 621.92; 661.183.48

UNELE CORELAŢII COMPOZIŢIE — PROPRIETĂŢI LA SITE MOLECULARE DE TIP NaA

DE

EVELINE POPOVICI şi M. CRUCEANU

1. Introducere

Reţeaua tridimensională a sitelor moleculare zeolitice este realizată prin înlănţuirea tetraedrelor de siliciu ($[SiO_4]^{4-}$) şi de aluminiu ($AlO_4]^{5-}$), la care compensarea sarcinii negative excedentare, rezultată prin substituirea izomorfă a siliciului din reţea cu aluminiul, este realizată cu ioni de metal, echivalenţi ca sarcină [1]. Gradul de substituire izomorfă a siliciului din reţea se exprimă analitic prin valoarea raportului molar SiO_2/Al_2O_3. Atît proprietăţile adsorbtive [2] cît şi proprietăţile superficiale ale sitelor moleculare sînt influenţate de valoarea gradului de substituire izomorfă precum şi de natura şi poziţia cationilor asociaţi [3].

Literatura indică drept metode de modificare a raportului molar SiO_2/Al_2O_3 din compoziţia sitelor moleculare, extracţia unei părţi din aluminiu, prin folosirea soluţiilor clorhidrice şi a soluţiilor de acetilacetonă în mediul organic anhidru [4] sau introducerea unor solvenţi organici în mediul de cristalizare.

În lucrarea de faţă se studiază variaţia unor proprietăţi structural-adsorbtive care se evidenţiază în cazul sitelor moleculare de tip NaA, în urma extracţiei parţiale a aluminiului cu acetilacetonă.

2. Partea experimentală

Pentru experimentare au fost alese site moleculare tip NaA sintetizate pe cale hidrotermală [5], [7], cu raport molar SiO_2/Al_2O_3 cuprins între 1,70... ...2,20 (seria Si) şi care au fost supuse extracţiei parţiale a aluminiului folosind soluţie benzenică de acetilacetonă. Extracţia s-a efectuat timp de 5 ore la o temperatură de 50° ± 1°C, în balon cu agitator şi reflux folosind o soluţie de 25% acetilacetonă în benzen anhidru, la un raport soluţie : solid de 10 : 1. După extracţie produsele au fost separate prin filtrare, spălate cu acetonă şi apă decationizată, uscate la 110°C (seria ESi). Eventuala prezenţă a acetilacetonei adsorbită pe produse a fost investigată pe două căi : o cale chimică, care constă în punerea eşantionului în contact cu o soluţie sulfurică de alaun feric [9], care ar putea conduce la apariţia unei colorаţii roşii, caracteristice acetilacetonatului de fer şi o cale fizico-chimică — spectroscopia în IR.

La produsele din ambele serii s-a determinat compoziţia chimică, structura, stabilitatea termică, stabilitatea chimică şi aciditatea suprafeţei.

3. Rezultate şi interpretări

Rezultatele analizei chimice a produselor, pe baza cărora s-a calculat compoziţia celulei elementare [12], sînt prezentate în tabelul 1.

Tabelul 1

Datele analizei chimice

Produsul	Compoziţia chimică, [mmoli/g]				Compoziţia celulei elementare				
	Na_2O	Al_2O_3	SiO_2	SiO_2: : Al_2O_3	Na	Al	Si	O	γ
S_1	6,12	6,06	10,42	1,72	12,9	12,9	11,00	49,9	0,86
S_2	6,31	6,24	11,23	1,80	12,6	12,6	11,30	47,8	0,90
S_3	5,30	5,27	10,43	1,98	12,0	12,0	11,80	47,7	0,99
S_4	7,00	6,45	14,19	2,20	11,4	11,4	12,50	47,8	1,10
ES_1	5,43	4,46	9,36	2,10	11,6	11,6	12,18	47,5	1,05
ES_2	5,85	4,97	10,33	2,08	11,7	11,7	12,06	47,7	1,04
ES_3	5,04	4,75	10,54	2,22	11,4	11,4	12,60	48,0	1,11
ES_4	6,75	5,86	13,88	2,37	11,0	11,0	13,03	48,0	1,18

Datele analizei chimice arată că extracţia aluminiului, respectiv reducerea numărului de tetraedre anionice $[AlO_4]^{5-}$, este condiţionată de raportul, γ, dintre numărul de tetraedre de siliciu şi aluminiu din celulele sodalitice, caracteristice produselor iniţiale.

Din fig. 1, în care s-a reprezentat gradul de extracţie al Al_2O_3 în funcţie de γ, se constată că cu cît valoarea parametrului γ este mai mică decît unitatea cu atît se extrage mai mult aluminiu din reţea.

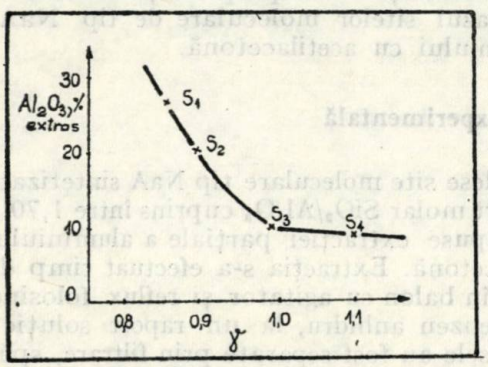

Fig. 1. — Variaţia conţinutului procentual de Al_2O_3 extras funcţie de valoarea raportului γ.

Se poate considera că eliminarea aluminiului din reţeaua cristalină a sitelor moleculare întîmpină rezistenţe atît de natură energetică cît şi sterică. Rezistenţele de natură sterică sînt legate de geometria carcasei, de posibilităţile de acces a soluţiei benzenice de acetilacetonă la aluminiul plasat pe suprafaţa internă a cavităţilor. Deoarece toate produsele cercetate sînt site moleculare de tip NaA se poate admite că în toate cazurile rezistenţele de natură sterică sînt de aceeaşi intensitate. În schimb dependenţa din fig. 1 pledează pentru ideea că rezistenţele de natură energetică, care se opun extracţiei unei părţi din aluminiu din reţeaua cristalină, sînt cu atît mai mici cu cît abaterea de la regula lui L ö w e n s t e i n ($\gamma \geqslant 1$) este mai mare, decît sînt condiţionate de compoziţia chimică.

Schematic, se poate presupune următoarea transformare posibilă în decursul extracţiei:

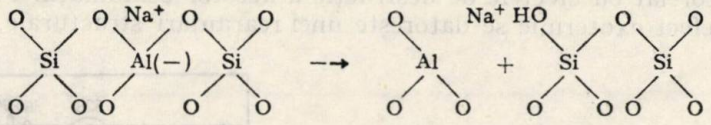

din care se întrevăd posibile modificări cristalografice.

Tabelul 2

Distanţe interplanare şi intensităţile corespunzătoare

$a_0 = 12{,}396$ S_1	$a_0 = 12{,}318$ ES_1	$a_0 = 12{,}360$ S_2	$a_0 = 12{,}316$ ES_2	$a_0 = 12{,}324$ S_3	$a_0 = 12{,}314$ ES_3
3,78(5)	3,77(5)	3,77(1)	—	5,68(1)	—
3,38(7)	3,38(5)	2,989(8)	2,986(9)	4,20(3)	4,20(3)
3,03(9)	3,00(9)	2,645(4)	2,645(3)	3,74(1)	—
2,65(9)	2,65(8)	1,913(1)	—	3,38(3)	3,38(2)
2,117(8)	2,117(5)	1,741(10)	1,743(10)	2,983(10)	2,983(8)
1,918(7)	1,918(8)	1,604(2)	1,603(1)	2,647(8)	2,643(5)
1,748(10)	1,747(10)	1,416(2)	1,416(3)	2,114(5)	2,110(6)
1,601(8)	1,601(8)	1,359(9)	1,357(9)	1,918(3)	1,920(5)
1,528(2)	—	1,306	—	1,742(10)	1,743(8)
1,482(1)	—	1,239	—	1,607(5)	1,608(5)
1,420(7)	1,421(7)	1,910(1)	1,910(1)	1,423(5)	1,421(4)
1,360(10)	1,361(10)	1,155(1)	1,155(1)	1,361(7)	—
1,298(2)	1,297(1)			1,245(5)	1,250(3)
1,235(9)	1,235(8)				
1,185(2)	—				
1,153(3)	1,154(2)				
1,117(1)	—				
1,077(3)	1,077(2)				
1,045(3)	1,044(3)				
1,016(2)	—				

Analiza roentgenografică a produselor (tabelul 2) arată că în urma extracţiei nu a avut loc destrucţia reţelei cristaline, deoarece se menţin liniile de difracţie caracteristice structurii produsului de tip NaA, dar se remarcă o micşorare a numărului planelor cristaline şi variaţii în intensitatea liniilor de difracţie. Aceste modificări structurale se reflectă şi în valoarea parametrului celulei elementare, evidenţiindu-se o contracţie a cărei valoare procentuală (fig. 2) este de asemenea dependentă de gradul extracţiei.

Este de presupus că extracţia unei părţi din aluminiu va reflecta însăşi stabilitatea edificiului cristalin. Analiza derivatografică (fig. 3) a scos în evidenţă faptul că, în limitele studiate ale raportului molar SiO_2/Al_2O_3, produsele din seria Si prezintă stabilitate termică pînă la temperaturi de peste 800°C, în timp ce la produsele din seria ESi se constată apariţia unui efect exoterm plasat între 440°...600°C, însoţit de pierdere în greutate.

Deoarece analiza spectrofotometrică în IR nu a detectat prezența substanțelor organice absorbite pe solid, efectul exotermic care apare nu poate fi corelat cu efectele de destrucție a acestor combinații. Presupunem că acest efect exotermic se datorește unei rearanjări structurale, pe seama

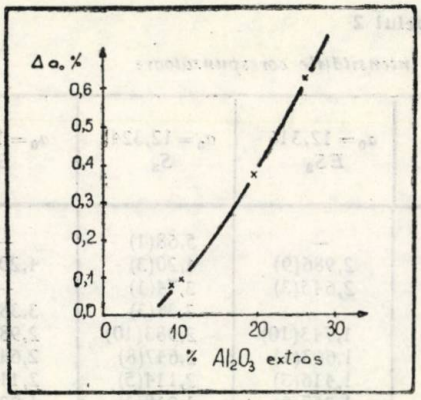

Fig. 2. — Variația contracției procentuale a parametrului celulei elementare, în funcție de cantitatea procentuală de Al_2O_3 extrasă.

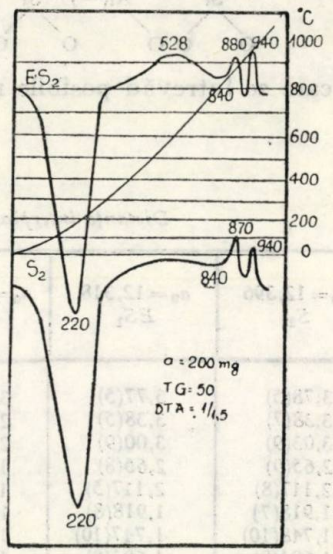

Fig. 3. — Curbele DTA ale produselor S_2 și ES_2.

unui proces de condensare a unor grupări hidroxilice, cu eliminarea moleculelor de apă. Acest efect exoterm de condensare a grupărilor hidroxilice de pe suprafață predomină în intensitate, față de procesul endoterm de dehidroxilare. Probabilitatea procesului de condensare a două grupări hidroxilice depinde de gradul de extracție, de valoarea raportului SiO_2/Al_2O_3, de apropierea grupărilor hidroxilice de pe suprafață. Astfel, s-a constatat că efectul exoterm este mai intens la produsele S_4 și S_2 care au un grad de extracție mai mare.

Deoarece presupunem ca fiind posibilă condensarea grupelor hidroxilice de pe suprafață este de așteptat să apară modificări ale acidității suprafeței. Determinarea acidității totale prin metoda adsorbției piridinei din soluția sa în *n*-heptan [11], [13] pe produse în forma Ca^{2+}, deshidratate la 400°C. a condus la rezultatele din tabelul 3.

Fiind cunoscut faptul că structura sitelor moleculare are o stabilitate redusă în mediu acid, s-a considerat necesar să se verifice dacă aceasta a fost modificată prin extracție. Determinarea stabilității chimice a produselor s-a efectuat prin titrarea unei probe de zeolit cu soluție apoasă de HCl, cînd se observă un efect de tamponare [10] la un pH a cărei valoare constituie un indiciu asupra stabilității sale relative față de acizi. Cu cît valoarea pH-ului este mai mică cu atît stabilitatea este mai mare și viceversa. Re-

Tabelul 3

Stabilitatea chimică și aciditatea produselor

Produsul	S m²/g	Stabilitatea chimică pH	Aciditatea	
			mval/g	mval/m² . 10^3
S_1	711,08	3,7	1,681	2,36
S_2	616,25	3,5	1,888	3,06
S_3	601,87	2,5	1,763	2,93
S_4	753,90	2,0	1,912	2,54
ES_1	740,15	3,5	1,776	2,41
ES_2	680,00	3,5	1,893	3,01
ES_3	689,12	3,5	2,114	3,11
ES_4	790,24	3,5	2,156	2,73

zultatele sînt prezentate în tabelul 3, în care, ca urmare a extracției unei părți din aluminiul rețelei anionice a sitelor moleculare, se observă o scădere a stabilității chimice a produselor, o variație a acidității suprafeței și schimbări în valoarea suprafeței specifice.

4. Concluzii

1. Extracția unei părți din aluminiul rețelei anionice a sitelor moleculare de tip NaA întîmpină rezistențe atît de natură energetică cît și sterică. Rezistențele energetice sînt condiționate de raportul dintre numărul de tetraedre de siliciu și aluminiu din celulele sodalitice.

2. Parametrul celulei elementare a sitelor moleculare de tip NaA, din care s-a extras o parte din atomii de aluminiu, prezintă o contracție care depinde de valoarea gradului de extracție.

3. Stabilitatea termică și chimică a produselor care au suferit tratamentul chimic cu acetilacetonă, sînt diminuate.

4. Eliminarea progresivă a aluminiului permite obținerea unor produse cu aciditate modificată și deci cu utilizări industriale variate.

Primită la 8 februarie 1980

Institutul politehnic, Iași
Catedra de chimie generală și tehnologică

BIBLIOGRAFIE

1. Breck D. W., J. Am. Chem. Soc., **78**, 2 338 (1967); Ibid., **78**, 5 693 (1956); Ibid., **78**, 3 972 (1956).
2. Barrer R. M., Brit. Chem. Eng., 4, 5 (1959).
3. Келцев Н. В., Старовоиства, „Синтетические цеолиты". Изд. АН СССР, М., 1962, 239.
4. Rouquerol F., Imelik B., Bull. Soc. Ch. France, **9**, 2 802 (1966).
5. Popovici Ev., *Studiul sintezei sitelor moleculare zeolitice în prezența solvenților organici.* Teză de doctorat, Univ. „Al. I. Cuza", Iași, 1973.

6. Cruceanu M., Popovici Ev., Pat. R.S.R., *55 824*, (1968).
7. Cruceanu M., *Zeoliţi sintetici cu proprietate de site moleculare*. Teză de doctorat, Inst. polit., Iaşi, 1966.
8. Betehtin A. G., *Curs de mineralogie* (trad. din l. rusă). Ed. Tehn., Buc., 1962, 354–72.
9. Barthomeuf D., Bull. Soc. Chim Fr., 1415 (1967).
10. Young S., Pat. USA, *1 548 382* (1968).
11. Tung S. E., J. Catal., 10, 166–182 (1968).
12. Дубинин М. М., *Синтетические цеолиты*. Изд. АН СССР, М., 1962, 86.
13. Pop A., Stud. Univ. Babeş-Bolyai, Chem., 12 (2), 89 (1967).
14. Hirshler I., J. Catal., 5, 428 (1963).

SOME CORRELATIONS COMPOSITION–PROPERTIES ON THE MOLECULAR SIEVES OF THE NaA TYPE

(Summary)

The influence of partial extraction of the aluminum by acetylacetone from framework of the molecular sieve type NaA, on the structural-adsorptive properties of the obtained products was investigated.

One notes, particularly, the influence of the molecular ratio SiO_2/Al_2O_3 both on the extraction and on the acidity of products.

BULETINUL INSTITUTULUI POLITEHNIC DIN IAŞI
Tomul XXIX (XXXIII), Fasc. 1—4, 1983
Secţia II
CHIMIE şi INGINERIE CHIMICĂ

D.C. 661.183.12

ADSORPTION BEHAVIOUR OF SOME ORGANIC CHLORODERIVATIVES ON VOLCANIC TUFFS

BY

GH. MIHĂILĂ, N. BÎLBĂ, P. ONU, C. LUCA and N. NAUM

1. Introduction

The waste gases resulted from the hydrocarbons chlorination process, depending on the real conditions of employed technology, contain also besides respective chloroderivatives chlorine traces. Both chlorine and chloroderivatives are strong pollutants of environment, demaging fauna and flora. At present, throughout the world, there are employed for pollutants agents separation from waste industrial gases different adsorbants such as active carbon, silicagel, synthetic zeolites, molecular sieves, etc., products with relative high cost. Taking into account the fact that volcanic tuffs with high content of zeolite [1] exhibit appreciable adsorptive properties and a low cost, the present paper deals with the results as regards adsorption of some organic chloroderivatives on volcanic tuffs, activated thermically, by ion exchange and by mineral acid treatment.

This study was performed in order to establish the activation conditions that lead to adsorbants with high adsorption capacity and good selectivity suitable for chloroderivatives adsorption from waste industrial gases. Adsorption was studied under both static and dynamic conditions. Under static conditions, adsorption was performed on a quartz spring balance and, under dynamic conditions, on a manually operated thermoanalyzer constructed from a standard analytical balance.

2. Experimental

The volcanic tuffs to be studied were obtained from Pîglişa and Mirşid deposits, Romania. Their mean chemical composition is given in Table 1 [2].

The experiments have been carried out on volcanic tuffs samples having granule size between 0.5 and 1.0 mm. Their BET specific surface area was 13.65 and 46.81 m^2/g for native tuff of Pîglişa and Mîrşid, respectively. Small values of this property are proper to solids of Ith order to which prevalent is the outer surface. Since the BET specific surface area of Mîrşid tuff is larger than that of Pîglişa one, all adsorption experiments were carried out on the former kind.

In order to improve the specific surface area and respective their adsorption capacity, the Mîrşid tuff samples were activated thermically, by ion exchange and by hydrochloric acid treatment.

Table 1

Oxidic Chemical Composition of Volcanic Tuffs

Oxide	%	Oxide	%
SiO_2	55 ...72	K_2O	1.5 ... 3.0
Al_2O_3	11 ...13	Na_2O	1.0 ... 3.0
Fe_2O_3	0.6 ... 1.8	TiO_2	0.1 ... 0.4
CaO	3.0 ... 4.0	MnO	0.009... 0.01
MgO	0.05... 1.5	Calcination loss	10 ...12

2.1. Thermic Activation

This activation has consisted in calcination of the tuff samples in an electric furnace, for two hours, at 500°C, temperature previously found to be optimum by two ways : adsorption against water vapour and benzene vapour and on the basis of TG curve, recorded on a Mettler thermobalance. The samples calcinated at this temperature exhibit a maximum specific surface area corresponding to a maximum water removal from tuff structure.

2.2. Activation by Ion Exchange

Looking over the chemical composition of volcanic tuff, presented in Table 1, it comes out that clinoptilolite can occurs in both forms with sodium and potassium or with calcium and magnesium. By replacing the Na^+ and K^+ ions with the Ca^{2+} ions by ion exchange, the space available for large molecules adsorption increases, because the volume occupied by two sodium ions is larger than that occupied by only one calcium ion.

Activation has consisted in two steps, i.e., ion exchange and calcination at 500°C for two hours. The ion exchange was carried out with a solution of 0.2 M $CaCl_2$ at 20°C, in two runs, followed by washing with distilled water untill complet removal of chlorine ions and drying. This activation lead to a small increase of specific surface area but the samples exhibit more accurate pore size distribution.

2.3. Chemical Activation

Treating the samples with mineral acids leads to removal of a larger part of cations and some aluminium atoms from tuff structure [3]. For this reason, tuff samples with granule size of 0.5...1.0 mm have been treated with hydrochloric acid solution with concentration ranging from 0.8 to 22.8 %, at 80°...90°C, for two hours, followed by washing and drying and, finally, calcinated for two hours at 500°C. Specific surface area of the samples activated as above was 66.3, 103.4, 141.4 and 193.1 m^2/g for HCl concentration of 0.8, 4.2, 11.3 and 22.8%, respectively.

Adsorption of 1,2-dichlorethane, 1,1,1-trichlorethane, 1,1,2,2-tetrachlorethane, pentachlorethane and phenylchloride was studied on the volcanic tuff samples activated thermically (M_{500}) by ion exchange with

Table 1

Oxidic Chemical Composition of Volcanic Tuffs

Oxide	%	Oxide	%
SiO_2	55 ...72	K_2O	1.5 ... 3.0
Al_2O_3	11 ...13	Na_2O	1.0 ... 3.0
Fe_2O_3	0.6 ... 1.8	TiO_2	0.1 ... 0.4
CaO	3.0 ... 4.0	MnO	0.009... 0.01
MgO	0.05... 1.5	Calcination loss	10 ...12

2.1. Thermic Activation

This activation has consisted in calcination of the tuff samples in an electric furnace, for two hours, at 500°C, temperature previously found to be optimum by two ways : adsorption against water vapour and benzene vapour and on the basis of TG curve, recorded on a Mettler thermobalance. The samples calcinated at this temperature exhibit a maximum specific surface area corresponding to a maximum water removal from tuff structure.

2.2. Activation by Ion Exchange

Looking over the chemical composition of volcanic tuff, presented in Table 1, it comes out that clinoptilolite can occurs in both forms with sodium and potassium or with calcium and magnesium. By replacing the Na^+ and K^+ ions with the Ca^{2+} ions by ion exchange, the space available for large molecules adsorption increases, because the volume occupied by two sodium ions is larger than that occupied by only one calcium ion.

Activation has consisted in two steps, i.e., ion exchange and calcination at 500°C for two hours. The ion exchange was carried out with a solution of 0.2 M $CaCl_2$ at 20°C, in two runs, followed by washing with distilled water untill complet removal of chlorine ions and drying. This activation lead to a small increase of specific surface area but the samples exhibit more accurate pore size distribution.

2.3. Chemical Activation

Treating the samples with mineral acids leads to removal of a larger part of cations and some aluminium atoms from tuff structure [3]. For this reason, tuff samples with granule size of 0.5...1.0 mm have been treated with hydrochloric acid solution with concentration ranging from 0.8 to 22.8 %, at 80°...90°C, for two hours, followed by washing and drying and, finally, calcinated for two hours at 500°C. Specific surface area of the samples activated as above was 66.3, 103.4, 141.4 and 193.1 m^2/g for HCl concentration of 0.8, 4.2, 11.3 and 22.8%, respectively.

Adsorption of 1,2-dichlorethane, 1,1,1-trichlorethane, 1,1,2,2-tetrachlorethane, pentachlorethane and phenylchloride was studied on the volcanic tuff samples activated thermically (M_{500}) by ion exchange with

$CaCl_2$ (M_{CaCl_2}) and by treatment with hydrochloric acid of different concentration ($M_3=2\%$; $M_{33}=6\%$; $M_{333}=12\%$).

Static adsorption was carried out on a gravimetrical plant with quartz spring as previously reported [4] and dynamic adsorption was carried out on a manually operated thermoanalyser, represented in Fig. 1.

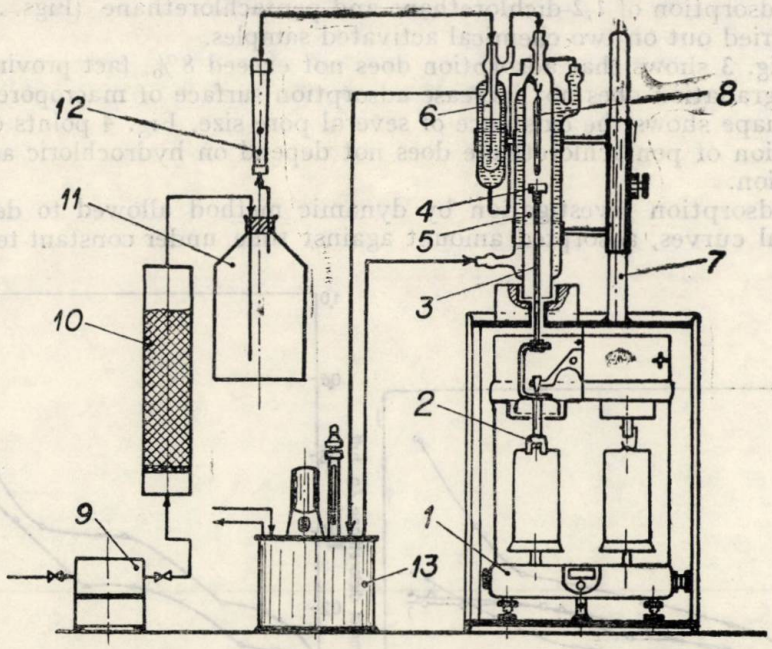

Fig. 1. — Gravimetrical plant for adsorption study under dynamic conditions: *1* — standard analytical balance ; *2* — plate interlock ; *3* — glass rod ; *4* — crucible ; *5* — thermostated tube ; *6* — thermostated bubbler ; *7* — holder ; *8* — thermometer ; *9* — screw-type axial flow fan ; *10* — drying tower with soda lime packed ; *11* — buffer ; *12* — rotameter ; *13* — thermostat.

Static and dynamic adsorption were carried out for all samples at 20°C, under saturation pressure in the case of static method and in air stream saturated with pollutant in the case of the dynamic method.

3. Results and Discussion

The adsorption isotherms obtained by statical method are represented in Figs. 2...4.

Looking over the isotherms plotted on Fig. 2, the following remarks can be reported :

a) Adsorpted amount does not exceed 7% and the adsorption order depends on boiling temperature of pure components and molecule configuration. Adsorpted amount of studied chloroderivatives is situated as follows : 1,2-dichlorethane > 1,1,1-trichlorethane > 1,1,2,2-tetrachlorethane > phenylchloride.

b) The adsorption isotherms are of IInd type, proper for macroporous solids [5].

c) Adsorption is due only to large size pores and is not a selective one, therefore the volcanic tuff cannot be utilized for chloroderivatives separation from one another.

Adsorption of 1,2-dichlorethane and pentachlorethane (Figs. 3 and 4) was carried out on two chemical activated samples.

Fig. 3 shows that adsorption does not exceed 8%, fact proving that acid degradation does not increase adsorption surface of macropores. Their steps shape shows the existence of several pore size. Fig. 4 points out that adsorption of pentachlorethane does not depend on hydrochloric acid concentration.

Adsorption investigation by dynamic method allowed to determine kinetical curves, adsorpted amount against time, under constant temperat-

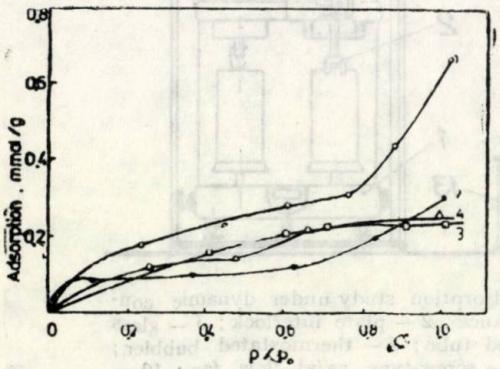

Fig. 2. — Adsorption isotherms of four chloroderivatives on Mîrșid volcanic tuff, activated at 500°C: *1* — 1,2-dichlorethane; *2* — 1,1,1-trichlorethane; *3* — 1,1,2,2-trichlorethane; *4* — phenyl chloride.

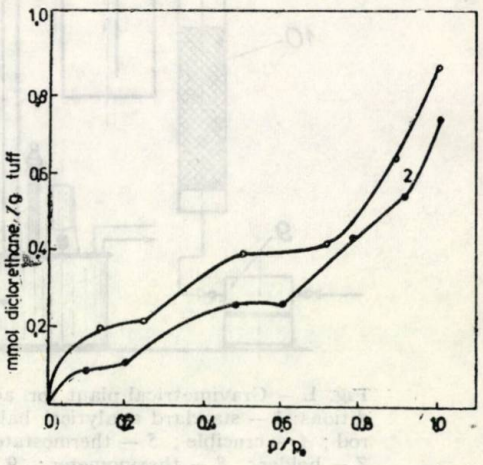

Fig. 3. — Adsorption isotherms of 1,2-dichlorethane on chemically activated volcanic tuff: *1* — M_{333}; *2* — M_3.

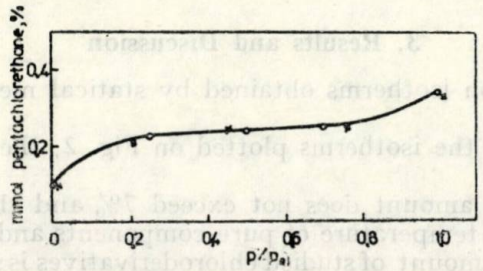

Fig. 4. — Adsorption isotherms of pentachlorethane on chemically activated volcanic tuff; o — M_{333}; x — M_3.

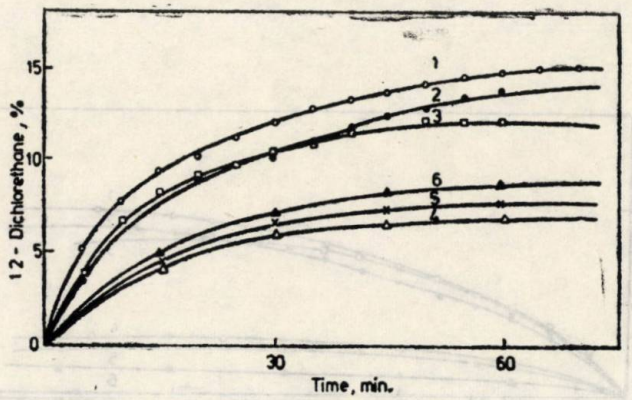

Fig. 5. — Adsorption of 1,2-dichlorethane: *1* — M_{500}; *2* — M_{CaCl_2}; *3* — M_{350}; *4* — M_3; *5* — M_{33}; *6* — M_{333}.

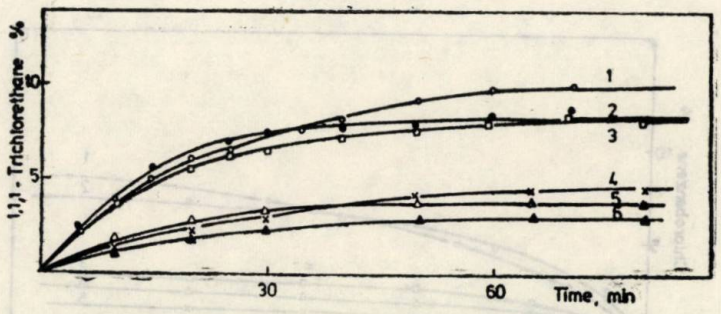

Fig. 6, — Adsorption of 1,1,1-trichlorethane: *1* — M_{500}; *2* — M_{350}; *3* — M_{CaCl_2}; *4* — M_3; *5* — M_{33}; *6* — M_{333}.

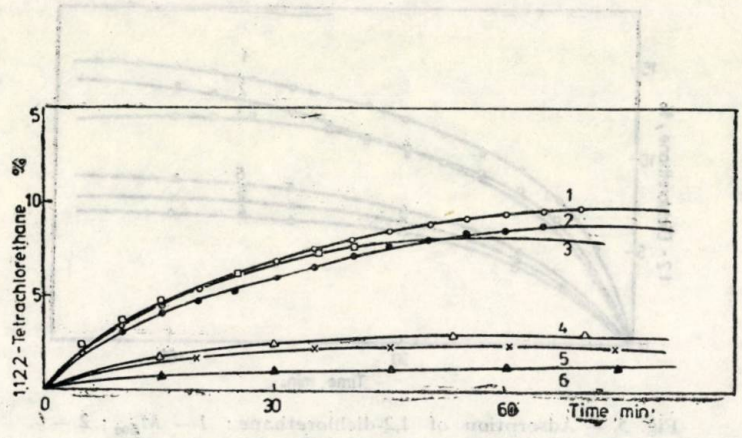

Fig. 7. — Adsorption of 1,1,2,2-trichlorethane : *1* — M_{500} ; *2* — M_{350} ; *3* — M_{CaCl_2} ; *4* — M_3 ; *5* — M_{33} ; *6* — M_{333}.

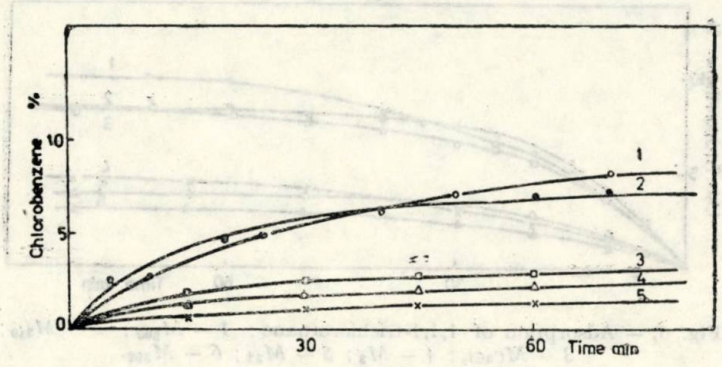

Fig. 8. — Adsorption of phenyl chloride ; 1 — M_{350} ; 2 — M_{500} ; *3* — M_3 ; *4* — M_{33} ; *5* — M_{333}.

ure of the four chloroderivatives on the same samples. The kinetical curves obtained are represented in Figs. 5...8.

Looking over the kinetical curves represented in Figs. 5...8 the following observations can be reported :

a) The samples activated thermically at 500°C (M_{500}) exhibit the highest adsorption capacity against all chloroderivatives studied, i.e., 14.0% 1,2-dichlorethane, 10.0% 1,1,1-trichlorethane and 1,1,2,2-tetrachlorethane and 7.0 % phenyl chloride.

b) Activation by ion exchange with calcium chloride solution and calcination at 500°C does not bring notable modifications of adsorption capacity.

c) Acid treatment of the samples with hydrochloric acid of different concentration followed by their calcination at 500°C led to products with adsorption capacity of two or three times less than that of those activated only thermically.

Taking into account the relative high value of adsorption capacity against organic chloroderivatives of the Mirșid volcanic tuff samples, granule size of 0.5...1.0 mm, activated at 500°C, for two hours, they can be employed successfully as depolluting agents of the gases containing these compounds.

4. Conclusions

Investigation of the adsorption behaviour of some organic chloroderivatives on activated volcanic tuffs, carried out by static and dynamic methods, lead to the following statements :

1. Thermal activation at 500°C, for two hours, of Mirșid volcanic tuff, produces adsorbants with appreciable adsorption capacity against chloroderivatives (Figs 5...8).

2. Activation by ion exchange with calcium chloride solution followed by thermal activation at 500°C, for two hours, did not increase adsorption capacity of the samples.

3. Chemical activation by treatment with hydrochloric acid of different concentration at the same ratio, solution to tuff, gives samples with microporous structure and larger specific surface area, but with less adsorption capacity against chloroderivatives.

4. Adsorption of chloroderivatives takes place exclusively on the outer surface of the tuff granules.

Received, April 29, 1982

Polytechnic Institute, Jassy,
Department of General and
Technological Chemistry

REFERENCES

1. Peterson D. L., Helfferich F., Blytas G. C., Phys. Chem. Solids, **26**, 835—840 (1965).
2. Fodor I., Piso P., Bărbat A., Bengeanu M., Felvinczi S., Ciceu S., Todan A., Symp. „New Mining and Dressing Technologies of Non-metallics", Cluj-Napoca, Nov. 26—28, 1979, 3, Paper *1*.

3. Коридзе З. И., Крупеникова А. Ю., Андроникашвили Т. Г., *Клиноптилолит*, Тр. симп. по вопр. и прим. клиноптилолита, Тбилиси, 1977, 96.

4. Ababi V., Bîlbă N., Onu P., Mihăilă Gh., Naum N., Luca C., Bul. Inst. polit., Iași, **XXVI(XXX)**, *3—4*, s. III, 51—59 (1980).

5. Gregg S. J., Sing K. S. W., *Adsorption, Surface Area and Porosity*. Academic Press, London—New York, 1967, 54.

COMPORTAREA UNOR DERIVAȚI CLORURAȚI ORGANICI LA ADSORBȚIE PE TUFURI VULCANICE

(Rezumat)

S-a cercetat comportarea la adsorbție a 1,2-dicloretanului, 1,1,1-tricloretanului, 1,1,2,2-tetracloretanului, pentacloretanului și monoclorbenzenului pe probe de tuf vulcanic din zăcămîntul de la Mîrșid, activate termic, prin schimb ionic și prin tratare cu soluție de acid clorhidric. Adsorbția s-a cercetat prin metoda statică, folosind o balanță cu spirală din fir de cuarț și prin metoda dinamică, folosind o balanță ce permite măsurarea variației masei probei plasate într-un curent de aer saturat cu derivat clorurat. Activarea termică a tufului vulcanic de Mîrșid conduce la probe cu proprietăți adsorptive apreciabile față de derivații cloruraț studiați. Activarea prin schimb ionic și prin tratament acid a condus la probe cu capacitate de adsorbție mai redusă decît a celora activate numai termic. Adsorbția are loc numai pe suprafața exterioară a granulelor de tuf.

BULETINUL INSTITUTULUI POLITEHNIC DIN IAŞI
Tomul XXIX (XXXIII), Fasc. 1—4, 1983
Secţia II
CHIMIE şi INGINERIE CHIMICĂ

D.C. 66.097 ; 662.743 ; 547.532

MATHEMATICAL MODELLING OF A CATALYTIC REACTOR FOR BENZENE HYDROGENATION

I. ONE-DIMENSIONAL MODEL

BY

I. CURIEVICI, SAVEL MATACHE, VIORICA NICU, ŞT. UNGUREANU, C. PETRILĂ and ELENA IONESCU

1. Problem Statement

Benzene hydrogenation in order to obtain cyclohexane, as an intermediate compound for caprolactam synthesis, is achieved by means of a solid—gas catalytic process [1].

The diagram of the hydrogenation installation is given in Fig. 1. The reactor for hydrogenation (*1*) is of the multitubular heat-exchanger type having catalyst inside tubes and cooling agent (water at boiling temperature) outside ones. The steam generated in the intratubular space is used for other technological processes, passing through a steam separator (*2*). The inlet reacting mixture is preheated in a counter-current heat exchanger (*3*) by outlet spent gases.

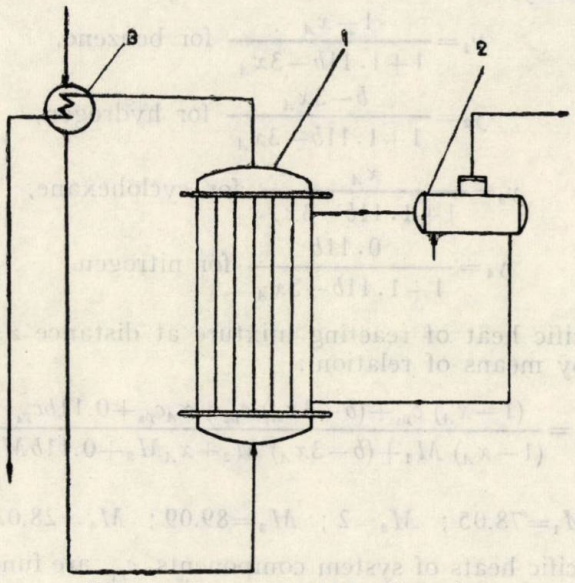

Fig. 1. — Benzene hydrogenation plant.

The catalyst consisting of nickel as active component on Al_2O_3 or Cr_2O_3 inert support is in the form of cylindrical pellets, 4...6 mm diameter and 4...6 mm high.

2. Initial Data and Simplifying Assumptions

2.1. Data on Reactor Geometry

The hydrogenation pilot-reactor studied in the present paper is a heat-exchanger type one having seven tubes, 6 m long each. In the model, the tube diameter, d, is considered as a parameter, the number of tubes being fixed and gas charge on tubes constant ; as a result, a change in the tubes diameter, d, will cause a variation of gas charge on tube.

2.2. Data on Reacting Mixture

The raw materials used in the process are industrial hydrogen (with 10% volume nitrogen) and industrial benzene having a sulphur content under 1 ppm.

Inlet reacting mixture has excess hydrogen. The hydrogen/benzene molar ratio in the feed mixture, b, is considered as a parameter too, which can vary between 4.15 and 11 [1].

Inlet temperature of reactants is $T_0=393.16°K$.

We consider 1 mol benzene in the feed mixture as a basis for the calculus of components molar ratios, so that the feed mixture will contain 1 mol benzene, b mols hydrogen, and 0.11 b mols nitrogen, a total of $(1+1.11b)$ mols.

The molar ratios of the reacting system components, y_i, $(i=1, 2, 3, 4)$, at a given constant conversion x_A and a given distance, z, from reactor input, respectively, will be :

$$y_1=\frac{1-x_A}{1+1.11b-3x_A} \quad \text{for benzene,} \tag{1a}$$

$$y_2=\frac{b-3x_A}{1+1.11b-3x_A} \quad \text{for hydrogen,} \tag{1b}$$

$$y_3=\frac{x_A}{1+1.11b-3x_A} \quad \text{for cyclohexane,} \tag{1c}$$

$$y_4=\frac{0.11b}{1+1.11b-3x_A} \quad \text{for nitrogen.} \tag{1d}$$

The specific heat of reacting mixture at distance z (conversion x_A) is computed by means of relation :

$$c_{p_a}=\frac{(1-x_A)\,c_{p_1}+(b-3x_A)\,c_{p_2}+x_Ac_{p_3}+0.11bc_{p_4}}{(1-x_A)\,M_1+(b-3x_A)\,M_2+x_AM_3+0.11bM_4}, \tag{2}$$

where

$$M_1=78.05\ ;\quad M_2=2\ ;\quad M_3=89.09\ ;\quad M_4=28.02. \tag{3}$$

The molar specific heats of system components, c_{p_i}, are function of temperature having the form :

(4) $$c_{pi}=4\,185.5\,(a_i+b_iT+c_iT^2+d_iT^3),\ (i=1,\,2,\,3\,,\,4).$$

The constants in relation (4) are given in Table 1.

Table 1

Nr.	Component	a_i	b_i	c_i	d_i
1	Benzene	-8.65	0.1158	-7.54×10^{-5}	1.854×10^{-8}
2	Hydrogen	6.88	6.6×10^{-5}	2.78×10^{-7}	0
3	Cyclohexane	-11.53	0.13965	-52.02×10^{-6}	0
4	Nitrogen	6.3	0.001819	-3.45×10^{-7}	0

Inlet benzene molar flow rate is constant and equal to

(5) $$F_A=6.88\times10^{-5}\ \text{Kmol/s}.$$

2.3. Data on Cooling Agent

Boiling water under 3 atm. pressure and temperature

(6) $$T_a=406.16°\text{K}$$

is used as cooling agent.

2.4. Thermodynamic and Kinetic Data

The benzene hydrogenation process follows reaction :

(7) $$C_6H_6+3H_2 \rightleftarrows C_6H_{12},\ \Delta_R H^0_{298}=-49.25\ \text{Kcal/mol}.$$

Standard free energy of reaction is negative up to 560.86°K [2], therefore the hydrogenation process must be effected below this temperature.

The reaction is exothermal, relation between thermal effect and temperature having the form given by K i r c h o f f 's law [3] :

(8) $$\Delta_R H=-18.1875\times10^7-98.4430\times10^3T+49.4977T^2+31.4512\times10^{-3}T^3-19.3998\times10^{-6}T^4.$$

The reaction is a first order one [1] with respect to benzene, thus the reaction rate is

(9) $$-r_A=ky_1.$$

Experimental work has established two separate domains for the rate constant dependence on temperature [1]. Below 393.16°K this dependence takes an exponential form :

(10) $$k=10^3\ \exp\,(e_1+e_2/T).$$

Values of constants e_1 and e_2, computed by means of a linear regression analysis, are :

(11) $$e_1=-3.45\ ;\ e_2=-2\,456.88$$

For temperatures higher than 393.16°K, the rate constant remains unmodified with temperature variation :

$$k = 6.183 \times 10^{-2} \text{ Kmol/m}^3\text{s}. \tag{12}$$

2.5. Simplifyng Assumptions

In the mathematical modeling of reactor the following simplifying assumptions were made :

a) Reactor works in steady-state.

b) Reactor is a plug-flow one. Deviation from ideal plug-flow is the smaller when inner tube diameter is the greater. The effects of this deviation on reacting mass concentration and temperature profiles are negligible compared to those due to radial conductivity and effective radial diffusiveness.

c) Binary mixture of catalyst bed is considered as a continuous homogeneous medium [4]. Papers quoted ([4]...[7]) show this last assumption as able to lead to satisfactory results.

d) Effective axial diffusiveness of components is negligible because $L/d_p > 50$ [6].

e) Effective radial diffusiveness is negligible too. This assumption leads to an one-dimensional model of reactor, giving the axial profiles of concentration and temperature.

3. Balance Equations

3.1. The Material Balance

The material balance relates to benzene concentration.

The inlet molar flow rate of benzene, F_A, is considered as a basis for calculus. The coordinate axis z, having reactor input as origin and reacting mass flow direction as positive direction, is an independent variable, benzene conversion to cyclohexane, $x_A(z)$, and mass reacting temperature, $T(z)$, being the dependent variables.

Taking into account the mentioned assumptions, the differential form of material balance with respect to benzene is given by equation :

$$F_A \frac{dx_A(z)}{dz} = \frac{\pi d^2}{4} N[-r_A(z)]. \tag{13}$$

The equation for reaction rate, according to relation (9), is :

$$-r_A(z) = k \frac{1 - x_A}{1 + 1.11b - 3x_A}. \tag{14}$$

Using Eqs. (13) and (14) we obtain the material balance equation :

$$\frac{dx_A(z)}{dz} = \frac{0.785\, Nk(1 - x_A)d^2}{F_A(1 + 1.11b - 3x_A)}. \tag{15}$$

Since k (Eq. (15)) is a function of temperature and temperature depends on z, the model requires one more equation — the heat balance equation.

3.2. Heat Balance

The heat balance equation of a multitubular reactor cooled by a cooling agent at a constant temperature, is :

$$\frac{dT(z)}{dz} = \frac{(-r_A)(-\Delta_R H)}{Gc_{p_a}} - \frac{4K}{dGc_{p_a}}[T(z)-T_a]. \tag{16}$$

The high heat-transfer coefficients existing between boiling water and steel makes it possible to neglect the shell-side resistance along with the metal tube wall as compared to the internal heat-transfer resistance. Thus, the overall heat-transfer coefficient, K, is given by relation [6] :

$$K=1.1624\,\frac{8\lambda_r\alpha_w}{8\lambda_r+d\alpha_w}. \tag{17}$$

Wall heat-transfer coefficient, α_w, is given by relation :

$$\alpha_w=\alpha_w^0+0.01152\,\frac{d}{d_p}\left(\frac{d_pG}{\mu}\right), \tag{18}$$

where the static contribution, α_w^0, is :

$$\alpha_w^0=\frac{8.4\lambda_r^0}{d^{1.33}}. \tag{19}$$

The diameter of a sphere having the same geometric surface area per unit volume of catalyst particle, $d_p=0.005$ m.

Efective radial thermal conductivity in catalyst bed, λ_r, is :

$$\lambda_r=\lambda_r^0+\frac{0.0025}{1+46\,(d_p/d)^2}\left(\frac{d_pG}{\mu}\right), \tag{20}$$

where the static contribution, λ_r^0, is [1] :

$$\lambda_r^0=0.311 \text{ Kcal/m.h. grad.} \tag{21}$$

Mass flow rate, G, can be computed by equation :

$$G=\frac{F_A(78.05+5.09\,b)}{(\pi d^2/4)N}. \tag{22}$$

Dynamic viscosity of reacting mixture is given by equation :

$$\mu=\frac{\sum_{i=1}^{n} y_iM_i}{\sum_{i=1}^{n} y_iM_i/\mu_i}. \tag{23}$$

Table 2

Nr.	Component	μ_i, [Kg/m.s.]
1	Benzene	110.7×10^{-7}
2	Hydrogen	113.9×10^{-7}
3	Cyclohexane	100.76×10^{-7}
4	Nitrogen	191.6×10^{-7}

Dynamic viscosities of components, μ_i, ($i=1, 2, 3, 4$), computed for temperature $T=433.16$°K, are shown in Table 2 ; molar ratios, y_i, given by Eqs. (1 *a*)...(1 *d*) and molecular mass, M_i, have the values (3).

4. One-Dimensional Model

The one-dimensional model of a catalytic multitubular reactor for benzene hydrogenation to cyclohexane is given by the differential equation system :

$$(24)\quad \begin{cases} \dfrac{dx_A(z)}{dz} = \dfrac{0.785\, k(1-x_A)\, Nd^2}{F_A(1+1.11\, b-3x_A)}, \\ \dfrac{dT(z)}{dz} = \dfrac{k(1-x_A)\,(-\Delta_R H)}{Gc_{Ta}(1+1.11\, b-3x_A)} - \dfrac{4K}{dGc_{Ta}}[T(z)-T_a], \end{cases}$$

with initial conditions :

$$(25)\quad x_A(0)=0,\ T(0)=T_0.$$

5. Conclusions

The solutions of system (24), obtained by numerical integration on computer, lead to the following conclusions :

a) Temperature profile along the tubes has a maximum (hot spot) which increases as internal diameter of tubes increases and inlet hydrogen/benzene ration decreases.

b) The distance of hot spot from reactor input is the greatest as the tubes diameter is the smaller and inlet hydrogen/benzene ratio is the higher.

c) Conversion of benzene in the outlet reacting mixture is the higher as hydrogen/benzene ratio is the smaller and tubes diameter is the larger.

In Fig. 2 the curves $x_A(z)$ and $T(z)$ were drawn for $b=4.15$, $d=0.03$ m, $N=7$ and nominal operating conditions of the reactor, as an exemple.

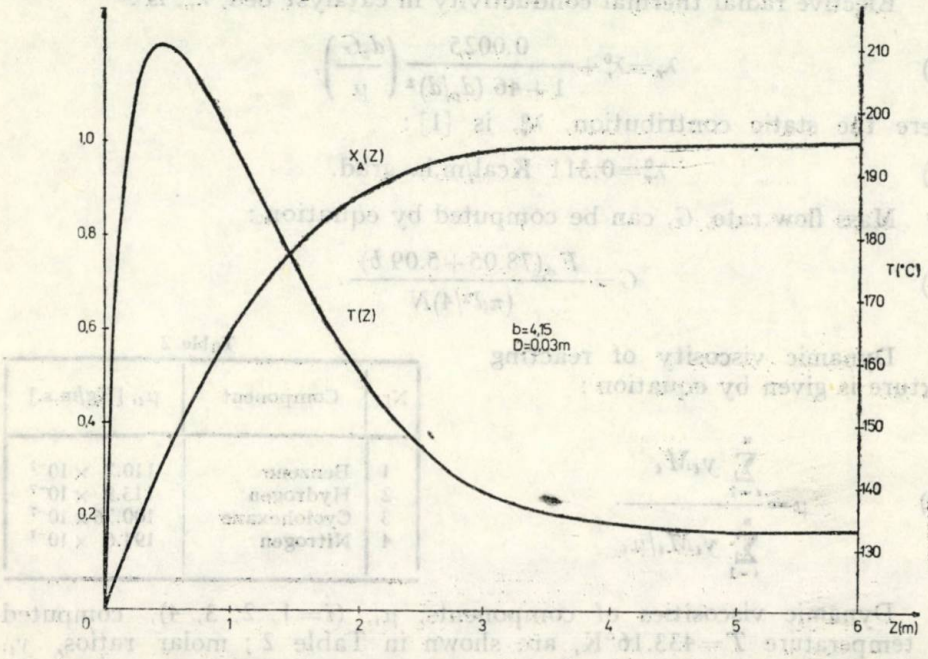

Fig. 2. — Benzene conversion, x_A, and mixture temperature, T, profiles along the tubes.

Notations

a_i, b_i, c_i, d_i — constants in relation (4), where subscripts mean : 1 — benzene ; 2 — hydrogen ; 3 — cyclohexane ; 4 — nitrogen ;
b — hydrogen/benzene molar ratio in feed mixture ;
c_{pa} — specific heat of reacting mixture, [J/kg. grad] ;
c_{pi} — specific heat of reacting mixture components, [J/kmol.grad] ;
d — internal diameter of tubes, [m] ;
d_p — the diameter of a sphere having the same geometric surface area per unit volume of catalyst particle, [m] ;
F_A — inlet benzene molar flow rate, [Kmol/s] ;
G — mass flow rate of feed, [kg/m^2.s] ;
k — reaction rate constant, [Kmol/m^3.s] ;
K — overall heat-transfer coefficient, [J/m^2.s.grad] ;
L — reactor lenght, [m] ;
M_i — molecular mass of reacting mixture components, [kg/Kmol] ;
N — number of tubes ;
r_A — reaction rate relative to benzene, [Kmol/m^3.s] ;
T — reacting mixture temperature, [°K] ;
T_a — cooling agent temperature, [°K] ;
x_A — benzene conversion to cyclohexane ;
y_i — molar ratio of reacting mixture components ;
z — distance from reactor input, [m] ;
α_w — wall heat-transfer coefficient, [Kcal/m^2.h .grad] ;
$\Delta_R H$ — thermal effect of reaction, [J/Kmol] ;
λ_r — effective radial thermal conductivity in catalyst bed, [Kcal/m.h.grad] ;
μ — dynamic viscosity of reacting mixture, [Kg/m.s] ;
μ_i — dynamic viscosity of reacting mixture components, [Kg/m.s.].

Received, June 6, 1981

Polytechnic Institute, Jassy,
Department of Chemical Engineering
and
Research Center for Chemical Threads and Fibres,
Săvinești

REFERENCES

1. Matache S., Ionescu E., Igna M., *Fabricarea ciclohexanului.* Research Center for Chimical Threads and Fibres, Săvinești, 1970.
2. Stephenson R. M., *Introduction to the Chemical Process Industries.* Reinhold Publ. Corp., New York, 1966.
3. Karapetiants M. H., *Exemples and Problems in Chemical Thermodynamics.* Mir Publ., Moscow, 1976.
4. Mihail R., *Modelarea reactoarelor chimice.* Ed. Tehn., Buc., 1976.
5. Rase H. F., *Chemical Reactor Design for Process Plants.* Vol. I, *Principles & Techniques.* John Wiley & Sons, N. Y.—London—Sydney—Toronto, 1977.
6. Rase H. F., *Chemical Reactor Design for Process Plants.* Vol. II, *Case Studies & Design Data.* John Wiley & Sons, N.Y.—London—Sydney—Toronto, 1977.
7. Franks R. G., *Modelarea și simularea în ingineria chimică,* (transl. from English). Ed Tehn., Buc., 1979.

MODELAREA MATEMATICĂ A UNUI REACTOR CATALITIC PENTRU HIDROGENAREA BENZENULUI

(Rezumat)

Se prezintă modelarea matematică, în regim staționar, a unui reactor catalitic multitubular pentru hidrogenarea benzenului la ciclohexan, considerînd curgerea cu deplasare totală și neglijînd dispersia axială și difuzivitatea radială. Modelul este integrat pe calculator, cu date numerice obținute pe o instalație pilot, pentru diverse valori ale raportului molar hidrogen/benzen și al diametrului țevilor reactorului, ca parametri, trasîndu-se profilele conversiei și temperaturii în lungul reactorului.

BULETINUL INSTITUTULUI POLITEHNIC DIN IAŞI
Tomul XXIX (XXXIII), Fasc. 1—4, 1983
Secţia II
CHIMIE şi INGINERIE CHIMICĂ

D.C. 661.846.24

CHEMICAL ENGINEERING RESEARCHES ON THE PROCESS OF $Mg(OH)_2$ PREPARATION

I. THEORETICAL RESEARCHES

BY

LIVIA IFRIM, CORNELIA LEONTE, Al. SZÉP and C. CALISTRU

1. Introduction

Nowadays, magnesium oxide industry is based on the use of two groups of methods, determined by the available raw materials of the productive countries [1]...[3] : a) methods starting from the use of the sea-water ; b) methods processing natural raw materials (magnesite, dolomite) for magnesium compounds.

The methods belonging to the second group are of a great interest for our country, which is the owner of important dolomite vars.

Among the well-known methods which are applied on an industrial scale (the ones belonging to the second group) those in which the technology of obtaining MgO was linked with the ammonia process (Solvay), called for a special attention.

This way, a higher valorification of the raw materials used in the processes, was achieved [4].

The link between the magnesium oxide industry and that of the ammonia process, can be realized by taking into account different technological variants [5]...[11].

This paper is dealing with the research done on the process of the MgO preparation by means of its precipitation with $Ca(OH)_2$ from a solution with some aqueous chlorides, within a technological scheme integrated to the soda manufacture. The link between the two industries is realized by decomposing the solution from heating scruber (RHCD) with dolomitic lime-milk, and the precipitation of $Mg(OH)_2$ is obtained by treating $MgCl_2$ previously obtained with $Ca(OH)_2$ [7].

Due to the generalization which are drawn, the results and the conclusions would be used both for the improvement of the corresponding technological line and for the technological processes, similar to the first ones.

2. The Macrokinetic Mechanism of the Process

The process used in order to obtain $Mg(OH)_2$ within the integrated scheme, can be expressed by means of the following characteristic equation [12] :

$$\{[Ca(OH)_2]_s + [Mg(OH)_2]_s + [A'']_s + [H_2O]_l\}_{susp} +$$
$$+ [MgCl_2 + CaCl_2 + NaCl + NH_4Cl + NH_3 + A'' + H_2O]_l \rightarrow$$
$$\rightarrow \{[Mg(OH)_2]_s + [Ca(OH)_2]_s + [A'']_s + [CaCl_2 + MgCl_2 + NaCl +$$
$$+ NH_4Cl + NH_3 + A'' + H_2O]_l\}_{susp} + [NH_3 + H_2O]_g.$$

As it can be noticed from the characteristic equation, within the final suspension, beside the $Mg(OH)_2$ important component as well as $Ca(OH)_2$, some impurities can appear. The presence of the components over a certain value depreciate the finite product value. Their content may fall down under the admitted limit, by means of assuring a proper quality and relation of the reactant phases. Such conditions are going to be experimentally established.

The elementary processes of transformation, taken into account within the characteristic equation, are the following :

(1) $Ca(OH)_{2[]s} \rightleftarrows Ca(OH)_{2[]l}$, (2) $Ca(OH)_2 + MgCl_2 \rightleftarrows CaCl_2 + Mg(OH)_2$,

(3) $Ca(OH)_2 + 2NH_4Cl \rightleftarrows CaCl_2 + 2NH_3 + 2H_2O$,

(4) $Mg(OH)_{2[]l} \rightleftarrows Mg(OH)_{2[]s}$, (5) $NH_{3[]l} \rightleftarrows NH_{3[]g}$, (6) $H_2O_{[]l} \rightleftarrows H_2O_{[]g}$.

$Mg(OH)_2$ precipitation process can take place after one of the following macrokinetic mechanisms :

a) $Ca(OH)_2$ dissolution — a double exchange reaction including the formation and growth of $Mg(OH)_2$ germs (f.g.g.).

b) $MgCl_2$ adsorbtion on the $Ca(OH)_2$ grain — the double exchange reaction — $Mg(OH)_2$ germs formation and growth.

The structural schemes present in each of two possible mechanisms are presented in Figs. 1 and 2, respectively :

$$\text{—Diss. } Ca(OH)_2 \rightarrow -T_{Ca(OH)_{2[]l}} \rightarrow \Big| -m \rightarrow -\text{rch} \rightarrow -\text{f.g.g.}_{[]s} \rightarrow$$
$$\text{———} T_{MgCl_{2[]l}} \text{———————} \rightarrow \Big|$$

Fig. 1 .— Macrokinetic mechanism for $Mg(OH)_2$ precipitation process (I).

$$-T_{MgCl_{2[]l}} \rightarrow -T_{MgCl_{2[]ash}} \rightarrow -\text{Ads} \rightarrow -\text{rch} \rightarrow -\text{f.g.g.}_{[]s} \rightarrow$$

Fig. 2. — Macrokinetic mechanism for $Mg(OH)_2$ precipitation process (II).

The realization of the process, taking into account one of the two mechanisms, is determined by the real conditions of its achievement. In practice, this aspect has a special importance due to its implications regarding both the rate of the global precipitation process and the quality of the obtained $Mg(OH)_2$. Thus, under the conditions in which the process takes place, following the : dissolution — reaction — formation and germs growth mechanism, the new phase appears in the liquid volume. Under the conditions in which the process develops following the adsorbtion — reaction — formation and germs growth mechanism, $Mg(OH)_2$ is formed on calcium hydroxide grains, in a crust (ash) form.

3. Process Stoichiometry

In order to get a complete stoichiometric definition of the reaction mass, the Eqs. (1)...(6) defining the elementary transformation processes, previously reported, must be taken into account. The description of the process at this level seems to be sufficiently complex, showing a series of difficulties in the material balance calculation of the reaction — mass components and phases.

By introducing some simplification which do not obviously affect the material balance, the $Mg(OH)_2$ precipitation process can be expressed by means of not more that three independent equations, namely :

(7) $$MgCl_2+Ca(OH)_2 \rightleftarrows Mg(OH)_2+CaCl_2,$$

(8) $$2NH_4Cl+Ca(OH)_2 \rightleftarrows CaCl_2+2NH_3+2H_2O, \quad (9)\ NH_{3[]l} \rightleftarrows NH_{3[]g}.$$

In this case, the changes that take place within the reaction—mass could be expressed by means of the degrees of transformation, defined as it follows :

$$\eta_{MgCl_2}=\frac{m^{01}_{MgCl_2}-m^{1}_{MgCl_2}}{m^{01}_{MgCl_2}}=\frac{m^{01}_{Ca(OH)_2}-m^{1}_{Ca(OH)_2}}{\frac{M_{Ca(OH)_2}}{M_{MgCl_2}}m^{01}_{MgCl_2}}=$$

$$=\frac{m^{1}_{CaCl_2}-m^{01}_{CaCl_2}}{\frac{M_{CaCl_2}}{M_{MgCl_2}}m^{01}_{MgCl_2}}=\frac{m^{1}_{Mg(OH)_2}-m^{01}_{Mg(OH)_2}}{\frac{M_{Mg(OH)_2}}{M_{MgCl_2}}m^{01}_{MgCl_2}},$$

$$\eta_{NH_4Cl}=\frac{m^{02}_{NH_4Cl}-m^{2}_{NH_4Cl}}{m^{02}_{NH_4Cl}}=\frac{m^{02}_{Ca(OH)_2}-m^{2}_{Ca(OH)_2}}{\frac{M_{Ca(OH)_2}}{2M_{NH_4Cl}}m^{02}_{NH_4Cl}}=$$

$$=\frac{m^{2}_{NH_3}-m^{02}_{NH_3}}{\frac{M_{NH_3}}{M_{NH_4Cl}}m^{02}_{NH_4Cl}}=\frac{m^{2}_{CaCl_2}-m^{02}_{CaCl_2}}{\frac{M_{CaCl_2}}{2M_{NH_4Cl}}m^{02}_{NH_4Cl}}=\frac{m^{2}_{H_2O}-m^{02}_{H_2O}}{\frac{M_{H_2O}}{2M_{NH_4Cl}}m^{02}_{NH_4Cl}},$$

$$\eta_{NH_3}=\frac{m^{03}_{NH_3[]l}-m^{3}_{NH_3[]l}}{m^{03}_{NH_3[]l}}=\frac{m^{3}_{NH_3[]g}}{m^{03}_{NH_3[]l}}.$$

The balance equation on components and phases are obtained by means of substitution and explanation. These are expressed by using the values of the degrees of transformation and are presented in Table 1. For a most operative usage of mathematical models of the material balance for the scientific management of the process it is necessary that these were expressed by means of values which are directly determined. Such values, which are called „parameters for material balance", must be determined experimentaly. They are : $\bar{x}_{CaCl_2[]l}$, $\bar{x}_{MgCl_2[]l}$, $\bar{x}_{NH_3[]l}$.

The transformation relations between the two modes of presentation are the following :

Table 1
Primary Equations for Material Balance

Phase	Component	Balance equations
Solid	$Mg(OH)_2$	$m_{Mg(OH)_{2[]s}} = m^0_{Mg(OH)_{2[]s}} + \frac{M_{Mg(OH)_2}}{M_{MgCl_2}} m^0_{MgCl_{2[]l}} \eta_{MgCl_2}$
	$Ca(OH)_2$	$m_{Ca(OH)_{2[]s}} = m^0_{Ca(OH)_{2[]s}} - \frac{M_{Ca(OH)_2}}{M_{MgCl_2}} m^0_{MgCl_{2[]l}} \eta_{MgCl_2} - \frac{M_{Ca(OH)_2}}{2M_{NH_4Cl}} m^0_{NH_4Cl_{[]l}} \eta_{NH_4Cl}$
	A″	$m_{A''_{[]s}} = m^0_{A''_{[]s}}$
	Total	$m_{[]s} = m^0_{[]s} + \frac{M_{Mg(OH)_2}}{M_{MgCl_2}} m^0_{MgCl_{2[]l}} \eta_{MgCl_2} - \frac{M_{Ca(OH)_2}}{M_{MgCl_2}} m^0_{MgCl_{2[]l}} \eta_{MgCl_2} - \frac{M_{Ca(OH)_2}}{2M_{NH_4Cl}} m^0_{NH_4Cl_{[]l}} \eta_{NH_4Cl}$
Liquid	$MgCl_2$	$m_{MgCl_{2[]l}} = m^0_{MgCl_{2[]l}} (1 - \eta_{MgCl_2})$
	$CaCl_2$	$m_{CaCl_{2[]l}} = m^0_{CaCl_{2[]l}} + \frac{M_{CaCl_2}}{M_{MgCl_2}} m^0_{MgCl_{2[]l}} \eta_{MgCl_2} + \frac{M_{CaCl_2}}{2M_{NH_4Cl}} m^0_{NH_4Cl_{[]l}} \eta_{NH_4Cl}$
	NH_4Cl	$m_{NH_4Cl_{[]l}} = m^0_{NH_4Cl_{2[]l}} (1 - \eta_{NH_4Cl})$
	NaCl	$m_{NaCl_{[]l}} = m^0_{NaCl_{[]l}}$
	H_2O	$m_{H_2O} = m^0_{H_2O_{[]l}} + \frac{M_{H_2O}}{M_{NH_4Cl}} m^0_{NH_4Cl_{[]l}} \eta_{NH_4Cl} + m^0_{H_2O_{[]l susp}}$
	NH_3	$m_{NH_{3[]l}} = \left(m^0_{NH_{3[]l}} + \frac{M_{NH_3}}{M_{NH_4Cl}} m^0_{NH_4Cl_{[]l}} \eta_{NH_4Cl} \right) (1 - \eta_{NH_3})$
	A″	$m_{A''_{[]l}} = m^0_{A''_{[]l}}$
	Total	$m_{[]l} = m^0_{[]l} + m^0_{MgCl_{2[]l}} \eta_{MgCl_2} \frac{M_{CaCl_2} - M_{MgCl_2}}{M_{MgCl_2}} + m^0_{H_2O_{[]l susp}} + m^0_{NH_4Cl_{[]l}} \eta_{NH_4Cl} \frac{M_{CaCl_2} - 2M_{NH_4Cl} + 2M_{H_2O} + 2M_{NH_3}}{2M_{NH_4Cl}} - m^0_{NH_{3[]l}} + \frac{M_{NH_3}}{M_{NH_4Cl}} m^0_{NH_4Cl} \eta_{NH_4Cl} \eta_{NH_{3[]l}}$
Gaz-eous	NH_3	$m_{NH_{3[]g}} = \left(m^0_{NH_{3[]l}} + \frac{M_{NH_3}}{M_{NH_4Cl}} m^0_{NH_4Cl_{[]l}} \eta_{NH_4Cl} \right) \eta_{NH_{3[]l}}$

Table 2

Secondary Equations for Material Balance

Phase	Component	Balance equations
Solid	$Mg(OH)_2$	$m_{Mg(OH)_2} = m^0_{Mg(OH)_2[]s} + \frac{M_{Mg(OH)_2}}{M_{MgCl_2}} (m^0_{[]l} \bar{x}^0_{MgCl_2[]l} - m_{[]l} \bar{x}_{MgCl_2[]l})$
	$Ca(OH)_2$	$m_{Ca(OH)_2[]s} = m^0_{Ca(OH)_2[]s} - \frac{M_{Ca(OH)_2}}{M_{CaCl_2}} (m_{[]l} \bar{x}_{CaCl_2[]l} - m^0_{[]l} \bar{x}^0_{CaCl_2[]l})$
	A''	$m_{A''[]s} = m^0_{A''[]s}$
	Total	$m_{[]s} = m^0_{[]s} + m^0_{[]l} \left(\frac{M_{Ca(OH)_2}}{M_{CaCl_2}} \bar{x}^0_{CaCl_2[]l} + \frac{M_{Mg(OH)_2}}{M_{MgCl_2}} \bar{x}^0_{MgCl_2[]l} \right) - m_{[]l} \left(\frac{M_{Ca(OH)_2}}{M_{CaCl_2}} \bar{x}_{CaCl_2[]l} + \frac{M_{Mg(OH)_2}}{M_{MgCl_2}} \bar{x}_{MgCl_2[]l} \right)$
Liquid	$MgCl_2$	$m_{MgCl_2[]l} = m_{[]l} \bar{x}_{MgCl_2[]l}$
	$CaCl_2$	$m_{CaCl_2[]l} = m_{[]l} \bar{x}_{CaCl_2[]l}$
	NH_3	$m_{NH_3[]l} = m_{[]l} \bar{x}_{NH_3[]l}$
	A''	$m_{A''[]l} = m^0_{A''[]l}$
	NH_4Cl	$m_{NH_4Cl} = m^0_{[]l} \left(\bar{x}^0_{NH_4Cl[]l} + \frac{2M_{NH_4Cl}}{M_{CaCl_2}} \bar{x}^0_{CaCl_2[]l} + \frac{2M_{NH_4Cl}}{M_{MgCl_2}} \bar{x}^0_{MgCl_2[]l} \right) - m_{[]l} \left(\frac{2M_{NH_4Cl}}{M_{CaCl_2}} \bar{x}_{CaCl_2[]l} + \frac{2M_{NH_4Cl}}{M_{MgCl_2}} \bar{x}_{MgCl_2[]l} \right)$
	H_2O	$m_{H_2O} = m^0_{H_2O[]l} + m^0_{H_2O[]l\,susp} - \frac{2M_{H_2O}}{M_{CaCl_2}} \left(m^0_{[]l} x^0_{CaCl_2[]l} - m_{[]l} \bar{x}_{CaCl_2[]l} \right) - \frac{2M_{H_2O}}{M_{MgCl_2}} \left(m^0_{[]l} \bar{x}^0_{MgCl_2[]l} - m_{[]l} \bar{x}_{MgCl_2[]l} \right)$
	Total	$m_{[]l} = \frac{m^0_{[]l} \left(1 - \bar{x}^0_{NH_3[]l} - \frac{M_{Ca}}{M_{CaCl_2}} x^0_{CaCl_2[]l} - \frac{M_{Mg}}{M_{MgCl_2}} \bar{x}^0_{MgCl_2[]l} \right) + m^0_{H_2O[]l\,susp}}{1 - \bar{x}_{NH_3[]l} - \frac{M_{Ca}}{M_{CaCl_2}} \bar{x}_{CaCl_2[]l} - \frac{M_{Mg}}{M_{MgCl_2}} \bar{x}_{MgCl_2[]l}}$
Gaz-eous	NH_3	$m_{NH_3[]g} = m^0_{[]l} \left(\bar{x}^0_{NH_3[]l} - \frac{2M_{NH_3}}{M_{CaCl_2}} \bar{x}^0_{CaCl_2[]l} - \frac{2M_{NH_3}}{M_{MgCl_2}} \bar{x}^0_{MgCl_2[]l} \right) - m_{[]l} \left(\bar{x}_{NH_3[]l} - \frac{2M_{NH_3}}{M_{CaCl_2}} \bar{x}_{CaCl_2[]l} - \frac{2M_{NH_3}}{M_{MgCl_2}} \bar{x}_{MgCl_2[]l} \right)$

$$m^0_{MgCl_2[]l}\eta_{MgCl_2}=m^0_{[]l}\bar{x}^0_{MgCl_2}-m_{[]l}\bar{x}_{MgCl_2[]l},$$

$$m_{NH_4Cl[]l}\eta_{NH_4Cl}=\frac{2M_{NH_4Cl}}{M_{CaCl_2}}(m_{[]l}\bar{x}_{CaCl_2[]l}-m^0_{[]l}\bar{x}^0_{CaCl_2[]l}-$$

$$-\frac{2M_{NH_4Cl}}{M_{MgCl_2}}(m^0_{[]l}\bar{x}^0_{MgCl_2[]l}-m_{[]l}\bar{x}_{MgCl_2[]l}),$$

$$\left(m^0_{NH_3[]l}+\frac{M_{NH_3}}{M_{NH_4Cl}}m^0_{NH_4Cl}\right)\eta_{NH_4Cl}\eta_{NH_3}=m^0_{[]l}\left(\bar{x}^0_{NH_3}-\frac{2M_{NH_3}}{M_{CaCl_2}}\bar{x}^0_{CaCl_2}-\right.$$

$$\left.-\frac{2M_{NH_3}}{M_{MgCl_2}}\bar{x}^0_{MgCl_2[]l}\right)-m_{[]l}\bar{x}_{NH_3[]l}-\frac{2M_{NH_3}}{M_{CaCl_2}}\bar{x}_{CaCl_2[]l}-\frac{2M_{NH_3}}{M_{MgCl_2}}\bar{x}_{MgCl_2[]l}.$$

By substitution we get the mathematical models of the material balance, expressed in a secondary form, which are reported in Table 2.

The checking up of the mathematical models for the material balance was achieved by drawing out the real balance of the process, for a pilot unit. For its materialization, the following values of the „parameters" were used :

$$\bar{x}_{CaCl_2[]l}=0.03643,\ \bar{x}_{MgCl_2[]l}=0.0002,\ \bar{x}_{NH_3[]l}=0.0041.$$

Table 3

Real Material Balance

Admitted materials				Evacuated materials			
Phase	Component	$m^0_{A_i}$	$\bar{x}^0_{A_i}$	Phase	Component	m_{A_i}	$\bar{x}_A$
Liquid	$MgCl_2$	12.336	0.01028	Liquid	$MgCl_2$	0.3688	0.00020
	$CaCl_2$	50.82	0.04235		$CaCl_2$	67.1811	0.03643
	NH_4Cl	2.352	0.00196		NH_4Cl	0.016824	0.000009123
	NH_3	7.188	0.00599		NH_3	7.56087	0.0041
	NaCl	94.344	0.07862		NaCl	94.344	0.051159
	H_2O	1 032.96	0.8608		H_2O	1 674.6446	0.90810
	Total	1 200.00	1		Total	1 844.1162	1
Suspension	$Ca(OH)_2$	11.2239	0.01700	Solid	$Ca(OH)_2$	0.31652	0.0204
	$Mg(OH)_2$	7.8771	0.01194		$Mg(OH)_2$	15.1980	0.9796
	H_2O	640.8989	0.97106		Total	15.5145	1
	Total	660	1	Gazeous	NH_3	0.36914	1
Total		1 860	—	Total		1 860	—

The results which were obtained were reported in Table 3. Analysing the data reported in these table one can drawn the conclusion that the proposed mathematical models describes with a great accuracy the analysed process. This fact allows us to use it as an efficient and operative instrument in the scientific management of the process. The parameters which are necessary in the concretization of the material balance are of a small number and can be easily determined by means of higher control analysis of the process.

Table 4

The Macrokinetic Modelling of $Mg(OH)_2$ Precipitation Process

Macrokinetic mechanism	Macrokinetic model	Model Equation	The condition assuring such a performance of the process	The place of $Mg(OH)_2$ precipitation
A process of dissolution — reaction — germs formation and growth-type	Dissolution $Ca(OH)_2$	$-\bar{r}_D = -\frac{dn_{Ca(OH)_2}}{S\,d\tau} = k_D C_{Ca(OH)_2}$	$r_m \ll r(ch+f.g.g_{[]s})$ $r_D \ll r_T(Ca(OH)_2+MgCl_2)$	On the grain surface with ash formation
	Transfer $Ca(OH)_{2[]l}$	$-r_T = -\frac{dn_{Ca(OH)_2}}{S\,d\tau} = k_T C_{Ca(OH)_2}$	$r_m \ll r\ (ch+f.g.g_{[]s})$ $r_{T\,Ca(OH)_2} \ll r_D$ $r_{T\,MgCl_2} \gg r_{T\,Ca(OH)_2}$	Inside the liquid phase
	Transfer $MgCl_{2[]l}$	$-r_T = -\frac{dn_{MgCl_2}}{S\,d\tau} = k_T C_{MgCl_2}$	$r_m \ll r(ch+f.g.g_{[]s})$ $r_{T MgCl_2} \ll r_D,\ r_{T Ca(OH)_2}$	Inside the liquid phase
	Transformation process $(m-r_{ch}-f.g.g_{[]s})$	$-r_{ch} = -\frac{dn_{Ca(OH)_2}}{S\,d\tau} = k_T C^m_{Ca(OH)_2} C^n_{MgCl_2}$ $\frac{dV_{[]s}}{(1-V_{[]s})d\tau} = V_p \frac{dN_p}{dV_{[]l}} + N_p \frac{dV_p}{d\tau}$	$r_m \gg r(ch+f.g.g_{[]s})$	Inside the liquid phase
A process of an adsorbtion—reaction—germs formation and growth type	Transfer $MgCl_{2[]l}$	$-\bar{r}_T = -\frac{dn_{MgCl_2}}{S\,d\tau} = k_T C_{MgCl_2}$	$\bar{r}_{tr} \gg \bar{r}_T$ $\bar{r}_{T MgCl_2} \ll \bar{r}_{T MgCl_2[]ash}$	On the surface of the unreacted core
	Transfer $MgCl_{2[]l\,ash}$	$-\bar{r}_T = -\frac{dn_{MgCl_2}}{S\,d\tau} = -D\frac{dC_{MgCl_2}}{dr}$	$\bar{r}_{tr} \gg \bar{r}_T$ $r_{T MgCl_2} \gg \bar{r}_{T MgCl_2[]ash}$	On the surface of the unreacted core
	Transformation process (ads.$-r_{ch}-f.g.g_{[]s}$)	$-r_{Ca(OH)_2} = -\frac{dn_{Ca(OH)_2}}{S\,d\tau} = k_r C^m_{Ca(OH)_2} C^n_{MgCl_2}$	$r_{tr} \ll \bar{r}_T$	On the surface of the unreacted core or inside a certain area

4. The Macrokinetic and Mathematic Modelling of the Process

4.1. Possible Macrokinetic Models

Within the two possible macrokinetic mechanisms employed in the proceeding of the precipitation process, we can notice that the average process can take place by a series of simple or combined macrokinetic models.

The main macrokinetic simple models, employed in the precipitation process and the corresponding kinetic equations are presented in Table 4.

Beside the simple macrokinetic models, the precipitation process can take place by using the combined macrokinetic models of the type : $Ca(OH)_2$ disolving — $Ca(OH)_2$ transfer, $MgCl_2$ transfer — $Ca(OH)_2$ transfer, a.s.o.

For a practical achievement of the double-exchange process we are especially interested in the quality of $Mg(OH)_2$ precipitate, concerning both the purity, the sedimentation and filtration characteristics.

Under the specified conditions of the reaction mass structure, the following could be taken for some limit-steps : $Ca(OH)_2$ dissolution and the formation and growth of the new phase germs. As our intention is to obtain a precipitate with a certain grain structure and at the same time, as pure as possible, the necessary limit step of the process must be that one corresponding to the $Mg(OH)_2$ germs formation and growth.

By means of this model, the factors with a special influence on the process achievement will be underlined, and, in consequence, the ways in which one could obtain a product with imposed characteristics will be shown.

5. Conclusions

It was studied the process of $Mg(OH)_2$ preparation with $Ca(OH)_2$ in a solution which contains chlorines.

The main macrokinetic mechanisms of the process are established ; the corresponding macrokinetic models are underlinden and, consequently, the implications in its practical achievement are shown.

The mathematical models for the material balance are elaborated and the minimal number of the measurements that must be done for a stoichiometric definition of the reaction — mass are specified.

Notations

Dis — dissolution,
T — transfer,
n — number of moles,
x — mole fraction,
$\bar{x}$ — mass fraction,
η — transforming degree,
A″ — inert products,

r_{ch} — rate of chemical reaction
r_T — rate of transfer process
r_{tr} — rate of overall transformation process (mixing—reaction f.g.g.)
K_r — chemical reaction rate constant,
K_D — dissolution rate constant,
K_T — mass transfer coefficient,
m — mixing.

Indices

l, s, g — liquid, solid, gas,
[] — phase symbol,
0 — initial value

Received, April 30, 1981

Polytechnic Institute, Jassy, Department of Inorganic Substances Technology and Building Materials

REFERENCES

1. Позин М. Е., *Технология минеральных солей*. Госхимиздат, М., 1967.
2. Pascal P., *Nouveau traité de chimie minérale*. Vol. IV, Paris, 1958.
3. Winnacker K., Kuchler L., *Tehnologia chimică anorganică*, (transl. from German). Vol. I, Ed. Tehn., Buc., 1962.
4. * * * *Ullmanns Encyclopädie der Technischen Chemie*. Bd. 12, Berlin, 1960, 91.
5. Kiss St., Lazăr A., Paczai V., Patent R.S.R., nr. *59 717*, 1975.
6. Hints M., Bîrzu D., Revista de chimie, *6*, 509 (1977).
7. Kiss Şt., Lazăr A., Suciu A., Hopîrteanu E., Patent R.S.R., nr. *59779*, 1975.
8. Kiss Şt., Lazăr A., Mînăscurtă V., Suciu I., Hopîrteanu E., Patent R.S.R., nr. *59 631*, 1975.
9. Карпенко В. Г., Патент СССР, № *4 473*, 1964.
10. Kiss Şt., Lazăr A., Mînăscurtă V., Hopîrteanu E., Suciu I., Patent R.S.R., nr. *59 776*, 1976.
11. Беляев Е. К., Тр. науки и проект. инст. осн. химии, *47*, 7—13 (1978).
12. Calistru C., Leonte C., *Tehnologia substanţelor anorganice*. EDP, Buc., 1972.

CERCETĂRI DE INGINERIE CHIMICĂ ÎN CADRUL PROCESULUI DE OBŢINERE A $Mg(OH)_2$

I. Cercetări teoretice

(Rezumat)

Se cercetează procesul obţinerii $Mg(OH)_2$ prin precipitarea $MgCl_2$ cu $Ca(OH)_2$ în cadrul unei scheme tehnologice grefate cu industria sodei amoniacale.

Se stabilesc mecanismele macrocinetice după care este posibil să se desfăşoare procesul de precipitare şi implicaţiile pe care acestea le pot avea asupra calităţii precipitatului obţinut.

Se elaborează modelele matematice de bilanţ de masă într-o formă care permite utilizarea acestora ca un instrument eficient şi rapid de conducere ştiinţifică a procesului de precipitare.

BULETINUL INSTITUTULUI POLITEHNIC DIN IAŞI
Tomul XXIX (XXXIII), Fasc. 1—4, 1983
Secţia II
CHIMIE şi INGINERIE CHIMICĂ

CZ. 542. 943. 7; 639. 841. 8

CONTROLUL PROCESULUI DE OXIDARE CATALITICĂ A AMONIACULUI PRIN INTERMEDIUL MODELELOR MATEMATICE DE BILANŢ

DE

CAROLINA HAGIU şi C. CALISTRU

1. Introducere

Oxidarea catalitică a amoniacului — proces chimic fundamental în tehnologia acidului azotic — se realizează la scară industrială utilizînd catalizatori pe bază de platină, reacţiile principale fiind următoarele:

(1) $4NH_3+5O_2=4NO+6H_2O$, (2) $4NH_3+3O_2=2N_2+6H_2O$, (3) $4NH_3+4O_2=2N_2O+6H_2O$.

Pe lîngă reacţiile (1)...(3) pot avea loc procese secundare de descompunere a amoniacului, a oxidului de azot sau de interacţiune între amoniac şi oxid de azot.

Procesul industrial trebuie astfel condus încît să se desfăşoare cu precădere după reacţia (1); Savenkov [1], cercetînd selectivitatea catalizatorilor pe bază de platină, ajunge la concluzia că posibilitatea formării protoxidului de azot este neglijabilă, chiar în condiţiile unei cantităţi insuficiente de oxigen. Borisova [2], [3], Zasorin [4], [5] şi Atroşcenko [6], [7] cercetează procesul de oxidare a amoniacului considerînd că se desfăşoară numai după reacţia (1). Practica industrială demonstrează, însă, că pe catalizatori platină—rhodiu, gradul maxim de transformare a amoniacului în oxid de azot după reacţia (1) este de 97...98%, restul de amoniac transformîndu-se în azot elementar (reacţia (2)), astfel încît amestecul de gaze rezultat din reactor nu conţine amoniac. În aceste condiţii, pentru calculul bilanţului de masă şi termic al procesului este necesar să se ia în consideraţie desfăşurarea simultană a reacţiilor (1) şi (2).

În literatura consacrată procesului de oxidare catalitică a amoniacului [1]...[10] sînt puţine indicaţii referitoare la ecuaţiile necesare pentru calculul bilanţului de masă şi termic în acest proces; în majoritatea cazurilor se utilizează pentru calculul gradului de transformare ecuaţia:

$$\alpha=\frac{C^0_{NH_3}-C_{NH_3}}{C^0_{NH_3}}\cdot 100 \tag{4}$$

şi se corelează gradul de transformare (α) de parametrii tehnologici (temperatură, presiune) şi constructivi (diametrul reactorului, numărul de site şi caracteristicile acestora) [2]...[5] prin intermediul unei ecuaţii cinetice de ordinul 1 [8], [9], [5]. Este evident că ecuaţia (4) poate fi utilizată numai în condiţiile în care se presupune desfăşurarea procesului fără variaţie de volum.

În [10] se prezintă modelele matematice secundare de bilanţ de masă pentru procesul de oxidare catalitică a amoniacului, considerînd desfăşurarea lui după reacţiile independente (1) şi (2), mărimile necesare utilizării acestora fiind conţinutul de oxid de azot şi azot în gazele formate.

Azotul fiind un compus greu de analizat iar în instalaţiile industriale determinîndu-se efectiv oxidul de azot şi oxigenul, se impune cunoaşterea

modelelor matematice de bilanț de masă, exprimate în funcție de aceste mărimi.

De asemenea este necesară cunoașterea modelelor matematice de bilanț termic care oferă posibilitatea calculului conținutului caloric al gazelor rezultate din reactor, respectiv a cantității de abur ce poate fi obținută prin recuperarea căldurii.

În cele ce urmează se elaborează modelele matematice de bilanț de masă și termic pentru procesul de oxidare catalitică a amoniacului considerînd desfășurarea simultană a reacțiilor (1) și (2), mărimile necesare utilizării acestora fiind cele care se determină efectiv în instalația industrială (x_{NO} și x_{O_2}) ; se verifică valabilitatea modelelor matematice elaborate și se concretizează modul de utilizare a acestora pe baza datelor experimentale industriale.

Se stabilește o ecuație pentru calculul gradului de transformare a amoniacului în oxid de azot luînd în considerație și variația de volum în desfășurarea procesului.

2. Model matematic de bilanț de masă

Considerînd desfășurarea simultană a reacțiilor (1) și (2), se definesc gradele de transformare :

$$(5)\qquad \eta_{NH_3}^{NO}=\eta_1=\frac{n_{NH_3}^{01}-n_{NH_3}^{1}}{n_{NH_3}^{01}}=\frac{n_{O_2}^{01}-n_{O_2}^{1}}{\frac{5}{4}n_{NH_3}^{01}}=\frac{n_{NO}}{n_{NH_3}^{01}}=\frac{n_{H_2O}^{1}}{\frac{3}{2}n_{NH_3}^{01}},$$

$$(6)\qquad \eta_{NH_3}^{N_2}=\eta_2=\frac{n_{NH_3}^{02}-n_{NH_3}^{2}}{n_{NH_3}^{02}}=\frac{n_{O_2}^{02}-n_{O_2}^{2}}{\frac{3}{4}n_{NH_3}^{02}}=\frac{n_{N_2}-n_{N_2}^{0}}{\frac{1}{2}n_{NH_3}^{02}}=\frac{n_{H_2O}^{2}}{\frac{3}{2}n_{NH_3}^{02}}$$

și relațiile de concretizare :

$$(7)\qquad n_{NH_3}^{0}=n_{NH_3}^{01}+n_{NH_3}^{02},\quad n_{NH_3}=n_{NH_3}^{1}+n_{NH_3}^{2},\quad n_{O_2}^{0}=n_{O_2}^{01}+n_{O_2}^{02},$$
$$n_{O_2}=n_{O}^{1}+n_{O_2}^{2},\quad n_{H_2O}=n_{H_2O}^{1}+n_{H_2O}^{2}.$$

Prin intermediul ecuațiilor (5)...(7) se stabilesc modelele matematice primare de bilanț de masă prezentate în tabelul 1.

Modelele matematice primare de bilanț nu pot fi utilizate pentru calculul bilanțurilor de masă, mărimile $n_{NH_3}^{01}$ și $n_{NH_3}^{02}$ neputînd fi determinate experimental. Ele se utilizează numai ca expresii intermediare pentru stabilirea modelelor matematice secundare de bilanț exprimate prin mărimi determinabile experimental. Ca mărimi determinabile se aleg conținutul în oxid de azot (x_{NO}) și în oxigen (x_{O_2}), care se determină efectiv în instalațiile industriale.

Din ecuațiile primare de bilanț pentru componentele O_2 și NO, prezentate în tabelul 1, rezultă următoarele relații de transformare :

$$(8)\qquad n_{NH_3}^{01}\eta_1=n_{NO}\ \text{ și }\ n_{NH_3}^{02}\eta_2=\frac{4}{3}n_{O_2}^{0}-\frac{4}{3}n_{O_2}-\frac{5}{3}n_{NO}.$$

Tabelul 1

Modele matematice primare de bilanţ de masă

Componentul	Modelul de bilanţ, [kmol/h]
NH_3	$n_{NH_3}=n^0_{NH_3}-n^{01}_{NH_3}\eta_1-n^{02}_{NH_3}\eta_2$
O_2	$n_{O_2}=n^0_{O_2}-\frac{5}{4}n^{01}_{NH_3}\eta_1-\frac{3}{4}n^{02}_{NH_3}\eta_2$
NO	$n_{NO}=n^{01}_{NH_3}\eta_1$
H_2O	$n_{H_2O}=\frac{3}{2}(n^{01}_{NH_3}\eta_1+n^{02}_{NH_3}\eta_2)$
N_2	$n_{N_2}=n^0_{N_2}+\frac{1}{2}n^{02}_{NH_3}\eta_2$
A″	$n_{A''}=n^0_{A''}$
Total	$n_{[]g}=n^0_{[]g}+\frac{1}{4}(n^{01}_{NH_3}\eta_1+n^{02}_{NH_3}\eta_2)$

Utilizînd relaţiile (8) şi modelele matematice primare de bilanţ (tab. 1) se elaborează modelele matematice secundare de bilanţ de masă prezentate în tabelul 2.

Practica industrială demonstrează că faza gazoasă rezultată din reactorul de oxidare catalitică a amoniacului nu conţine amoniac, acesta transformîndu-se total în oxid de azot. În aceste condiţii, din egalitatea :

$$n_{NH_3}=n^0_{NH_3}-\frac{4}{3}n^0_{O_2}+n_{[]g}\left(\frac{4}{3}x_{O_2}+x_{NO}\right)=0 \tag{9}$$

rezultă :

$$n_{O_2}=n^0_{O_2}-\frac{3}{4}n^0_{NH_3}-\frac{1}{2}n_{NO} \tag{10}$$

şi modelele matematice secundare de bilanţ de masă au forma prezentată în tabelul 3.

Pentru utilizarea ecuaţiilor prezentate în tabelul 3, în calculul bilanţului de masă, este necesară cunoaşterea, pe lîngă mărimile iniţiale, a conţinutului de oxid de azot (x_{NO}) în gazele rezultate din reactorul de oxidare.

Prin intermediul ecuaţiilor din tabelul 3 se stabileşte relaţia pentru calculul gradului de oxidare a amoniacului în oxid de azot :

$$\eta^{NO}_{NH_3}=\frac{\left(1+\frac{1}{4}x^0_{NH_3}\right)x_{NO}}{x^0_{NH_3}}. \tag{11}$$

Tabelul 2

Modele matematice secundare de bilanț de masă (forma a)

Componentul	Modelul de bilanț, [kmol/h]
NH_3	$n_{NH_3}=n^0_{[]g}\left[x^0_{NH_3}-\frac{4}{3}x^0_{O_2}+\frac{\left(\frac{4}{3}x_{O_2}+\frac{2}{3}x_{NO}\right)\left(1+\frac{1}{3}x^0_{NO}\right)}{1+\frac{1}{3}x_{O_2}+\frac{1}{6}x_{NO}}\right]$
O_2	$n_{O_2}=\frac{n^0_{[]g}\left(1+\frac{1}{3}x^0_{O_2}\right)x_{O_2}}{1+\frac{1}{3}x_{O_2}+\frac{1}{6}x_{NO}}$
NO	$n_{NO}=\frac{n^0_{[]g}\left(1+\frac{1}{3}x^0_{O_2}\right)x_{NO}}{1+\frac{1}{3}x_{O_2}+\frac{1}{6}x_{NO}}$
H_2O	$n_{H_2O}=n^0_{[]g}\left[x^0_{H_2O}+2x^0_{O_2}-\frac{\left(1+\frac{1}{3}x^0_{O_2}\right)(x_{O_2}+x_{NO})}{1+\frac{1}{3}x_{O_2}+\frac{1}{6}x_{NO}}\right]$
N_2	$n_{N_2}=n^0_{[]g}\left[x^0_{N_2}+\frac{2}{3}x^0_{O_2}-\frac{\left(1+\frac{1}{3}x^0_{O_2}\right)\left(\frac{2}{3}x_{O_2}+\frac{5}{6}x_{NO}\right)}{1+\frac{1}{3}x_{O_2}+\frac{1}{6}x_{NO}}\right]$
A″	$n_{A''}=n^0_{[]g}x^0_{A''}$
Total	$n_{[]g}=n^0_{[]g}\frac{1+\frac{1}{3}x^0_{O_2}}{1+\frac{1}{3}x_{O_2}+\frac{1}{6}x_{NO}}$

Tabelul 3

Modele matematice secundare de bilanț de masă (forma b)

Componentul	Model matematic de bilanț, [kmol/h]
NH_3	$n_{NH_3}=0$
O_2	$n_{O_2}=n^0_{[]g}\left[x^0_{O_2}-\frac{3}{4}x^0_{NH_3}-\frac{1}{2}\left(1+\frac{1}{4}x^0_{NH_3}\right)x_{NO}\right]$
NO	$n_{NO}=n^0_{[]g}\left(1+\frac{1}{4}x^0_{NH_3}\right)x_{NO}$
H_2O	$n_{H_2O}=n^0_{[]g}\left(x^0_{H_2O}+\frac{3}{2}x^0_{NH_3}\right)$
N_2	$n_{N_2}=n^0_{[]g}\left[x^0_{N_2}+\frac{1}{2}x^0_{NH_3}-\frac{1}{2}\left(1+\frac{1}{4}x^0_{NH_3}\right)x_{NO}\right]$
A″	$n_{A''}=n^0_{[]g}x^0_{A''}$
Total	$n_{[]g}=n^0_{[]g}\left(1+\frac{1}{4}x^0_{NH_3}\right)$

3. Modele matematice de bilanț termic

Procesul de oxidare catalitică a amoniacului fiind puternic exoterm, ecuația generală de bilanț termic se exprimă sub forma :

$$H^0_{[]g}+H_r=H_{[]g}+H_p. \tag{12}$$

Concretizarea termenilor ecuației generale de bilanț termic se realizează prin intermediul modelelor matematice de bilanț de masă și a mărimilor termice corespunzătoare.

Luînd în considerație desfășurarea procesului după reacțiile paralele (1) și (2) și ținînd cont de modelele matematice secundare de bilanț de masă (tab. 3), căldura de reacție H_r se exprimă prin relația :

$$\begin{aligned} H_r&=n_{NO}\Delta_{R_1}H^0_T+2(n_{N_2}-n^0_{N_2})\Delta_{R_2}H^0_T= \\ &=n^0_{[]g}\left[\left(1+\frac{1}{4}x^0_{NH_3}\right)x_{NO}(\Delta_{R_1}H^0_T-\Delta_{R_2}H^0_T)+x^0_{NH_3}\Delta_{R_2}H^0_T\right]. \end{aligned} \tag{13}$$

Efectele termice ale reacțiilor chimice principale, preluate din [11] și recalculate în unități S.I., sînt prezentate în tabelul 4. Concretizarea termenilor $H^0_{[]g}$ și $H_{[]g}$ implică cunoașterea capacităților calorice ale componentelor masei de reacție. Expresiile acestora [12], recalculate în S.I., sînt prezentate de asemenea în tabelul 4.

Tabelul 4

Relații pentru calculul capacității calorice și a efectelor termice de reacție

Componentul	Relația de calcul a capacității calorice	Unitatea de măsură	Domeniul de valabilitate, [°K]
NH_3	$24{,}785+0{,}0375\ T-73{,}855\cdot10^{-7}\ T^2$	Kj/Kmol.grd.	273...2 073
O_2	$25{,}665+0{,}0125\ T-33{,}745\cdot10^{-7}\ T^2$	Kj/Kmol.grd.	273...2 073
N_2	$26{,}376+0{,}00761\ T-14{,}444\cdot10^{-7}\ T^2$	Kj/Kmol.grd.	273...2 073
NO	$25{,}832+0{,}01088\ T-27{,}632\cdot10^{-7}\ T^2$	Kj/Kmol.grd.	273...2 073
H_2O	$28{,}847+0{,}01374\ T-14{,}360\cdot10^{-7}\ T^2$	Kj/Kmol.grd.	273...2 073
$\Delta_{R_1}H^0_T=229\,415{,}7-11{,}723\ T+0{,}01054\ T^2-2{,}229\cdot10^{-6}\ T^3$, [Kj/Kmol]			
$\Delta_{R_2}H_T=319\,761{,}6-11{,}827\ T+0{,}01185\ T^2-2{,}274\cdot10^{-6}T^3$, [Kj/Kmol]			

Utilizînd modelele matematice secundare de bilanț de masă (tab. 3), relațiile din tabelul 4 și calculînd aditiv entalpia fazei gazoase inițiale și finale, se obțin ecuațiile :

$$H^0_{[]g}=n^0_{[]g}[A\,T^0+B\cdot10^{-2}T^{0^2}-C\cdot10^{-6}T^{0^3}-D] \tag{14}$$

și

$$\begin{aligned} H_{[]g}=n^0_{[]g}[&(A+12{,}43x^0_{NH_3}-0{,}188x_{NO}-0{,}047x^0_{NH_3}x_{NO})T+ \\ &+(B-0{,}126x^0_{NH_3}+0{,}038x_{NO}+0{,}0095x^0_{NH_3}x_{NO})\cdot10^{-2}T^2- \\ &-(C-2{,}346x^0_{NH_3}+0{,}154x_{NO}+0{,}0385x^0_{NH_3}x_{NO})\cdot10^{-6}T^3- \\ &-(D+2\,765x^0_{NH_3}-26{,}99x_{NO}-6{,}747x^0_{NH_3}x_{NO})], \end{aligned} \tag{15}$$

în care :

$$(16)\quad \begin{cases} A = 24{,}785x^0_{NH_3} + 26{,}376x^0_{N_2} + 25{,}665x^0_{O_2} + 28{,}847x^0_{H_2O}, \\ B = 1{,}875x^0_{NH_3} + 0{,}38x^0_{N_2} + 0{,}625x^0_{O_2} + 0{,}685x^0_{H_2O}, \\ C = 2{,}461x^0_{NH_3} + 0{,}4813x^0_{N_2} + 1{,}1248x^0_{O_2} + 0{,}478x^0_{H_2O}, \\ D = 8\,975{,}87x^0_{NH_3} + 8\,186{,}76x^0_{N_2} + 8\,173{,}43x^0_{O_2} + 9\,192{,}06x^0_{H_2O}. \end{cases}$$

Înlocuind ecuațiile (13)...(16) și efectele termice de reacție cu expresiile lor din tabelul 4, în ecuația (9), se obține modelul matematic de bilanț termic :

$$(17)\quad \begin{aligned} & n^0_{[]g}[AT^0 + B\cdot 10^{-2}T^{0^2} - C\cdot 10^{-6}T^{0^3} + (0{,}292x_{NO} + 0{,}073x^0_{NH_3}x_{NO} - \\ & - 24{,}257x^0_{NH_3} - A)T + (1{,}311x^0_{NH_3} - 0{,}169x_{NO} - 0{,}0422x^0_{NH_3}x_{NO} - \\ & - B)\cdot 10^{-2}T^2 + (0{,}199x_{NO} + 0{,}151x^0_{NH_3}x_{NO} - 4{,}62x^0_{NH_3} + C)\cdot 10^{-6}T^3 + \\ & + (322\,526{,}6x^0_{NH_3} - 90\,376{,}89x_{NO} - 22\,593{,}147x^0_{NH_3}x_{NO})] - H_p = 0. \end{aligned}$$

Mărimile necesare pentru utilizarea modelului matematic de bilanț termic sînt cele inițiale (debitul de fază gazoasă, compoziția și temperatura acesteia) și conținutul de oxid de azot (x_{NO}) în gazele nitroase obținute după reactorul de oxidare.

4. Verificarea modelelor matematice de bilanț

Datele experimentale necesare utilizării modelelor matematice de bilanț, determinate pe o instalație industrială de oxidare catalitică a amoniacului, sînt prezentate, ca valori medii, în tabelul 5.

Tabelul 5

Date experimentale necesare utilizării modelelor matematice de bilanț

Mărimi necesare	Unitate de măsură	Valoare experimentală medie
Debit amestec NH_3 — aer	m^3N/h	11 200
$x^0_{NH_3}$	fracții de volum	0,105
$x^0_{O_2}$		0,188
$x^0_{N_2}$		0,707
Temp. inițială T^0	°K	513
Temp. finală T	°K	1 153
x_{NO}	fracții de volum	0,0992

Pe baza modelelor matematice secundare de bilanț de masă (tab. 3) și a datelor experimentale (tab. 5) se calculează bilanțul real de masă, rezultatele fiind prezentate în tabelul 6.

Tabelul 6

Bilanțul real de masă

Mărimi intrate			Mărimi ieșite		
Componentul	Kmol/h	kg/h	Componentul	kmol/h	kg/h
NH_3	52,5	892,5	NH_3	0	0
O_2	94,0	3 008,0	O_2	29,17	933,56
N_2	353,5	9 898,0	N_2	354,29	9 920,37
			NO	50,90	1 527,06
			H_2O	78,75	1 417,50
Total	500	13 798,5	Total	513,11	13 798,49

Se constată că modelele matematice de bilanț elaborate se verifică pe baza datelor experimentale industriale, deci procesele de transformare (1) și (2) descriu cantitativ procesul de oxidare catalitică a amoniacului.

Utilizînd modelul matematic de bilanț termic (ecuația (17)) și datele experimentale prezentate în tabelul 5, admițînd $H_p=0$, se calculează temperatura gazelor la ieșirea din stratul de catalizator, obținînd $T=1\,176{,}7°$ K ; temperatura măsurată în reactorul industrial (1 153° K) este mai mică decît valoarea calculată, această diferență datorîndu-se pierderilor de căldură ce nu au fost luate în considerație în calcul.

5. Concluzii

Se elaborează modelele matematice de bilanț de masă și termic pentru procesul de oxidare catalitică a amoniacului pe catalizatori platină — rhodiu, considerînd desfășurarea simultană a reacțiilor cu formare de oxid de azot și azot. De asemenea, se stabilește o ecuație pentru calculul gradului de oxidare a amoniacului la oxid de azot, luînd în considerație variația de volum la desfășurarea procesului.

Se precizează mărimile necesare pentru utilizarea modelelor matematice de bilanț de masă și termic ; acestea sînt mărimile inițiale (debit de fază gazoasă, compoziția și temperatura ei) și conținutul de oxid de azot în gazele rezultate din reactor.

Se atestă exactitatea și valabilitatea modelelor matematice de bilanț de masă și termic, verificarea acestora făcîndu-se pe baza datelor experimentale obținute într-o instalație industrială de oxidare catalitică a amoniacului.

Notații și indici

$C^0_{NH_3}$, C_{NH_3} — concentrația inițială și finală aa moniacului, [% vol],

H — entalpia masei de reacție, [Kj/h],

H_p — pierderi de căldură, [Kj/h],
H_r — căldură de reacţie, [Kj/h],
$\Delta_R H_T^0$ — efect termic de reacţie, [Kj/kmol. grd.],
n_{A_i} — număr de moli ai componentului A_i,
T — temperatură, [K],
x_i — fracţia molară a componentului A_i,
η — grad de transformare,
0 — iniţial,
fără indice — final,
[]g — fază gazoasă.

Primită la 9 iunie 1981

Institutul politehnic, Iaşi,
Catedra de tehnologia substanţelor anorganice şi a materialelor de construcţii

BIBLIOGRAFIE

1. Савенков А. С., Вятсын Л. Л., Атрощенко В. И., Тезисы докл. 12го Укр. Респ. Конф. Физ. Хим., 1977, 1955—1956.
2. Борисова Р. Г., Хамаха Л. Н., Хим. пром., *11*, 844 (1976).
3. Борисова Р. Г., Хамаха Л. Н., Хорошин В. П., Укр. хим. ж., *9*, 940 (1976).
4. Засорин А. П., Орзулова П. Г., Атрощенко В. И., ЖПХ, **4**, 1722 (1967).
5. Засорин А. П., Хим. пром., *6*, 475 (1975).
6. Атрощенко В. И., Каргин С. И., *Технология азотной кислоты*. Изд. Химия, М., 1970.
7. Атрощенко В. И., Галашкина М. М., Приб. сист. упр., **21**, *10*, 10—11 (1967).
8. Засорин А. П., Атрощенко В. И., *Химическая технология*. Изд. ХГУ, Харков, 1969.
9. Бергер И. И., Борёсков Г. К., Хим. пром., *1*, 2 (1952).
10. Calistru C., Hagiu C., *Tehnologia acidului azotic*. Inst., polit., Iaşi, 1970.
11. Beskov S. D., *Calcule tehnochimice*, (trad. din l. rusă). Ed. Tehn., Buc., 1970.
12. Karapetiantz M. N., *Chemical Thermodynamics*. Mir Publ., M., 1978.

CONTROLE OF CATALYTIC OXYDATION PROCESS OF AMMONIA BY MEANS OF BALANCE MATHEMATICAL MODELS

(Summary)

The mathematical material and termic balance models are derived for the catalytic process of ammonia oxydation taking into account the simultaneous development of NO and N_2 forming reactions and the required ammounts for their use are indicated.

Based on industrial experimental data the validity of derived models is checked and the mode of their use for controlling the reactor of ammonia oxidation is given.

BULETINUL INSTITUTULUI POLITEHNIC DIN IAŞI
Tomul XXIX (XXXIII), Fasc. 1—4, 1983
Secţia II
CHIMIE şi INGINERIE CHIMICĂ

D.C. 669.054.8; 669.33; 669.5

ON THE POSSIBILITY OF RECOVERING COPPER AND ZINC FROM ACID SOLUTIONS*)

BY

MARIA APOSTOLESCU, ŞT. IVĂŞCAN and FLORIN BANDRABUR

1. Introduction

The approached subject represents an actual problem regarding the recovery of the useful materials existing sometimes in great amounts in the residual solutions from the either chemical or nonchemical factories [1]...[3].

The present paper deals with recovery of copper and zinc from the solutions (residual water) resulted after washing the sulphurous gases evolved în the equipment of obtaining sulphuric acid at the Chemical Metallurgical Combinat.

The great amounts of residual water (about 20 m^3), resulted daily after washing the sulphurous gases, cause copper losses of about 150 t in a year, that means above 10 millions lei [7]. The necessity of recovering the two nonferrous metals useful for the national economy is thus evident.

The chemical composition of residual water [4]...[6] is given in Table 1. The copper and zinc concentrations are see to be of 18 g/l and 6 g/l, respectively.

Table 1

Initial Average Composition of the Waste Solutions

Component	Copper	Zinc	Arsenic	Iron	Lead	Nickel	Cadmium	Bismuth	NH_3	H_2SO_4
g/l	18	6.75	4.1	2.9	0.008	0.002	0.35	0.25	—	53

The other elements are not important, excepting for the arsenic, due to their low concentrations. The arsenic concentration, of 4 g/l, requires its removal before the copper and zinc recovery.

*) Paper presented at the IInd National Congres of Chemistry, Bucharest, 1981,

2. Experimental

In the present paper the separation of copper and zinc from the residual solutions by electrolysis and cementation is studied [8], [9]. The previous removal of arsenic and iron was required due to their negative influence on the recovery of useful ions.

In order to remove the arsenic and iron, residual solutions were treated with either calcium hidroxide or calcium oxide to pH=2.5...3, when calcium arsenite precipited with decreasing in the arsenic content till 0.5 g As/l. Some of the zinc amount is retained by the precipitate thus formed. In order to avoid the zinc losses the arsenic separation was tested by means of an ion-exchanger such as Amberlitte-IR in its K—H form. Thus the whole amount of arsenic was retained and the zinc losses completely avoided.

Further, the iron present in the solutions was separated by treating with small amounts of hydrogen peroxide for Fe^{+2} oxidation and then with ammonium hidroxide till pH=9...10. The ferric hydroxide was filtred off and the remaining solution heated for removing the ammonia excess. The oxidation of ferrous ion as well as the elimination of the ammonia excess could also be performed by air bubbling into the solution.

The solution containing ammonia in a rather low amount was then acidified to pH=1.5...2 with concentrated H_2SO_4 and submitted further to cementation and electrolysis for the separation of copper and zinc. The concentration of the acidified solution is given in Table 2.

Table 2

Average Composition of the Waste Solutions after Chemical Working

Component	Copper	Zinc	Arsenic	Iron	Lead	Nickel	Cadmium	Bismuth	NH_3	H_2SO_4
g/l	16.2	6.0	0.4	—	0.007	0.0018	0.25	0.18	16.3	82.2

The cementation consists in treating the acid solution with zinc powder for reducing the copper ions to the metallic copper :

$$Cu^{+2} + Zn \rightarrow Cu + Zn^{+2}.$$

The metallic copper slightly oxidized to the black cuprous oxide was filtred and then converted to copper sulphate by treating with H_2SO_4 in the presence of an oxidizing agent. The obtained solution may be submitted to electrolysis in order to obtain the metallic copper [10].

The electrolysis was performed in an electrochemical reactor with platinum, graphite or lead insoluble anodes, the last ones being the most efficient. During the electrolysis the current yield was found to decrease in time (Table 3).

Table 3

Variation of Current Yield in Time for Copper Extraction

Nr.	Cu		I A	τ h	η %
	theoretical deposit g	practical deposit g			
1	0.297	0.262	0.25	1	81
2	0.594	0.451	0.25	2	75
3	0.891	0.624	0.25	3	70
4	1.188	0.782	0.25	4	66
5	1.485	0.896	0.25	5	60.3

The solution enriched in zinc was submitted to the electrolytical extraction of zinc by using lead anodes and aluminium cathodes. The current yield was also found to decrease in time (Table 4).

Table 4

Variation of Current Yield for Zinc Extraction

Nr.	Zn		I A	τ h	η %
	theoretical deposit g	practical deposit g			
1	0.306	0.284	0.25	1	93
2	0.612	0.514	0.25	2	84
3	0.918	0.660	0.25	3	72
4	1.224	0.746	0.25	4	61
5	1.530	0.734	0.25	5	48

In both cases the current yield decreasing is caused by the decrease in the concentration of the copper and zinc ions as well as by the cathodic reduction of the hydrogen ions in case of the zinc separation.

The purity of the metals obtained by electroylsis was of 99%.

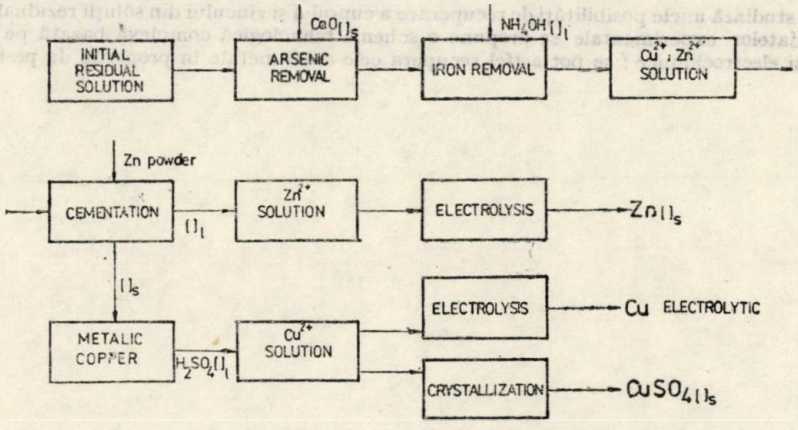

Fig. 1. — Process Scheme for the Recovery of Copper and Zinc from Residual Acid Solutions.

Based on the laboratory data the scheme represented in Fig. 1 is proposed for copper and zinc recovery from the waste acid solutions.

3. Conclusions

1. The posibility of copper and zinc recovery from the residual acid solutions is studied.
2. A technology for recovering these metals by electrolysis and cementation is proposed.
3. The metals of 99% purity are obtained in a rather high yields.

Received, March 12, 1982

Polytehnic Institute, Jassy, Department of Inorganic Substances Technology and Building Materials

REFERENCES

1. Popa F. et al., Symp. „Chemical Process Enginering", Piatra-Neamţ, 1975.
2. Negulescu M. C., *Epurarea apelor industriale*. Ed. Tehn., Buc., 1968.
3. Pilitewski D., Wasser, Luft, Betrieb, *9* (1979).
4. Popa G., Moldoveanu S., *Analiza chimică cantitativă cu reactivi organici*. Ed. Tehn., Buc., 1969.
5. Macarovici C., *Analiza chimică cantitativă anorganică*. Ed., Acad. R.S.R., Buc., 1979.
6. Savencu S. et al., *Chimie analitică cantitativă*. EDP, Buc., 1963.
7. Oniciu L., *Chimie fizică—electrochimie*. EDP, Buc., 1977.
8. Facsko Gh., *Tehnologie electrochimică*. Ed. Tehn., Buc., 1969.
9. Bandrabur F., *Cercetări privind recuperarea cuprului din deşeuri industriale*. Ph. D. Diss., Polyt. Inst, Jassy, 1981.

CERCETĂRI PRIVIND POSIBILITATEA DE RECUPERARE A CUPRULUI ŞI ZINCULUI DIN SOLUŢII ACIDE

(Rezumat)

Se studiază unele posibilităţi de recuperare a cuprului şi zincului din soluţii reziduale acide. În baza datelor experimentale se propune o schemă tehnologică complexă bazată pe procese chimice şi electrochimice ; se pot astfel recupera cele două metale în proporţie de peste 90%.

BULETINUL INSTITUTULUI POLITEHNIC DIN IAŞI
Tomul XXIX (XXXIII), Fasc. 1—4, 1983
Secţia II
CHIMIE şi INGINERIE CHIMICĂ

D.D. 547.791

1, 2. 4-TRIAZOLIUM-YLURES

VII. ARYLATION DES TRIAZOLIUM-PHENACYLURES PAR LES CHLORONITRO DÉRIVÉS DU BENZENE

PAR

CRISTINA LUCHIAN, VIRGIL BĂRBOIU, GH. SURPĂŢEANU et MAGDA PETROVANU

1. Introduction

Dans des travaux antérieurs [1]...[6] on a étudié l'obtention et la réactivité de quelques 1, 2, 4-triazolium-ylures.

Il est connu [7], [8] que les sels de cycloimmonium contenant un groupement méthylène actif peuvent réagir avec le chlorure de picryle et ses analogues en milieu basique fournissant des ylures à carbanions disubstitués fortement colorés.

Tenant compte de ces données de la littérature nous avons étudié, dans le présent travail, le comportement de quelques 1, 2, 4-triazolium-ylures dans les réactions avec le chlorure de picryle et le 2,4-dinitrochlorbenzène dans le but d'obtenir des triazolium-ylures à carbanions disubstitués.

2. Résultats et discussions

Dans une première étape on a étudié la réaction des ylures (III) et (IV) *in situ* avec le chlorure de picryle en solution chloroformique ou en mélange chloroforme—acétonitrile. On obtient les ylures (V) et (VI) fortement colorés en violet très foncé et très stables. Les structures des ylures (V) et (VI) ont été établies par voies chimique et spectrale. Dans le spectre IR on remarque une bande intense à $\nu = 1\,600$ cm^{-1} correspondant au groupement carbonylique. On a déduit les structures des produits (V) et (VI) en analysant le spectre ^{1}H - RMN du produit (VI) plus facile à interpréter en région aromatique. Ainsi, on observe que les protons H_a et H_b sont équivalents (du point de vue chimique et magnétique, $\delta = 8{,}62$ ppm). Les protons H_3 et H_5 du cycle triazolique ne sont pas équivalents, le proton H_5 étant fortement desécranné ($\delta = 11{,}04$ ppm) à cause de la formation d'une liaison d'hydrogène entre H_5 et l'oxygène du groupement NO_2 ou carbonylique voisin.

Des arguments supplémentaires en faveur des structures des ylures (V) et (VI) sont fournis par les transformations chimiques subies par ces

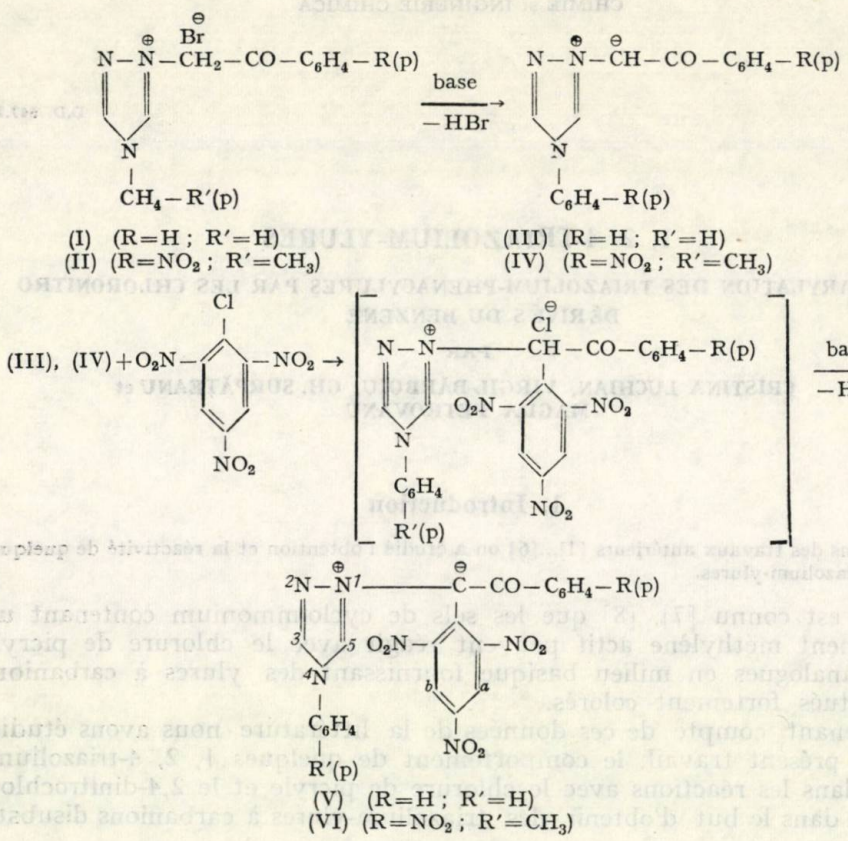

ylures en milieu fortement basique. Ainsi, lorsque l'on traite les ylures (V) et (VI) par la pipéridine il se produit l'élimination de l'acide nitreux et cyclisation, conduisant aux produits (VII) et (VIII) colorés en orange, insolubles dans la plupart des solvants et ayant des points de fusion élevés. Les analyses chimiques et spectrales IR et ^{1}H - RM N confirment pour ces produits une structure triazolo - [2, 3a] - isoindolique. Les spectres IR des produits (VII) et (VIII) présentent des bandes d'absorption à $\nu = 1\,580$ cm^{-1}, respectivement $\nu = 1\,600$ cm^{-1}, correspondant aux groupements carbonyliques. Le spectre ^{1}H - RMN du produit (VIII) montre une non-équivalence magnétique (donc aussi chimique) des protons H_4 et H_6 qui donnent un signal *AB*. On constate aussi la disparition du signal du proton triazolique qui dans les ylures (V) et (VI) est engagé dans une liaison d'hydrogène..

Les produits (VII) et (VIII) peuvent subir des transformations chimiques ultérieures en présence de l'acide sulphurique. On constate l'élimination du radicale benzoylique respectivement *p*-nitrobenzoylique et la formation du 3-phényl-5, 7-dinitro-triazolo-[2, 3a] - isoindole (IX), respectivement du 3-(*p*-tolyl)-5,7-dinitro-triazolo-[2,3a]-isoindole (X), produits cristallisés, colorés en rouge foncé. Les résultats des analyses chimiques et spectrales (IR et ^{1}H - RMN) confirment les structures (IX) et (X).

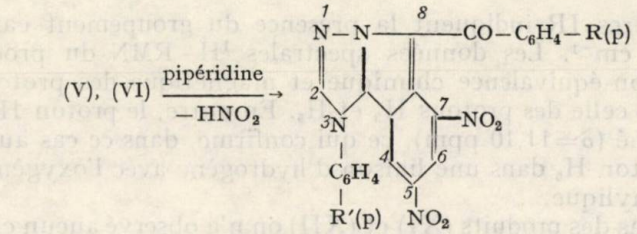

(VII) (R=H ; R′=H)
(VIII) (R=NO$_2$; R′=CH$_3$)

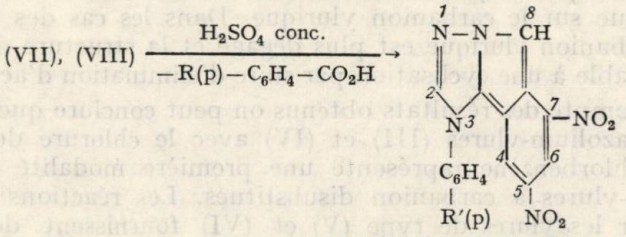

IX (R′=H) X(R′=CH$_3$)

Dans le spectre IR on observe la disparition des bandes à 1 600 cm^{-1}, ce qui confirme l'élimination du groupement benzoylique. Le spectre ^{1}H-RMN du produit (X) enregistré dans le DMSO-d_6, montre la non-équivalence chimique et magnétique des protons H_4 et H_6 et l'apparition d'un singulet à δ=8,05 ppm attribué au proton H_8. En comparaison avec le spectre ^{1}H - RMN du produit (VIII), dans le spectre ^{1}H - RMN du produit (X) on constate la disparition des signaux des protons aromatiques du groupement —CO—C$_6$H$_4$—NO$_2$, ce qui confirme l'élimination du groupement *p*-nitrobenzoylique.

Dans la seconde étape des recherches on a étudié la réaction des triazolium-phénacyclures (III) et (IV) *in situ* avec le 2,4-dinitrochlorbenzène dans le DMSO. On a obtenu les ylures à carbanions disubstitués attendus (XI) et (XII), cristallisés, colorés en rouge foncé. Les structures des ces ylures ont été confirmées par les analyses chimiques et spectrales.

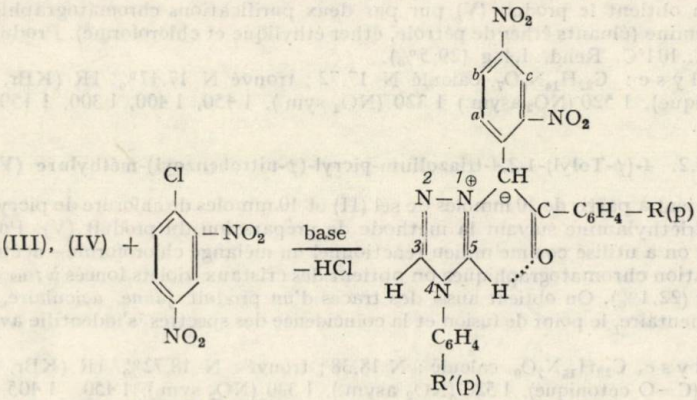

(XI) (R=H ; R′=H) (XII) (R=NO$_2$; R′=CH$_3$)

Les spectres IR indiquent la présence du groupement carbonylique vers $\nu = 1\,590$ cm^{-1}. Les données spectrales ^{1}H - RMN du produit (XII) montrent la non-équivalence chimique et magnétique des protons H_a, H_b et H_c ainsi que celle des protons H_3 et H_5. En outre, le proton H_5 est fortement desécranné ($\delta = 11,10$ ppm), ce qui confirme, dans ce cas aussi, l'engagement du proton H_5 dans une liaison d'hydrogène avec l'oxygène du groupement carbonylique.

Dans le cas des produits (XI) et (XII) on n'a observé aucun changement dans la réaction avec la pipéridine. Ceci conduit à la conclusion que dans le cas des ylures (V) et (VI) l'élimination de l'acide nitreux est dûe à l'encombrement stérique sur le carbanion ylurique. Dans les cas des ylures (XI) et (XII) le carbanion ylurique est plus dégagé et la structure des produits n'est pas favorable à une cyclisation par suite d'élimination d'acide nitreux.

Tenant compte des résultats obtenus on peut conclure que la réaction des 1, 2, 4-triazolium-ylures (III) et (IV) avec le chlorure de picryle et le 2,4-dinitrochlorbenzène représente une première modalité d'obtention des triazolium-ylures à carbanion disubstitués. Les réactions de cyclisation subies par les ylures de type (V) et (VI) fournissent de nouvelles structures hétérocycliques triazolo-[2, 3a] - isoindoliques difficilement accessibles par d'autres méthodes.

3. Partie expérimentale

Les spectres ^{1}H—RMN sont réalisés sur un spectromètre JMN-C-60-HL à 60 MHz, en utilisant le TMS comme référence interne. Les spectres IR ont été enregistrés sur un spectromètre SPECORD.

La préparation des sels de cycloimmonium (I) et (II) a été déjà décrite dans les Notes précédentes [1], [5].

3.1. 4-Phényl-1,2,4-triazolium-picryl-benzoyl-méthylure (V)

On mélange une suspension de 10 mmoles de sel (I) dans 30 ml de chloroforme avec un solution de 10 mmoles de chlorure de picryle dans 30 ml de chloroforme. On ajoute goutte à goutt 3 ml de triéthylamine dissoute dans 10 ml de chloroforme, en agitant continuellement à la tempé rature ambiante. La solution se colore en violet foncé. Après 2 h on lave la solution trois fois à l'eau et la phase organique est séchée sur du Na_2SO_4 anhydre. On réduit le volume de la solution à 3 ml et on obtient le produit (V) pur par deux purifications chromatographiques sur une colonne d'alumine (éluants éther de pétrole, éther éthylique et chloroforme). Produit violet foncé à $t_{fus.} = 100°...101°$C. Rend. 1,4 g (29,5%).

Analyse : $C_{22}H_{14}N_6O_7$, calculé N 17,72 ; trouvé N 17,47%. IR (KBr, cm^{-1}) : 1 600 (C=O cétonique), 1 520 (NO_2 asym.) 1 320 (NO_2 sym.), 1 450, 1 400, 1 300, 1 150 (C—C, C—N aromatiques).

3.2. 4-(*p*-Tolyl)-1,2,4-triazolium-picryl-(*p*-nitrobenzoyl)-méthylure (VI)

On l'obtient à partir de 10 mmoles de sel (II) et 10 mmoles de chlorure de picryle en présence de 3 ml de triéthylamine suivant la méthode de préparation du produit (V). Pour augmenter le rendement on a utilisé comme milieu réactionnel un mélange chloroforme—acétonitrile. Après deux purification chromatographiques on obtient des cristaux violets foncés à $t_{fus.} = 138°...140°$C Rend. 1,29 g (22,1%). On obtient aussi des traces d'un produit jaune, aciculaire, qui d'après l'analyse élémentaire, le point de fusion et la coïncidence des spectres s'indentifie avec le produit (VIII).

Analyse. $C_{23}H_{15}N_7O_9$, calculé : N 18,38 ; trouvé : N 18,72%. IR (KBr, cm^{-1}) : 3 020 (CH_3), 1 600 (C=O cétonique), 1 520 (NO_2 asym.), 1 330 (NO_2 sym.), 1 450, 1 405, 1 275, 1 150 (C—C, C—N aromatiques). RMN ($CDCl_3$, δ) : 2, 60 ppm, singulet, 3p (Ph—CH_3) ; 7,22...7,36...7,78...

8,02 ppm, multiplet $AA'BB'$, 4p ($-CO-C_6H_4-NO_2(p)$) ; 7,35 ppm, quasisingulet, 4p($-C_6H_4-Me(p)$) ; 8,28 ppm, singulet, 1p (H_3) ; 8,62 ppm, singulet, 2p (H_a et H_b) ; 11,04 ppm, singulet, 1p (H_5).

3.3. 3-Phényl-5,7-dinitro-8-benzoyl-triazolo-[2,3a]-isoindole (VII)

On dissout 2,5 mmoles de produit (V) en 20 ml de DMSO et on ajoute 0,5 ml pipéridine en agitant continuellement à 20°C, pendant 2 h. La couleur, initialement violette, devient rouge-orange. Après 2 h on ajoute lentement CH_3COOH 3N jusqu'à la formation d'un précipité. On filtre le mélange réactionnel et le précipité est lavé à l'eau, l'alcool et l'éther éthylique. On obtient un produit jaune nacré qui soublime à 290°C.

Analyse. $C_{22}H_{13}N_5O_5$, calculé : C 61,82 ; H 3,04 ; N 16,39 ; trouvé : C 61,95 ; H 2,90 ; N 16,63%. IR (KBr, cm^{-1}) : 1 560 (C=O cétonique), 1 530 (NO_2 asym.), 1 620, 1 580, 1 450 1 430, 1 280, 1 200, 1 130 (C—C, C—N aromatiques), 1 305 (NO_2 sym.).

3.4. 3-(*p*-Tolyl)-5,7-dinitro-8-(*p*-nitrobenzoyl)-triazolo-[2,3a]-isoindole (VIII)

On le prépare d'après la méthode d'obtention du produit (VII), à partir de 2,5 mmoles de produit (VI) et 0,5 ml pipéridine. Produit orange à $t_{fus.}$ =248°C.

Analyse : $C_{23}H_{14}N_6O_7$, calculé : C 75,72 ; H 2,28 ; N 17,28 ; trouvé C 75,51 ; H 2,72 ; N 17,32%. IR (KBr, cm^{-1}) : 1 600 (C=O cétonique), 1 510 (NO_2 asym.), 1 630, 1 440, 1 380, 1 320, 1 250, 1 200, 1 120 (C—C, C—N aromatique), 1 340 (NO_2 sym.). RMN (DMSO—d_6, δ) : 2,52 ppm, singulet, 3*p* ($Ph-CH_3$) ; 7,32...7,47...7,58...7,72 ppm, multiplet $AA'MM'$, 4p, ($>N-C_6H_4-Me(p)$) ; 7,73...7,88...8,08...8,22 ppm, multiplet $AA'MM'$, 4p, ($-CO-C_6H_4-NO_2(p)$) ; 8,45 et 8,58 ppm, deux doublets AB avec scision de 1,5 Hz, 2p, (H_4 et H_6) ; 9,1 ppm, singulet 1p, (H_2).

3.5 3-Phényl-5,7-dinitro-triazolo-[2,3a]-isoindole (IX)

On traite 1 mmole de produit (VII) avec 1,6 ml H_2SO_4 conc. et le mélange est chauffé au bain-marie pendant 10 min. On refroidit la solution et on ajoute de l'eau. On obtient un mélange de cristaux blancs et rouge. Pour séparation on chauffe le mélange jusqu'à l'ébullition et on filtre immédiatement. Dans le filtrate on précipite, au refroidissement, cristaux blancs d'acide benzoïque et sur le filtre on obtient un précipité rouge de l'ylure (IX) pur ; $t_{fus.}$ =259°... 260°C.

Analyse. $C_{15}H_9N_5O_4$, calculé : C 55,72 ; H 2,78 ; N 21,36 ; trouvé : C 55,49 ; H 2,70 ; N 21,52%. IR (KBr, cm^{-1}) : 1 530 (NO_2 asym.) 1 610, 1 590, 1 490, 1 420, 1 300, 1 280, 1 220, 1 190 (C—C, C—N aromatiques), 1 340 (NO_2 sym.).

3.6. 3-(*p*-Tolyl)-5,7-dinitro-triazolo-[2,3a]-isoindole (X)

Selon le même mode opératoire du produit (IX). Cristaux blancs de l'acide *p*-nitro-benzoïque et cristaux rouges foncés de l'ylure (X) ; $t_{fus.}$ =270°...271°C.

Analyse. $C_{16}H_{11}N_5O_4$, calculé : C 56,97 ; H 3,26 ; N 20,77 ; trouvé : C 56,64 ; H 3,15 ; N 20,84%. IR (KBr, cm^{-1}) : 1 520 (NO_2 asym.) 1 625, 1 490, 1 445, 1 350, 1 270, 1 240, 1 230, (C—C, C—N aromatiques), 1 310 (NO_2 sym.). RMN (DMSO—d_6, δ) : 2,50 ppm, singulet, 3p ($Ph-CH_3$) ; 7,33...7,47...7,60...7,73 ppm, multiplet $AA'MM'$, 4p ($-C_6H_4-Me(p)$) ; 8,05 ppm, singulet, 1p (H_8) ; 8,55 ppm, multiplet AB, 2p (H_4 et H_6) ; 9,2 ppm, singulet, 1p (H_2).

3.7. 4-Phényl-1,2,4-triazolium-2,4-dinitrophényl-benzoyl-méthylure (XI)

On dissout 10 mmoles de sel (I) et 10 mmoles de 2,4-dinitro-chlorbenzène en 30 ml de DMSO. On ajoute, goutte à goutte, 3 ml de triéthylamine et on agite pendant 1 h à 20°C. La solution se colore en rouge foncé. On ajoute de l'eau et on filtre le précipité de l'ylure (XI) qui se sépare. On redissout l'ylure (XI) dans le DMSO, on chauffe à 80°C et après refroidissement on le précipite avec de l'eau. On filtre et par recristallisation dans de l'alcool éthylique on obtient des cristaux rouges foncés ; $t_{fus.}$ =97°C.

Analyse : $C_{22}H_{15}N_5O_5$, calculé N 16,31 ; trouvé N 16,69%.

3.8. 4-(*p*-Tolyl)-1,2,4-triazolium-2,4-dinitrophényl-(*p*-nitrobenzoyl)-méthylure (XII)

On l'obtient d'une façon analogue au produit (XI) à partir de 10 mmoles de sel (II) et 10 mmoles de 2,4-dinitrochlorbenzène. Cristaux rouges foncés à $t_{fus.}$ = 145...146°C.

Analyse : $C_{23}H_{16}N_6O_7$, calculé N 17,21 ; trouvé N 17,29%. IR (KBr, cm^{-1}) : 1 590 (C—O cétonique), 1 520 (NO_2), 1 570, 1 460, 1 300, 1 230, 1 115 (C—C, C—N aromatiques)

1 330 (NO_2). RMN (DMSO—d_6, δ) : 2,55 ppm, singulet, 3p (PH—CH_3) ; 7,00 ppm, doublet avec scission à 6,5 Hz, 1p (H_a); 7,85 ppm, multiplet avec scission à 6,5 et 3 Hz, 1p (H_b); 8,72 ppm, doublet avec scission à 3 Hz (H_c); les signaux des protons H_a, H_b et H_c forment un système *ABK*; 7,29 ppm, quasidoublet, 4p (—C_6H_4—Me(*p*)) ; 7,35...7,49...7,88...8,02 ppm, multiplet *AA'MM'*; 4p, (—CO—C_6H_4—NO_2(*p*)), 8,22 ppm, singulet, 1p (H_3) ; 11,10 ppm, singulet, 1p (H_5).

Reçue le 25 septembre 1980

Institut Polytehnique, Jassy,
Chaire de Chimie organique et macromoléculaire
et
Institut de Chimie macromoléculaire „P. Poni", Jassy

BIBLIOGRAPHIE

1. Petrovanu M., Luchian C., Surpăţeanu Gh., Bărboiu V., Rev. Roumaine Chim., **24**, 733 (1979).
2. Petrovanu M., Luchian C., Surpăţeanu Gh., Bărboiu V., Rev. Roumaine Chim., **24**, 1053 (1979).
3. Petrovanu, M. Luchian C., Surpăţeanu Gh., Constantinescu M., Bărboiu V., Rev. Roumaine Chim., **25**, 1091 (1980).
4. Petrovanu M., Luchian C., Surpăţeanu Gh., Constantinescu M., Bărboiu V., Bul. Inst. polit., Iaşi, **XXVI (XXX)**, *3—4*, s. II, 97 (1980).
5. Petrovanu M., Luchian C., Surpăţeanu Gh., Bărboiu V., Tetrahedron, **37**, 2805 (1981).
6. Petrovanu M., Luchian C., Surpăţeanu Gh., Bărboiu V., Tetrahedron, **37**, 2811 (1981).
7. Kröhnke F., Schmeiss H., Chem. Ber., **70**, 172 (1937).
8. Reusching D., B. Kröhnke F., Chem. Ber., **104**, 2103, 2110 (1971).

1, 2, 4-TRIAZOLIU-ILIDE

VII. Arilarea triazoliu-fenacilidelor cu clor nitroderivaţi ai benzenului

(Rezumat)

Continuînd cercetările în clasa triazoliu-ilidelor, s-a propus sintetizarea unor ilide carbanion disubstituite stabile. Prin reacţia ilidelor (III) şi (IV) cu clorura de picril şi cu 2, 4-dinitroclorbenzen s-au sintetizat ilidele stabile (V), (VI), (XI) şi (XII). Ilidele (V) şi (VI) suferă, în mediu bazic, ciclizări conducînd la derivaţi de triazolo-[2, 3 a]-isoindol.

BULETINUL INSTITUTULUI POLITEHNIC DIN IAȘI
Tomul XXIX (XXXIII), Fasc. 1—4, 1983
Secția II
CHIMIE și INGINERIE CHIMICĂ

D.C. 547.678.2

POLYACENAPHTHENEQUINONIMINIMIDES

BY

TATIANA LIXANDRU, MARIA DUMITRIU, MARIANA PĂSTRĂVANU and I. COCÎRLĂ

1. Introduction

The heterochain polymers show important properties in connection to their structure and the heteroatom presence which determines their applications in numerous fields.

The dicarbonylic components lead to polyconjugated systems and have a particular importance for obtaining polymers with $>C=N$-bonds on the macromolecular chain.

In previous papers [1], [2] studies have been raported on the obtaining of new polyazines and polyazomethines with acenaphtenequinone and its substituted derivatives with biuret reported.

2. Experimental

2.1. Materials

a) *Acenaphthenequinone*. Merk-Schuchardt product, m.p.=248°...253°C and 261°C when recrystallized from *m*-xylene.

b) *Chlorocenaphthenequinone* was obtained by the oxydation of 5-chloroacenaphtene [3], synthesised in its turn by the chlorination of acenaphthene with sulphurylchloride [4] The chloroacenaphthenequinone was purified by the recrystallization from acetic acid/water, m.p.= =218°C.

c) *5-Nitro- and 5,6-dinitro-acenaphthenequinone* were prepared according to the literature indication [5], [6], by the nitration of acenaphthenequinone. After recrystallization from acetic acid, m.p.=218°C (the 5-nitro-derivative) and 300°C (the 5,6-dinitro-derivative).

d) *Biuret*. Schuchardt product containing 85% biuret, 10.2% triuret, 2.7% urea, m.p.= = 140°C.

2.2. Method

A mixture of 0.01 mol quinone, 0.02 mol biuret and 2 g $ZnCl_2$ is solved in 20m^1 solvent. The reaction mixture is refluxed under stirring for 8 hours. In some cases, a solid red to brown product begins to separate, even without cooling. The product is filtred after cooling and washed with a diluted ammonia solution for removing $ZnCl_2$. By adding water the fraction soluble in the reaction medium is separated from the solution. The unreacted monomers are removed by repeated washings with either hot glacial acetic acid or ethylic alcohol.

The IR spectra were recorded with KBr on a UR-20 apparatus.

The thermogravimetrical analyses were made on a Paulik-Paulik-Erdey MOM-Budapest derivatograph, in air, within the 20°...900°C temperature range at a heating rate of 10°C/min.

The energies of activation and the reaction orders for the thermodestruction processes were calculated by the Coats-Redfern method and the data processed on a Felix computer.

3. Results and Discussion

3.1. Reactivity of Dicarbonylic Components

The reactivity of the dicarbonylic components in the polycondensation reaction was estimated based on EHT calculation (Extended Hückel Theory) [8], [9], the interatomic distances being chosen according to the literature data [10].

Some estimations on the relative reaction capacity of the carbonyl carbon atoms could be made based on the charge distributions given in the molecular diagrams *I*...*IV* (Fig. 1).

The reactivity of the substituted dicarbonylic compounds may be discussed in comparison with that of the unsubstituted one based on the electrophylic properties of the carbonylic carbon atoms estimated from the values of the atomic charges.

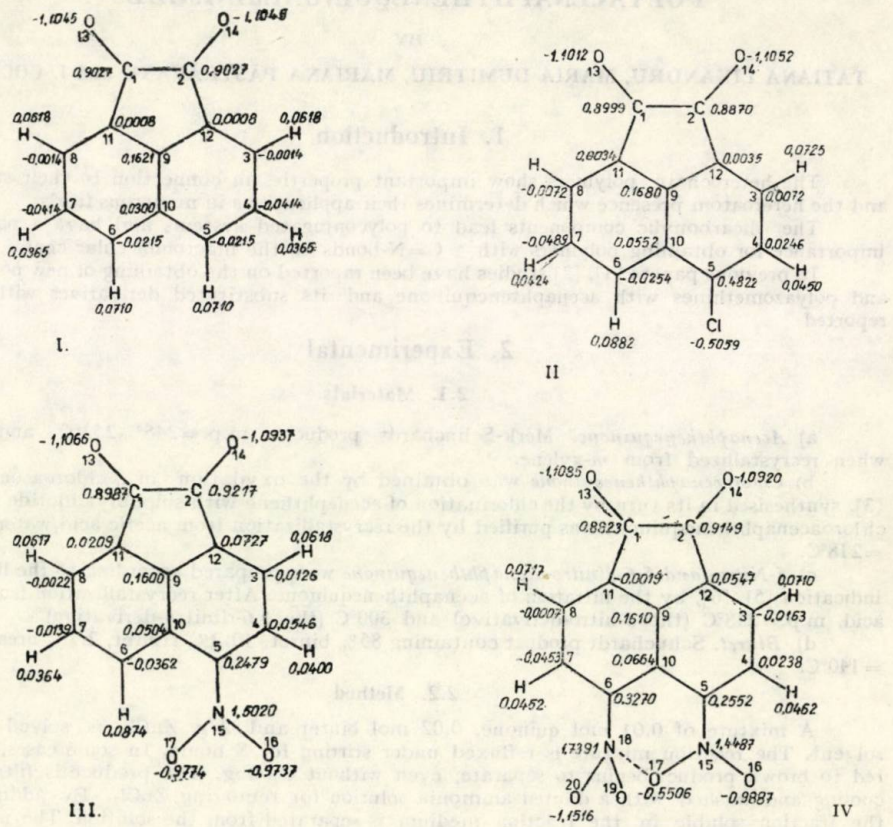

Fig. 1. — *I* — Acenaphthenequinone; *II*— 5-Chloroacenaphthenequinone; *III*— 5-Nitroacenaphthenequinone; *IV*— 5,6-Dinitroacenaphthenequinone.

The energies (E_{el}) and the atomic charges on the carbonylic carbon atoms (1 and 2) are given in Table 1.

The atomic charges on the 1 and 2 carbon atoms are noticed to vary with nature and number of the substituents as well as the molecular symmetry.

The energy calculation for 5,6-dinitroacenaphthenequinone showed the conformation to be stable when a nitro group is directed out of the molecular plane. The atomic charges on the nitrogen and oxygen atoms of the two nitro groups are different due to the interaction between the nitrogen atom of one nitro group and the oxygen atom of the other.

Table 1
Molecular Characteristics of Dicarbonilyc Components

No.	Dicarbonylic component	Atomic charges		Energy (E_{el}) eV
		C_1	C_2	
1	Acenapthenequinone	0.9027*)	0.9027*)	− 1 217.97
2	5-Chloroacenaphthenequinone	0.8999*)	0.8870)	1 334.38
3	5-Nitroacenaphthenequinone	0.8987	0.9217*)	− 1 549.39
4	5,6-Dinitroacenaphthenequinone	0.8823	0.9149*)	− 1 873.12

*) A_dN attack.

By taking into account the first reaction stage, namely the nucleophylic attack on the carbonylic atom A_dN, the reactivity of the four dicarbonylic components are noticed to decrease in the following order :

5-nitroacenaphthenequinone (III) > 5,6-dinitroacenaphthenequinone (IV) > acenaphthenequinone (I) > 5-chloroacenaphthenequinone (II).

3.2. Synthesis and Molecular Structure of the Polymers

The reactions of acenaphthenequinone and its substituted derivatives with hydrazine and aromatic diamines leading to hydrazones, azomethine bases, substituted quinoxaline derivatives or macromolecular compounds (polyazines or poyazomethines) are described in numerous papers [1], [2], [11]...[20].

In order to obtain new macromolecular compounds based on acenaphthenequinone and its derivatives the polycondensation with biuret was performed.

The polycondensation was carried out in both protic (acetic acid) and aprotic (DMF) solvents at a quinone/biuret mole ratio of 1/2. The optimum reaction duration of 8 hours was settled. The product obtained from acenaphthenequinone was a red, crystalline compound while the others were amorphous, red-brown to black coloured. Some properties of the synthesized compounds are given in Table 2. The data from these table show the acenaphthenequinone to give only insoluble compound, the dinitric derivative only soluble product while the other quinones lead to both soluble and insoluble fraction.

The yields obtained in acetic acid are low compared to those obtained in dimethylformamide, probably because in DMF the reactions proceed at higher temperature which promotes the polycondensation. Secondly, the nucleophylicity of NH_2 group in biuret may be diminished as a consequence of protonation ; the blocking NH_2 group in biuret by acetic acid is also possible. For these reason DMF was choosen as a solvent for the polycondensation.

By the polycondensation of acenaphthenequinone and its substituted derivatives with hydrazine [1] and biuret both soluble and insoluble fractions in the reaction medium are obtained while the polycondensation with *m*- and *p*-phenylenediamines [2] lead to insoluble fraction only. This fact is indicative of a decrease in reactivity from hydrazine to biuret and phenyl-

Table 2

Characteristics of Polyiminimides

No.	Dicarbonylic component	Yield, [%]			Melting point, [°C]		Aspect		IR absorptions		
		Soluble	Insoluble	Total	Soluble	Insoluble	Soluble	Insoluble	$\nu_{C=N}$	Amid I	Amid II
I	Acenaphthenequinone	—	54.94	54.94	—	345	crystalline —	dark-red	1 620	1 705	1 580
II	5-Nitroacenaphthenequinone	12.95	14.26	27.21	306	345	amorphous dark-brown	red-brown	1 650	1 690	1 610
III	5,6-Dinitroacenaphthenequinone	20.51	—	20.51	337	—	amorphous black	—	1 640	1 680	1 610
IV	5-Chloroacenaphthenequinone	32.40	20.50	52.90	269	300	amorphous brown	brown	1 650	1 700	1 610

Table 3

Thermal Properties of Dicarbonylic Component and Polyiminimides

Compound	T_d	Stages of thermal degradation								
		I			*II*			*III*		
	°C	Temperature range °C	T_I °C	Weight losses %	Temperature range °C	T_{II} °C	Weight losses %	Temperature range °C	T_{III} °C	Weight losses %
Acenaphthenequinone	190	190...330	330	81.3	330...420	350	18.7	—	—	—
5-Chloroacenaphthenequinone	195	195...435	360	91.2	435...582	543	8.8	—	—	
5-Nitroacenaphthenequinone	220	220...394	300	33.5	394.. 620	513	47.2	620...740	690	19.3
5,6-Dinitroacenaphthenequinone	264	264...368	326	28.7	368...620	516	55.8	620...693	650	15.5
Polyacenaphthenequinoniminimide	340	340...625	460	96.0	—	—	—	—	—	—
Poly-(5,6-dinitroacenaphthenequinone)-iminimide	275	275...525	485	86.1	—	—	—	—	—	—

T_d — initial temperature of weight loss; T_I, T_{II}, T_{III} — temperature of the maximum distruction rate for stages *I*, *II*, *III* rom DTG curves)

enediamines. The diamine components with high reactivity promote the formation of compounds of low molecular weights which separate from the reaction medium. Besides, the delocalization of π electrons on the conjugated system in oligomers diminishes the reactivity of the end groups which causes a decrease in the capacity of continuing the polycondensation [21].

Since the polymers were insoluble in common organic solvents the molecular weights and viscosities could not be determined.

The structures of the synthesized compounds were elucidated by elemental analyses and IR spectral measurements.

All IR spectra show absorptions characteristic of the $\nu_{C=N}$ valence vibrations at 1 640...1 650 cm^{-1} (Table 2) as well as absorption bands at 1 680...1 700 cm^{-1} (amide I) and 1 570...1610 cm^{-1} (amide II). In all spectra the bands characteristic of aromatic ring and of substituents in the dicarbonylic component (1 330 cm^{-1} $\nu_{NO_2\,sym.}$, 1 530 cm^{-1} $\nu_{NO_2\,asym.}$).

The IR spectra and the elemental analysis data confirm the polyiminimidic structure of the synthesized polymers :

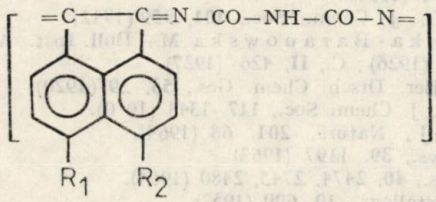

I. R_1, R_2=H,
II. R_1=H ; R_2=Cl,
III. R_1=H ; R_2=NO_2,
IV. R_1, R_2=NO_2

3.2. Properties of Polyiminimides

a) *Thermal stability*. The thermal properties of the polymers depend on both the stability of the recurring units and the bonds between them. The chain bonds must be somewhat rigid to diminish the free rotation ; in this connection, the double bonds as well as the bulky substituents confer stability to the system.

The thermal stability of polyiminimides was studied in comparison to that of dicarbonylic components for which the thermogravimetrical data indicate an increase in the following order :

acenaphthenequinone $\leqslant$ 5-chloroacenaphthenequinone $<$ 5-nitro-acenaphthenequinone $<$ 5,6-dinitroacenaphthenequinone (Table 3).

The polyacenaphthenequinoniminimides and the polydinitroacenaphthenequinoniminimides are stable up to 360° and 275°C, respectively ; the low weight losses up to 400°C are indicative of a good stability of these polymers.

b) *Paramagnetism*. The paramagnetic properties of the polymers were made evident by means of ERS spectra which show signals as singl lines of the L o r e n z type without hyperfine structure. The concentration in paramagnetic particle is of the 10^{22} spin/g order.

4. Conclusions

1. The polycondensation of biuret with acenaphthenequinone and its substituted derivatives was studied.

2. By means of the EHT method the influence of the substituents on the relative reaction capacity (A_dN) of acenaphthenequinone was estimated.

3. By studying the influence of the temperature, solvent and reaction duration the optimum parameters for the obtaining of new polyiminimidic macromolecular compounds were settled.

4. The synthesized compounds show a good thermal stability (up to 350°C) and paramagnetic properties (paramagnetic particle concentration of the 10^{22} sping/g order).

Received, September 25, 1980

Polytehnic Institute, Jassy, Department of Organic and Macromolecular Chemistry

REFERENCES

1 Păstrăvanu M., Dumitriu M., Lixandru T., Eur. Polym. J., **17**, 197–201 (1981).
2. Lixandru T., Dumitriu M., Păstrăvanu M., Bul. Inst. polit., Iași, **XXVII (XXXI)**, *3–4*, s. II, 95–101 (1981).
3. Crompton H., Walker W., J. Chem., Soc., **101**, 959 (1912).
4. Dziewonski K., Zabrzewska-Baranowska M., Bull. Inst. Acad. Polon. Sci. Letters Serie A, 347 (1926); C., **II**, 426 (1927).
5. Mayer F., Kaufmann W., Ber. Dtsch. Chem. Ges., **53**, 297(1920).
6. Rowe F. M., Devres S. J., J. Chem. Soc., **117**, 1344 (19 0).
7. Coats A. W., Redfern T. J., Nature, **201**, 68 (1964).
8. Hoffmann R., J. Chem. Phys., **39**, 1397 (1963).
9. Hoffmann R., J. Chem. Phys., **40**, 2474, 2745, 2480 (1964).
10. Ehrlich H. W. W., Acta Crystallogr., **10**, 699 (1957).
11. Francesconi L., Pirrazzoli F., Gazz. chim. Ital., **33**, 36 (1903).
12. Matei I., Lixandru T., Bul. Inst polit., Iași, **XII(XVI)**, *1–2*, 171 (1966).
13. Ampola G., Rechi V., R. Acad. Lincei Roma, (5), **8**, 210 (1899).
14. Guha S. K., J. Indian Chem. Soc., **9**, 423 (1932).
15. Prasad D., Dutta P. C., B., **70**, 2365 (1937).
16. Кипнамиов А. И., Крощенко М. М., Укр. хим. ж., **19**, 302 (1953).
17. Каришин А. П., Укр. хим. ж., **23**, 651 (1957).
18. Каришин А. П., Федосенко Т. П., Укр. хим. ж., 21, 373 (1955).
19. Коптюг Б. А., Володовский К. Б., Ворожцов Н. Н., Ж. общ. хим., **32**, 1616 (1962)
20. Goldstein H., Strenli M., Helv. Chim. Acta, **20**, 650 (1937).
21. Берлин А. А., Высокомолек. соед., **XV**, *2*, 256 (1973).

POLIACENAFTENCHINONIMINIMIDE

(Rezumat)

Prin policondensarea acenaftenchinonei și derivaților săi substituiți cu biuretul s-au obținut o serie de noi poliacenaftenchinoniminimide.

Cu ajutorul metodei EHT s-a apreciat influența substituenților asupra capacității relative de reacție (A_dN) a acenaftenchinonei. Cercetînd variația temperaturii, a solventului și a duratei de reacție s-au stabilit parametrii optimi pentru obținerea de noi compuși macromoleculari de tip poliiminimidic.

Produșii sintetizați prezintă o bună stabilitate termică (pînă la 350°C) și proprietăți paramagnetice (concentrația în particule paramagnetice de ordinul 10^{22} spini/g).

BULETINUL INSTITUTULUI POLITEHNIC DIN IAŞI
Tomul XXIX (XXXIII), Fasc. 1—4, 1983
Secţia II
CHIMIE şi INGINERIE CHIMICĂ

D.C. 542.957 ; 546.22

ORGANIC SULPHUR COMPOUNDS[1])

XVI. 2-HYDROXYKETONES. XI. A CONVENIENT SYNTHESIS OF SUBSTITUTED 2-DIALKYLAMINO-2,3-DITHIOL-2-YLIUM SALTS BY CYCLIZATION OF SOME 2-OXOALKYL DITHIOCARBAMATES IN A VILSMEIER-HARNISCH REACTION

BY

Al. CAŞCAVAL

1. Introduction

During our investigations on chromone synthesis in the V i l s m e i e r-H a r n i s c h reaction [1] we observed a facile cyclization of some 2-oxoalkyl dithiocarbamates (I) which afforded instead of the expected chromone ($II_{a\cdots d}$) new 2-dialkylamino-1,3-dithiol-2-ylium salts (III) in a good yield. These new heteronium salts are useful and reactive intermediates for the preparation of various heterocycles including tetrathiofulvalene (TTF).

2. Results and Discussions

2-Oxoalkyl dithiocarbamates ($I_{a\cdots h}$), easily accesible from α-haloketones and sodium- or dialkylammonium N, N-dialkyl dithiocarbamates [3], reacted with V i l s m e i e r reagent ($DMF+POCl_3$) in the H a r n i s c h conditions [3] to produce compounds ($III_{a\cdots h}$) (Scheme *A*) :

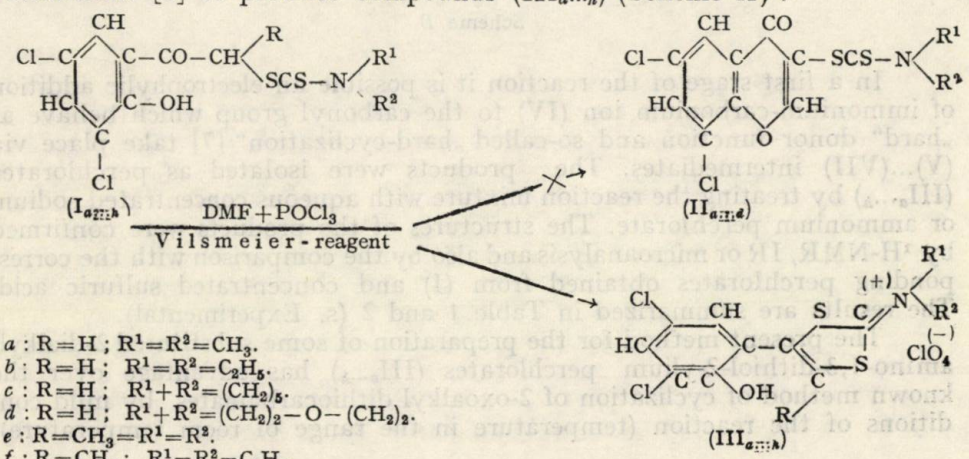

a : R=H ; $R^1=R^2=CH_3$.
b : R=H ; $R^1=R^2=C_2H_5$.
c : R=H ; $R^1+R^2=(CH_2)_5$.
d : R=H ; $R^1+R^2=(CH_2)_2-O-(CH_2)_2$.
e : $R=CH_3=R^1=R^2$.
f : $R=CH_3$; $R^1=R^2=C_2H_5$.
g : $R=CH_3$; $R^1+R^2=(CH_2)_5$.
h : $R=CH_3$; $R^1+R^2=(CH_2)_2-O-(CH_2)_2$.

Scheme *A*

[1]) XV and XI of this series, s. J. Heter. Chem. (in press).

The above cyclization of (I) is interesting in connection with the normal cyclization mode of (I) with strong acids as 70% perchloric acid [4] or concentrated sulfuric acid [5] leading to the salts (III) which are the important intermediates for the preparation of TTF derivatives [6].

The mechanism of this cyclization can be written as follows (scheme *B*) :

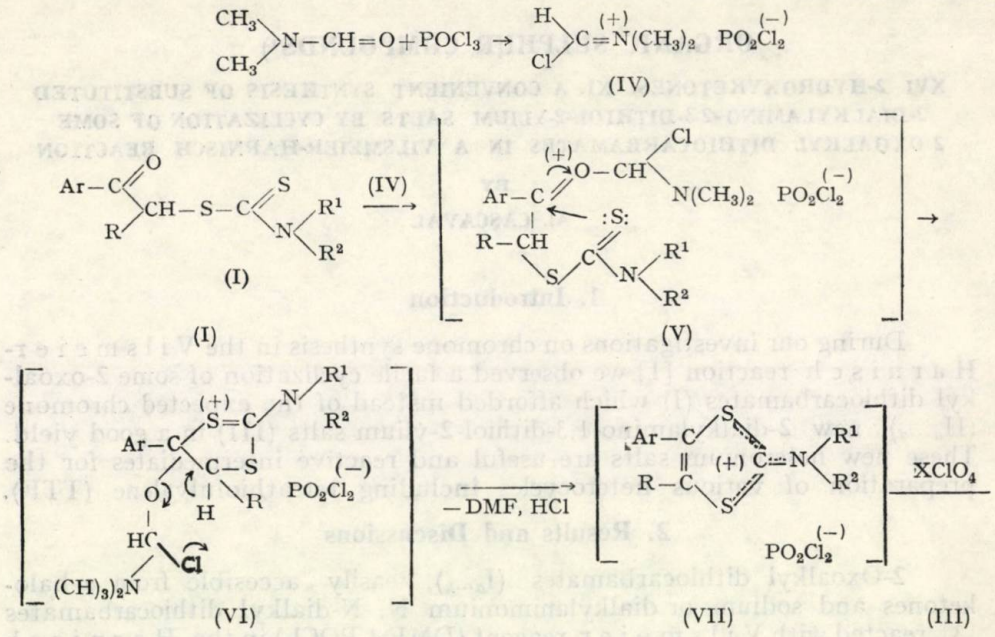

Ar=2(OH)-3,5-$Cl_2C_6H_2$; X=Na or NH_4.

Scheme *B*

In a first stage of the reaction it is possible an electrophylic addition of immonium-carbonium ion (IV) to the carbonyl group which behave as „hard" donor function and so-called „hard-cyclization" [7] take place via (V)...(VII) intermediates. The products were isolated as perchlorates ($III_{a...h}$) by treating the reaction mixture with aqueous concentrated sodium or ammonium perchlorate. The structures of the products were confirmed by ^{1}H-NMR, IR or microanalysis and also by the comparison with the corresponding perchlorates obtained from (I) and concentrated sulfuric acid. The results are summarized in Table 1 and 2 (s. Experimental).

The present method for the preparation of some substituted 2-dialkylamino-1,3-dithiol-2-ylium perchlorates ($III_{a...h}$) has advantage over the known method of cyclization of 2-oxoalkyl dithiocarbamates by mild conditions of the reaction (temperature in the range of room temperature).

3. Experimental

IR-spectra were recorded on a Spekord 71 IR spectrometer as KBr-pellets, ^{1}H-NMR spectra on a JNM-C-60 HL spectrometer in DMSO-d_6 at 20°C.

General Procedure for the Cyclization of 2-Oxoalkyl dithiocarbamates ($I_{a...h}$) to the Substituted 2-Dialkylamino-1,3-dithiol-2-ylium Perchlorates ($III_{a...h}$).

10 mmole (I) was dissolved by stirring in 20 ml dimethylformamide at the room temperature. By cooling into ice water the solution was treated dropwise with 5 ml phosphoryl chloride (temperature during this addition was maintained at 20°...30°C). The reaction mixture was the allowed to stand for one hour at room temperature. 250 ml of water was added and the solution was extracted twice with ether to remove the unreacted dithiocarbamate. The aqueous layer was treated with a sodium, or ammoniu perchlorate solution until a complete precipitation take place. The white product was filtered and crystallized from methanol. All results are listed in Tables 1 and 2. The same perchlorates were synthesized by E. Campaigne and R. D. Hamilton method [5] without depression of m.p. for the products.

Table 1

Data on Characterization (Microanalysis, IR-Spectra) *of the Perchlorates ($III_{a...h}$)*

Compound	Yield*) %		M.p. °C	%C Calcd. Found	%H Calcd. Found	%Cl Calcd. Found	%N Calcd. Found	IR(KBr) ν, [cm^{-1}]
	a	*b*						
(III_a)	64	77	228...229	32.48 32.45	2.46 2.52	26.17 26.24	3.44 3.93	3 400, 1 070 (ClO^{-4})
(III_b)	90	93	178	35.91 35.60	3.21 2.91	24.42 24.26	3.21 2.99	3 400, 1 100
(III_c)	75	75	155	37.63 37.81	3.13 3.25	23.84 23.77	3.13 3.50	3 500, 1 100
(III_d)	85	90	197	34.79 35.02	2.68 2.80	23.72 23.15	3.12 3.26	3 400, 1 090
(III_e)	60	50	218...219	34.25 34.62	2.85 2.71	25.30 24.99	3.33 3.42	3 300, 1 100
(III_f)	72	65	118...119	37.47 37.59	3.57 3.82	23.72 24.15	3.12 3.25	3 300, 1 100
(III_g)	52	52	189...190	39.10 39.32	3.47 3.62	23.10 23.20	3.04 3.50	3 300, 1 080
(III_h)	70	65	185	36.34 36.38	3.03 3.07	23.00 23.15	3.03 3.44	3 300, 1 070

*) *a* — Cyclization with $DMF/POCl_3$; *b* — Cyclization with conc. H_2SO_4.

Table 2

^1H-NMR Spectra of the Perchlorates ($III_{a...h}$)

Compound	Chemical shifts in δ, [ppm], (shape*), intensity and assignement of signals)
(III_a)	3.5(*s*, 6H, $2CH_3$) ; 4.1(*bs*, 1H, OH) ; 7.6...7.7(*m*, 2H, arom.) ; 8,05(1H, *s*)
(III_b)	1.2...1.4(*t*, 6H, $2CH_3$) ; 3.2...3.5(*m*, 5H, $2CH_2$+OH) ; 7.6...7.7(*m*, 2H, arom.); 8.15(*s*, 1H, CH=).
(III_c)	1.7...1.8(*m*, 6H, $3CH_2$) ; 3.6...3.9(*m*, 5H, $2CH_2$+OH) ; 7.7 (*m*, 2H, arom.) ; 8.0(*s*, 1H, CH=).
(III_d)	3.8...3.9(*bs*, 8H, $4CH_2$) ; 4.4(*bs*, 1H, OH) ; 7.6(*bs*, 2H, arom.) ; 8.0 (1H, *s*).
(III_e)	2.2...2.3(*s*, 3H, CH_3C) ; 3.4...3.6(*bs*, 7H, $2CH_3N$+OH) ; 7.3...7.7(*dd*, 2H, arom.).
(III_f)	1.2...1.4(*t*, 6H, $2CH_3$) ; 2.2...2.3(*s*, 3H, CH_3C=); 3.6...4.0(*q*, 4H, $2CH_2$) ; 4.3...4.5(*bs*, 1H, OH) ; 7.4...7.7(*dd*, 2H, arom.).
(III_g)	1.6...1.9(*bs*, 6H, $3CH_2$) ; 2.3...2.4(*s*, 3H, CH_3C=) ; 3.4...3.9(*m*, 5H, $2CH_2N$+ +OH) ; 7.3...7.7(*dd*, 2H, arom.).
(III_h)	2.2...2.3(*s*, 3H, CH_3C=); 3.7...4.0(*bs*, 9H, $4CH_2$+OH); 7.3...7.6 (*dd*, 2H, arom.).

*) *s*—singlet ; *bs*—broad singlet ; *m*—multiplet ; *dd*—double doublet ; *q*—quartet.

A k n o w l e d g e m e n t. The author is thankful to „Alexander von Humboldt" Stiftung, Bonn-Bad Godesberg, for awarding a fellowship in Freiburg i.Br.to undertake a part of this study.

Received, December 4, 1980

Polytechnic Institute, Jassy, Department of Organic and Macromolecular Chemistry

REFERENCES

1. C a ş c a v a l Al., Liebigs Ann., *669* (1980).
2. C a ş c a v a l Al., Tetrahedron (in press).
3. H a r n i s c h H., Liebigs Ann., *765*, 8 (1972).
4. C a m p a i g n e E., J a c o b s e n N. W., J. Org. Chem., **29**, 1703 (1964).
5. C a m p a i g n e E., H a m i l t o n R. D., J. Org. Chem., **29**, 1711 (1964).
6. N a r i t a M., P i t t m a n n C. U. Jr., Synthesis, 489 (1976).
7. U e n o Y., O k a w a r a M., Synthesis, 182 (1979).

COMPUŞI ORGANICI AI SULFULUI

XVI. 2-Hidroxicetone. XI. O convenabilă sinteză a sărurilor de 2-dialchilamino-1,3-ditiol-2-ilium substituite prin ciclizarea unor 2-cetoalchil ditiocarbamaţi într-o reacţie Vilsmeier-Harnisch

(Rezumat)

Se arată că 2-hidroxi-3,5-diclor-fenacil-N,N-dialchilditiocarbamaţii ($I_{a...d}$) şi 2-hidroxi-3,5-diclor-α-metilfenacil-N,N-dialchilditiocarbamaţii ($I_{e...h}$), în condiţiile reacţiei V i l s m e i e r - H a r n i s c h, conduc cu randamente bune la percloraţii de 2-dialchilamino-1,3-ditiol-2-ilium ($III_{a...h}$). Sînt prezentate procedeele de sinteză, mecanismele de reacţie iar produşii sintetizaţi sînt caracterizaţi din punct de vedere analitic şi spectral. Produşii obţinuţi pot fi intermediari folositori în sinteza derivaţilor de tetratiofulvalenă.

BULETINUL INSTITUTULUI POLITEHNIC DIN IAŞI
Tomul XXIX (XXXIII), Fasc. 1—4, 1983
Secţia II
CHIMIE şi INGINERIE CHIMICĂ

C.Z. 677.622.32

NOI PIGMENŢI AZOICI DE CONDENSARE

DE

VALERIA GORDUZA, GH. LUPUŞOR şi VIANORA PESCARU

1. Introducere

Sinteza unor noi pigmenţi organici, cu proprietăţi fizico-chimice îmbunătăţite, constituie o direcţie prioritară de investigaţie în chimia şi tehnologia coloranţilor.

2. Rezultate şi discuţii

Noii pigmenţi sintetizaţi se seriază încercărilor de îmbunătăţire a proprietăţilor fizico-chimice ale pigmenţilor prin mărirea masei moleculare, fiind din punct de vedere structural derivaţi azoici ai bis-β-oxi-naftil-arilidelor, de tip Cromophtal [1]...[3]:

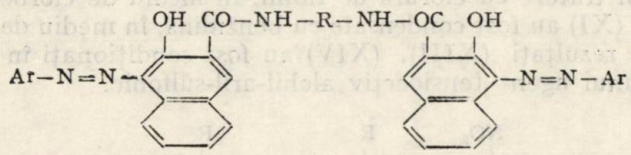

Ar — rest aromatic cu substituenţi electronoacceptori ; R — rest de diamină aromatică.

Sinteza acestor pigmenţi presupune obţinerea unui colorant monoazoic, care conţine grupare carboxilică, transformarea în clorură acidă şi acilarea cu aceasta a unei diamine aromatice, ultimele două reacţii efectuîndu-se în solvenţi inerţi, cu punct de fierbere înalt (clorbenzen, *o*-diclorbenzen, triclorbenzen, xilen) [4].

În sinteza şi condiţionarea pigmenţilor de acest tip se acordă o atenţie deosebită factorilor care influenţează procesul de formare a particulelor şi anume : forţe de agregare, diluţie, variaţii de temperatură şi pH, puritatea materiilor prime, agitarea, adaosul de agenţi tensioactivi, metoda de condiţionare.

Pigmenţii azoici de condensare se caracterizează prin rezistenţă la acţiunea solvenţilor şi temperatură înaltă, datorită maselor moleculare mari, fiind indicaţi pentru fabricarea lacurilor şi vopselelor, precum şi pentru colorarea maselor plastice.

Prezenţa grupărilor amidice în structura acestor pigmenţi conferă rezistenţă la lumină, în timp ce cea a grupărilor nitrice determină efecte batocrome şi mărirea puterii de colorare.

Plecînd de la dezideratul măririi masei moleculare s-au ales, în calitate de componente diazotate, amine din seria benzidinelor aril-aminate cu 2,4-dinitro-clorbenzen, studiate de Lupușor și colaboratorii [5], obținute conform schemei de reacție :

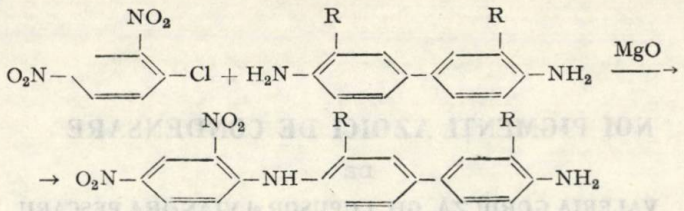

(II *a*) R=CH_3 ; (II *b*) R=OCH_3 ; (III) R=CH_3 ; (IV) R=OCH_3

Astfel de amine prezintă stabilitate termică, rezistență la acțiunea solvenților și efecte batocrome datorită poziției *orto-para* a grupărilor nitrice față de legătura aminică secundară.

N-(2′, 4′-dinitro-fenil)-*o*-tolidina (III) și N-(2′, 4′-dinitrofenil)-*o*-dianisidina (IV), purificate prin recristalizare din amestec alcool etilic—acetonă (1 : 1), au fost supuse diazotării cu cantitatea stoechiometrică de azotit de sodiu, în prezența acidului clorhidric în exces [6]. Clorurile de aril diazoniu obținute (V), (VI) au fost cuplate cu acid 2-hidroxi-naftalin-3-carboxilic (VII), la valori ale pH-ului cuprinse între 8,5 și 9 și la o temperatură de 5°C [7]. Coloranții monoazoici (VIII), (IX) au fost transformați în cloruri acide prin tratare cu clorură de tionil, în mediu de clorbenzen. Clorurile acide (X), (XI) au fost condensate cu benzidină, în mediu de clorbenzen, iar pigmenții rezultați (XIII), (XIV) au fost condiționați în mediu apos, în prezența unui agent tensioactiv alchil-aril-sulfonic.

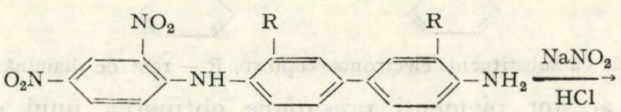

(III) R=CH_3 ; (IV) R=OCH_3 ;

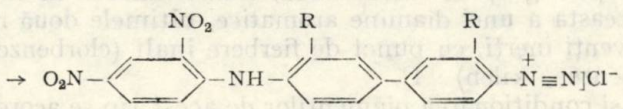

(V) R=CH_3 ; (VI) R=OCH_3

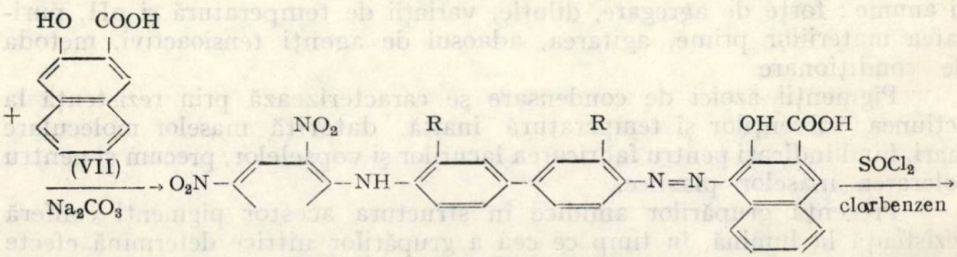

(VIII) R=CH_3 ; (IX) R=OCH_3.

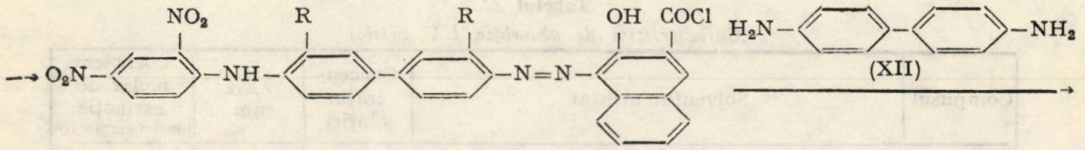

(X) R=CH_3; (XI) R=OCH_3

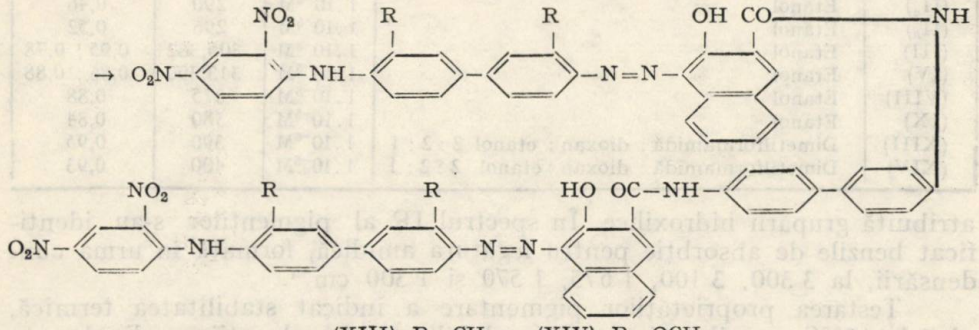

(XIII) R=CH_3; (XIV) R=OCH_3

Produșii obținuți au fost caracterizați prin analiză elementară (dozare azot prin metoda D u m a s) (tabelul 1). spectroscopie UV vizibil (tabelul 2) și spectroscopie IR (pastilă de KBr). De asemenea, au fost testate proprietățile pigmentare.

Tabelul 1

Analiza elementară a produșilor sintetizați

Compusul	Formula brută	Masa moleculară	% N	
			calculat	găsit
(III)	$C_{20}H_{18}N_4O_4$	378	14,81	14,68
(IV)	$C_{20}H_{18}N_4O_6$	410	13,66	13,50
(VIII)	$C_{31}H_{23}N_5O_7$	577	12,13	11,98
(IX)	$C_{31}H_{23}N_5O_9$	609	11,49	11,30
(XIII)	$C_{74}H_{54}N_{12}O_{12}$	1 302	12,90	12,55
(XIV)	$C_{74}H_{54}N_{12}O_{16}$	1 366	12,30	12,01

S-a remarcat insolubilitatea pigmenților sintetizați în solvenții organici uzuali, cît și în unele amestecuri de solvenți. Produșii se dizolvă în amestec N, N-dimetil-formamidă : dioxan : etanol, în proporție 2 : 2 : 1.

Valorile maximelor de absorbție și ale coeficienților molari de extincție, în domeniile UV vizibil, pentru pigmenții și intermediarii sintetizați, sînt prezentate în tabelul 2, în care se menționează solvenții și concentrațiile utilizate.

În spectrele IR ale compușilor sintetizați se remarcă absorbțiile caracteristice grupărilor funcționale constitutive. Astfel, intermediarii (III), (IV) prezintă frecvențe caracteristice pentru grupele nitrice (1 450, 1 580 cm^{-1}), grupa aminică secundară (1 310 cm^{-1}), grupa aminică primară (1 260, 1 600 cm^{-1}). În spectrele de absorbție ale coloranților monoazoici (VIII), (IX) s-au pus în evidență absorbții la 1 500 cm^{-1} atribuite legăturii azotice, la 970, 1 390 și 1 790 cm^{-1}, datorite grupării carboxilice și la 3 200 cm^{-1},

Tabelul 2

Caracteristici de absorbție UV vizibil

Compusul	Solventul utilizat	Concentrația soluției	λ_{max} nm	Coeficient molar de extincție $l.mol^{-1}.cm^{-1} \times 10^3$
(I)	Etanol	1.10^{-5}M	230,240	0,66 ; 0,68
(II_a)	Etanol	1.10^{-5}M	290	0,46
(II_b)	Etanol	1.10^{-5}M	296	0,52
(III)	Etanol	1.10^{-5}M	305,362	0,95 ; 0,78
(IV)	Etanol	1.10^{-5}M	313,390	0,86 ; 0,88
(VIII)	Etanol	1.10^{-5}M	375	0,88
(IX)	Etanol	1.10^{-5}M	380	0,84
(XIII)	Dimetilformamidă : dioxan : etanol 2 : 2 : 1	1.10^{-5}M	390	0,95
(XIV)	Dimetilformamidă : dioxan : etanol 2 : 2 : 1	1.10^{-5}M	400	0,93

atribuită grupării hidroxilice. În spectrul IR al pigmenților s-au identificat benzile de absorbție pentru legătura amidică, formată în urma condensării, la 3 300, 3 100, 1 675, 1 570 și 1 300 cm^{-1}.

Testarea proprietăților pigmentare a indicat stabilitatea termică, pînă la 170°C, a noilor pigmenți, insolubilitatea în solvenții uzuali, absența fenomenului de sublimare, puterea de colorare mare în nuanțe brun-roșietice, caracteristici corelate cu masa moleculară mare și prezența în structură a grupărilor amidice și nitrice. Friabilitatea pigmenților este corespunzătoare, conținutul în cenușă — 0,01%, testele de umiditate și conținut în substanțe solubile în apă — negative. Nu s-au observat modificări de culoare la tratarea cu soluții de acizi (soluție 5% de acid clorhidric) și alcalii (soluție 1% de hidroxid de sodiu și soluție 5% de carbonat de sodiu).

3. Partea experimentală

3.1. Obținerea coloranților azoici (VIII), (IX)

0,01 moli amină (III), IV) se suspendă în 50 ml apă și se tratează, sub agitare, cu 0,05 echivalenți de acid clorhidric ($d = 1,19$). Amestecul obținut se încălzește la fierbere, sub agitare, obținîndu-se o suspensie fină. Suspensia se răcește la 5°C, pe baie de gheață și se diazotează prin tratare cu 0,01 moli azotit de sodiu (soluție 20%). După perfectarea reacției excesul de acid azotos se distruge prin tratare cu acid sulfamic. Clorurile de aril-diazoniu formate (V), (VI) se trec, imediat după preparare, la cuplare cu acid 2-hidroxi-naftalin-3-carboxilic.

0,01 moli acid 2-hidroxi-naftalin-3-carboxilic (VII) se suspendă în 60 ml apă și se adaugă 10 ml soluție hidroxid de sodiu 1 N. Se încălzește la 80°C, pînă la obținerea unei soluții limpezi. Soluția se răcește la 5°C, la această temperatură adăugîndu-se, în porțiuni, sub agitare energică, sarea de diazoniu. În timpul cuplării se menține pH-ul la valoarea 8,5, prin utilizarea unei soluții tampon de carbonat de sodiu. Se agită timp de o oră la temperatura de 5°...10°C și apoi se încălzește amestecul de reacție la 80°C, menținîndu-se la această temperatură o oră. Colorantul precipitat se separă prin filtrare la vid și se spală cu apă.

3.3. Obținerea și condiționarea pigmenților (XIII), (XIV)

Într-un balon cu patru gîturi, de 250 ml, prevăzut cu agitator, pîlnie de picurare, termometru și refrigerent, se introduc 0,01 moli colorant monoazoic și 90 ml clorbenzen. Se încălzește pe baie de aer, eliminîndu-se prin distilare azeotropă eventualele urme de apă, la temperatura de 130°...132°C (volum distilat : 9 ml). Se răcește amestecul de reacție la 50°C, se schimbă refrigerentul descendent cu unul ascendent, se adaugă 0,5 ml dimetilformamidă și apoi, în decurs de 15 min., 0,02 moli clorură de tionil. Se încălzește amestecul de reacție la 130°...132°C și se menține la reflux două ore. Se verifică sfîrșitul reacției prin cromatografie pe hîrtie. Clorura acidă a colorantului monoazoic (X), (XI) este condensată cu 0,008 moli benzidină, sub agitare

și reflux, timp de patru ore. Se răcește la 90°C, se filtrează și se spală cu clorbenzen (de patru ori cîte 10 ml). Pasta obținută se suspendă în 85 ml apă, se adaugă 0,8 g carbonat de sodiu și 2 g detergent alchil-aril-sulfonic. Se fierbe suspensia, sub agitare, timp de o oră. Se filtrează fierbinte și se spală de cinci ori cu cîte 20 ml apă. Se usucă la 60°C. Randament 80%.

3.3. Controlul cromatografic al transformării în clorură acidă

O probă extrasă din amestecul de reacție se tratează cu anilină, în mediu de *o*-diclorbenzen la cald. Arilida formată se cromatografiază (hîrtie MN 260, eluent benzen : ciclohexan 1 : 1). În aceleași condiții se cromatografiază o probă martor (colorant monoazoic—anilină-diclorbenzen, la cald). Colorantul azoic rămîne la startul cromatogramei, iar arilida formată din clorura acidă migrează (R_f=0,71). Procesul se consideră terminat cînd la startul cromatogramei nu rămîn urme de colorant monoazoic.

4. Concluzii

1. Au fost sintetizați doi noi pigmenți azoici de condensare, pe baza unor intermediari arilaminați originali.

2. Reacțiile de arilaminare și diazotare au fost efectuate conform metodelor stabilite de L u p u ș o r și colaboratorii.

3. S-au stabilit metodele de cuplare a intermediarilor aril-aminați diazotați cu acidul 2-hidroxi-naftalin-3-carboxilic, transformarea în clorură acidă a derivaților monoazoici și condensarea acestora cu benzidină.

4. Caracterizarea produșilor sintetizați s-a efectuat prin analiză elementară și spectrală.

5. Testarea preliminară indică bune proprietăți pigmentare, corelate cu masa moleculară mare și prezența grupelor nitrice și amidice în structură.

Primită la 20 decembrie 1980

Institutul politehnic, Iași,
Catedra de chimie organică și macromoleculară

BIBLIOGRAFIE

1. V e n k a t a r a m a n K., *The Chemistry of Synthetic Dyes*. Vol. 5, Academic Press, New York, 1971, 314—474.
2. L e n o i r J., Peintures, Pigments, Vernis, **38**, *1*, 7 (1962).
3. L e n o i r J., Peintures, Pigments, Vernis, **38**, *5*, 384 (1962).
4. G e i s s l e r G., Fortschritte in der Entwicklung von Azopigmenten, Defazet, **27**, *10*, 464 (1973).
5. L u p u ș o r Gh., D u m i t r e s c u Sv., Bul. Inst. polit., Iași, **II (VI)**, *1—2*, 131 (1956).
6. L u p u ș o r Gh., G o r d u z a V., Bul. Inst. polit., Iași, **XXIII (XXVII)**, *3—4*, s. II, 59 (1977).
7. S a n i e l e v i c i H., F l o r u L., *Sinteza intermediarilor aromatici și a coloranților*. EDP, Buc., 1971, 262.

NEW CONDENSING AZOPIGMENTS

(Summary)

Two new condensing azo-pigments have been synthesized, starting from arilaminated intermediates.

The arilamination and diazotization reactions have been accomplished according to the methods developed by L u p u ș o r and co-workers

The methods of coupling the diazotized aril-aminated intermediates with 2-hydroxy-naphthalin-3-carboxylic acid were settled as well as those of converting the azo-derivatives in to the acid chloride and of condensing with benzidine.

The characterization of the synthesized products were accomplished by elemental and spectral analysis.

Preliminary tests indicate good pigment properties, correlated with the large molecular weight and the presence of nitro and amide group in their structure.

BULETINUL INSTITUTULUI POLITEHNIC DIN IAŞI
Tomul XXIX (XXXIII), Fasc. 1—4, 1983
Secţia II
CHIMIE şi INGINERIE CHIMICĂ

D.C. 678-13

REACTIVITY OF ACRYLIC MONOMERS

X. COPOLYMERIZATION OF ACRYLAMIDE AND METHACRYLAMIDE WITH n-BUTYL ACRYLATE

BY

SPIRIDON OPREA, EMIL DUMITRIU and IRINA-CARMEN DIEAC

1. Introduction

The acrylic monomers are regarded as one of the most important class of vinyl monomers, because they have numerous and various applications. Certainly, this fact is favoured by the great number of acrylic monomers with various properties, thus there is possibility to use them in different fields. An important source of new acrylic materials consists in the copolymerization of acrylic monomers. By copolymerization of acrylic monomers with other vinyl monomers, such as styrene, olefins, dienes, etc. or with monomers from the same group one obtain polymeric products having certains applications. In this context is remarked the preoccupation regarding the copolymerization of the acrylamides with acrylic esters. The numerous patents demonstrate a large field of applications: materials for textile finishing [1], [2], coatings [3]...[7], adhesives [8], elastomers [9], flocculants [10], carriers for biologically active substances [11], resins for paints [12], etc.

The knowledge of behaviour of the systems acrylamides — acrylates in the copolymerization processes show a real interest both practical and theoretical. In this sense the systems acrylamide — butyl acrylate and methacrylamide — butyl acrylate were chosen to be studied, the chosen monomers being among the most used acrylic monomers but their behaviour in the mentioned copolymerization processes do not have sufficient data.

2. Experimental

Acrylamide (AAm) was purified by recrystallization from benzene; m.p. = 84,5°C. Methacrylamide (MAm) was also purified by recrystallization from benzene; m.p. = 110°C. n-Butyl acrylate (BuA) was purified by distillation under vacuum to remove the inhibitor; the middle fraction was collected; b.p. = 38°C/10 mm Hg. 2,2′ — Azobis (izobutironitrile) (AIBN) was purified by recrystallization from ethanol.

The solvents used, dimethylsulfoxide (DMSO) and diethyl ether, were purified by the common methods.

2.1. Copolymerization

The copolymerization of (meth)acrylamide with n-butyl acrylate was carried out in DMSO solution at 60°C using AIBN as polymerization initiator. In the polymerizàtion ampoules was introduced the weighed amount of the (meth)acrylamide, then one part of DMSO was added to solubilize the (meth)acrylamide, after which the n-butyl acrylate was introduced and finally was added the remaining solvent which contains the disolved initiator (monomer concentration was 5 M; initiator concentration was 0.2% against monomers). The ampoules were degased and purged with nitrogen then they were closed and introduced into thermostat bath at 60°C. The proper time for low conversions (under 10%) was established by trial and error method. At proper time the ampoules were taken out from thermostat, cooled and the reaction mixture poured into diethyl ether. The polymers were purified by reprecipitation in the same system, then they were dried under vacuum. The copolymer compositions were determined by their nitrogen content using micro K j e l d a h l method. The reaction conditions and results are summarized in Tables 1 and 2.

Table 1

Copolymerization of Acrylamide (AAm) with n-Butyl Acrylate in DMSO Solution at 60°C

No crt.	Mole fraction AAm in monomer feed	Mole fraction AAm in copolymer	N_2 %	Conversion %
1	0.101	0.083	0.94	3.37
2	0.198	0.148	1.73	2.14
3	0.305	0.231	2.81	8.63
4	0.412	0.315	4.02	5.20
5	0.502	0.385	5.08	1.17
6	0.597	0.461	6.34	4.61
7	0.703	0.525	7.49	7.82
8	0.800	0.616	8.35	3.34
9	0.899	0.730	9.28	3.01

Table 2

Copolymerization of Methacrylamide (MAm) with n-Butyl Acrylate in DMSO Solution at 60°C

No crt.	Mole fraction MAm in monomer feed	Mole fraction MAm in copolymer	N_2 %	Conversion %
1	0.097	0.090	1.02	4.15
2	0.199	0.153	1.76	4.78
3	0.301	0.248	2.96	3.25
4	0.402	0.329	4.05	5.14
5	0.504	0.404	5.15	8.22
6	0.598	0.477	6.22	2.18
7	0.701	0.560	7.55	9.34
8	0.802	0.634	8.81	5.71

3. Results and Discussions

On the basis of the data from the Tables 1 and 2 the copolymer compositions against monomer feed were represented in Figs. 1 and 2. From these figures one can state that copolymerization systems show the features of systems having the reactivity ratio $r_1 < 1$ and $r_2 > 1$. As it can be seen from Figs. 1 and 2 the copolymer is always more poorer in acrylamide compared with the initial mixtures of monomers. The shape of curves having the specific feature of the systems for which r_1 is smaller than unity and r_2 is greater than unity, demonstrate the higher reactivity of the butyl acrylate.

Since the values of reactivity ratio illustrate more exactly this aspect further two methods were applied for copolymerization parameters r_1

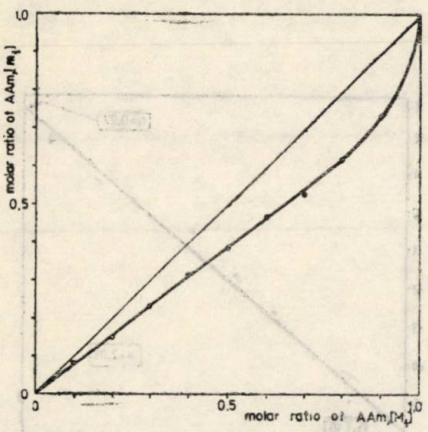

Fig. 1. — Composition diagram for acrylamide—butyl acrylate system.

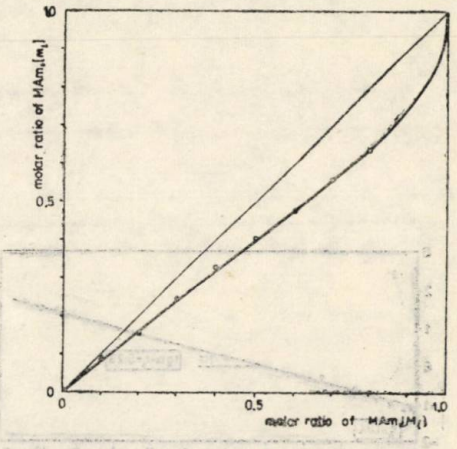

Fig. 2. — Composition diagram for methacrylamide—butyl acrylate system.

and r_2 evaluation. On account of the adopted experimental technique the methods used for reactivity ratios evaluation are based on differential equation of composition , namely :

$$\frac{d[M_1]}{d[M_2]} = \frac{[M_1]}{[M_2]} \cdot \frac{r_1[M_1]+[M_2]}{r_2[M_2]+[M_1]}, \tag{1}$$

where r_1 and r_2 are the copolymerization reactivity ratios. Applying the F i n e m a n-R o s s method [13] according to Eq. :

$$\frac{x}{y}(y-1) = r_1 \frac{x^2}{y} - r_2, \tag{2}$$

where :

$$x = \frac{[M_1]}{[M_2]}, \quad y = \frac{d[M_1]}{d[M_2]}$$

the plots represented in Figs. 3 and 4 are obtained for the two systems. The straightlines were plotted by the least square method and from their parameters the reactivity ratios were calculated.

As it is known, the disadvantage of F i n e m a n-R o s s method is due to the unequally weighted values of the experimental data; the experimental data at the range extremities have a great influence on the slope. Consequently it was applied the K e l e n-T ü d ö s method [14] :

$$\eta = \left(r_1 + \frac{r_2}{\alpha}\right)\xi - \frac{r_2}{\alpha}, \tag{3}$$

where :

$$\eta = \frac{G}{\alpha+F}, \quad \xi = \frac{F}{\alpha+F}, \quad \alpha = \sqrt{F_{min} F_{max}}, \quad F = \frac{x^2}{y}, \quad G = \frac{x(y-1)}{y};$$

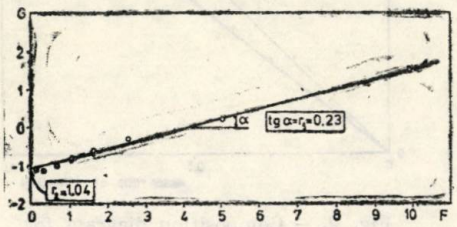

Fig. 3. — F i n e m a n - R o s s plot for copolymerization of acrylamide with n-butyl acrylate in DMSO solution at 60°C.

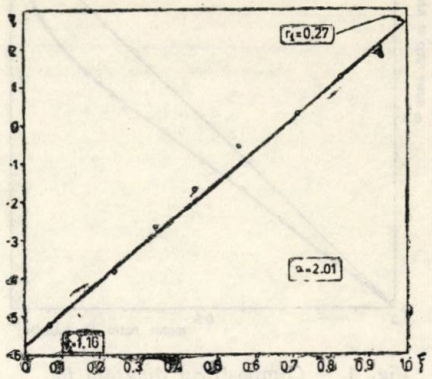

Fig. 4. — F i n e m a n - R o s s plot for copolymerization of methacrylamide with n-butyl acrylate in DMSO solution at 60°C.

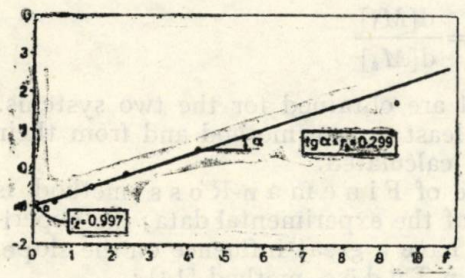

Fig. 5. — K e l e n - T ü d ö s plot for copolymerization of acrylamide with n-butyl acrylate in DMSO solution at 60°C.

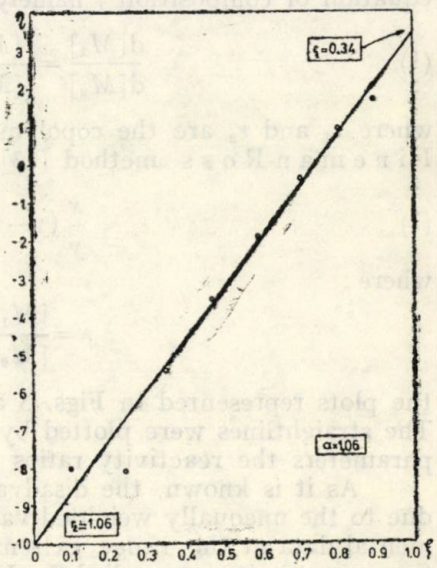

Fig. 6. — K e l e n - T ü d ö s plot for copolymerization of methacrylamide with n-butyl acrylate in DMSO solution at 60°C.

this method realises a more uniform distribution of the experimental data (Figs. 5 and 6). The straightlines were also plotted by the least square method and from their parameters the r_1 and r_2 values were calculated, (Table 3). From Figs. 5 and 6 one can observe that the experimental data are placed on the straight lines and therefore the kinetic model corresponds to the terminal model.

Table 3

Copolymerization Parameters for (Meth)acrylamide Butyl Acrylate Systems

Monomer M_1	r_1		r_2	
	Fineman-Ross method	Kelen-Tüdös method	Fineman-Ross method	Kelen-Tüdös method
Acrylamide	0.23	0.27	1.04	1.16
Methacrylamide	0.29	0.34	0.99	1.06

Analysing the r_1 and r_2 values from the Table 3 it can be observed similar behaviours, for studied systems, r_1 being smaller than unity and r_2 greater than unity. If it is considered the propagation stage for the kinetic chain :

(4)
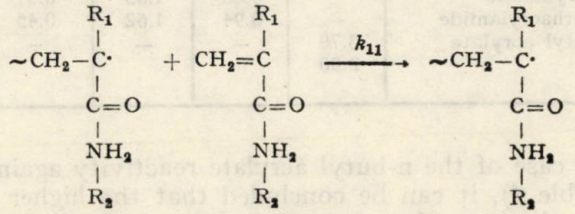

(5)
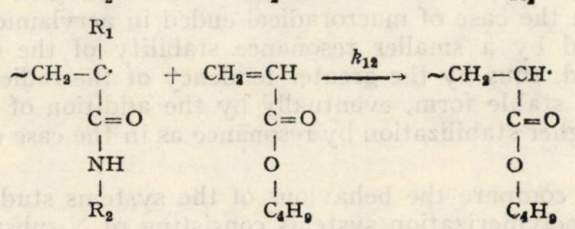

(6)
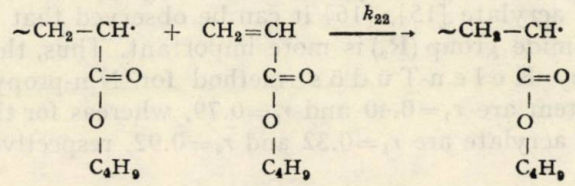

(7)
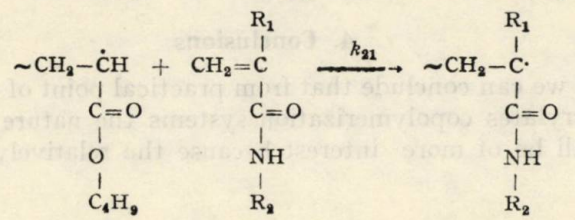

the above mentioned observation indicates that the reaction described by the kinetic Eqs. (5) and (6) take place with greater rate than the reactions (4) and (7). This means that n-butyl acrylate is more reactive than (meth) acrylamide. The difference in reactivity can be also proved by the relative reactivities $1/r_i$, (Table 4). Thus considering the data shown in the Table 4 if we compare the reactivities of acrylamides against the macroradical ended in n-butyl acrylate it can be observed that the relative reactivity of methacrylamide is some greater than those of the acrylamide. These differences can only explained on the basis of the influence of the methyl radical in the α position. The small difference between the values of Q and e parameters do not permit exact evidence of the influence, yet, as it is known, methyl group is an electron donor therefore the influence exercised can only be due to the property of the methyl group.

Table 4

Relative Reactivities of the Monomers

Radical	Monomer	$1/r_1$	$1/r_2$	e_1	Q_1 [17]	e_2	Q_2 [17]
~BA.	Acrylamide	—	0.86	1.65	0.37	—	—
	Methacrylamide	—	0.94	1.62	0.45	—	—
~AAm.	Butyl acrylate	3.70	—	—	—	1.06	0.50
~MAm.		2.90					

In the case of the n-butyl acrylate reactivity against the two macroradicals (Table 4), it can be concluded that the higher relative reactivity is present in the case of macroradical ended in acrylamide. This fact could be explained by a smaller resonance stability of the mentioned radical $Q=0.37$, and, thus by the greater tendency of the radical in transforming into a more stable form, eventually by the addition of a monomer which leads to a higher stabilization by resonance as in the case of n-butyl acrylate ($Q=0.50$).

If one compare the behaviour of the systems studied in this paper with the copolymerization systems consisting of N-substituted acrylamide and n-butyl acrylate [15], [16] it can be observed that the effect of substituent at amide group (R_2) is more important. Thus, the reactivity ratios calculated by K e l e n-T ü d ö s method for N-n-propylacrylamide-butyl acrylate system are $r_1=0.40$ and $r_2=0.79$, whereas for the N-n-butylacrylamide-butyl acrylate are $r_1=0.32$ and $r_2=0.92$, respectively.

4. Conclusions

Finally we can conclude that from practical point of view for the acrylamides — acrylates copolymerization systems the nature of amide substituent (R_2) will be of more interest because the relatively large differences

between the two copolymerization parameters r_1 and r_2 demonstrate the tendency of obtaining copolymers poorer in acrylamide than substrate (fact illustrated by the composition diagrams, too).

Received, May 31, 1980

Polytehnic Institute, Jassy
Department of Organic and Macromolecular Chemistry

REFERENCES

1. . * . BASF, Fr. *2 003 769*, 14 Nov. 1969; C.A., **72**, 101224 t (1970).
2. . . . BASF, Ger. *1 920 287*, 12 Nov. 1970; C.A., **74**, 23606 u (1971).
3. Kapalka E. J., Bittle H. G., U.S. *3 001 993*, 17 July 1957; C.A., 4894 i (1962)
4. . * . Mitsubishi Rayon Co., Ltd., Jap. 74 *52 224*, 21 May 1974; C.A., 171485 p (1974).
5. Kapalka E. J., Martin R. A., Fr. *1 158 078*, 29 Aug. 1969; C.A., **72**, 123053 p (1970).
6. . * . Bayer A.-G., Ger. *1 519 144*, 12 July 1973; C.A., **82**, 87804 e (1975).
7. Popa L., Lydick H. K., Ger. *1 814 115*, 13 Dec. 1967; C.A., **71**, 71408 r (1969).
8. Vosta A. J., U.S. *3 845 066*, 29 Oct. 1974; C.A., 113266 c (1975).
9. . * . B. F. Goodrich Co., Fr. *1 424 422*, 19 May 1964; C.A., **65**, 1329 b (1971).
10. . * . Dow Chemical Co., Ger *2 054 523*, 5 Nov. 1969; C.A., **75**, 77861 n (1971).
11. . * . Rehm G.m.b.H., Ger. *2 237 316*, 14 Feb. 1974; C.A., **82**, 74078 w (1975).
12. . * . Dainippon Ink and Chemicals, Inc., Jap. 74 *06 555*,4 July 1970; C.A., **82**, 60099 s (1975).
13. Fineman M., Ross S. A., J. Polym. Sci., **5** 259 (1950).
14. Kelen F., Tüdös F., J. Macromol. Sci.—Chem., **A9** (1975).
15. Oprea Sp., Dumitriu Em., Bul. Inst. polit.,'Iaşi, **XXVI (XXX)**, *1—2*, s. II, 71 (1980).
16. Oprea Sp., Dumitriu Em., Iordache V., Mat. Plast., **17**, *3*, 141 (1980).
17. Young L. J., *Polymer Handbook*. Interscience Publ., 1966.

REACTIVITATEA MONOMERILOR ACRILICI

XI. Copolimerizarea acrilamidei şi metacrilamidei cu acrilatul de n-butil

(Rezumat)

S-a studiat copolimerizarea acrilamidei şi metacrilamidei cu acrilatul de n-butil, în soluţie, la 60°C. Ambele sisteme arată ca acrilatul de n-butil este mai reactiv decît acrilamidele. S-a calculat raportul de reactivitate prin două metode diferenţiale. S-a observat că substituentul din poziţia α exercită o influenţă redusă asupra reactivităţii acrilamidei.

ÎNTREPRINDEREA PRELUCRARE MASE PLASTICE

IAŞI, ŞOS. ŢUŢORA 95

PHONE : 3.19.27

Manufactures and supplies

- **Thermocontractible Polyvinil Chloride Tubes for Protection and Electrotechnical Purposes**

  — Dimensions : $D_t = 15...80$ mm.

  — Wall thickness : 0.5...1.2 mm.

  — Cross contraction coefficient : min. 40%.

- **High Pressure Plastic Hoses**

Manufactured with polyamide lining (inner layer) type Rilsan, Besno P.40 or other polymers depending on the working pressure and the environment. Such hoses are being used in dyeing installations as well as in hydraulic and pneumatic equipments, with a regime pressure of at most 230 bar and temperatures ranging between +5...+40°C.

We mention several manufacturable sizes :

	Simple Braid	Double Braid
Inside diameter, [mm]	3.75±0.2	6.5±0.2
Outside diameter, [mm]	8.7 ±0.2	14.0±0.2
Thickness of PA tube wall, [inches]	0.7 ±0.1	1 ±0.1

The hoses are resistant to the action of oil-type dyestuffs, enamel varnish, epoxidic resin, gasoline, corrosive agents etc.

- **Polyvinyl Chloride Hose with Rigid Armature**

Outside diameter : 40 mm.

Wall thickness : 4 mm.

Minimum bending radius : 150 mm.

Sealing pressure : 10 daN/cm^2.

It may be used in sowing machines for transporting seeds and, most commonly, for transporting fluids which do not cat into polyvinyl chloride walls and which require constant transfer sections for small curvature radii.

Hoses with other diameters may be manufactured on demand.

INTREPRINDEREA DE ANTIBIOTICE
IAŞI
Telefon : (981) 4.27.70 : Telex : 022244

THE ANTIBIOTICS ENTERPRISE
IASSY
Phone : (981) 4.27.70 ; Telex : 022244

R6647 S. R. of Romania produces and delivers the following new pharmaceutical formulae based on medicinal plants extracts :

- ERGOCEPS — solution for internal use ;
  sin : Redergin, DH Ergotoxin, Hydergin.

Composition : a 0.1% solution comprising equal parts of :

— methane-sulphonate of dihydroergocryptine ;

— methane-sulphonate of dihydroergocornine ;

— methane-sulphonate of dihydroergocristine ;

with peripheral-sympatholytic vasodilating effect, it lowers the arterial tensions in hypertensive patients.

It is intended for peripheral and central circulatory disturbances, arterial hypertension and cervical sympathicus irritation syndrome.

- CORNHIDRAL — a 0,2% solution for internal use
  — methane-sulphonate of dihydroergotamine acting as :

vascular tonus regulator with a central mechanism (regulationg effect upon neuro-vegetative vasomotric centres) and a peripheral mechanism (direct tonic action on the venous wall).

It is suggested in the basic treatment of

— migrenes (cataminal, digestive, vascular and postcomotional) ;

— peripheral venous insufficiencies ;

— orthostatic, idiopathic or medicinal hypotension ;

— neurovegetative distoniae in hepatic biliary insufficiency, serpigo, epidermic paroditis, varicella, following upon a psichotropic treatment etc.

Exporter : CHIMIMPORT-EXPORT, Bucureşti
B-dul Republicii nr. 10, sect. 4
R. S. ROMÂNIA

Coli de tipar 7,5

Tiparul executat sub cd. 245
la Intreprinderea Poligrafică Iaşi,
str. 7 Noiembrie nr. 49

1984 OKT 2 6

40822